Universidad de Huelva

Departamento de Ingeniería Eléctrica y Térmica

Design of a non-linear controller to track de maximum power point of photovoltaic systems in electrical power systems with distributed generation

Memoria para optar al grado de doctora
presentada por:

Aránzazu Delgado Martín

Fecha de lectura: 26 de enero de 2016

Bajo la dirección del doctor:

Jesús Rodríquez Vázquez

Huelva, 2016

Universidad de Huelva

Universidad de Huelva

Doctorado en Ingeniería de Control, Sistemas Electrónicos e Informática Industrial

Design of a Non-linear Controller to Track de Maximum Power Point of Photovoltaic Systems in Electrical Power Systems with Distributed Generation

Doctoranda: **Dña. Aránzazu Delgado Martín**

Director de la tesis: **Dr. D. Jesús Rodríguez Vázquez**

Noviembre de 2015

Table of contents

1 Introduction, Objetives and Organization

1.1 Introduction - State of the Art.

The energy demand and the number of distributed generation systems are growing all over the world last years. For that reason, it is essential the use of renewable energy systems in addition to the conventional ones, [1]-[3]. Nowadays, renewable energy sources are widely used and, particularly, photovoltaic (PV) energy systems have become widespread everywhere. Photovoltaic energy supplies electricity to isolated houses and autonomous devices and provides electrical energy to inject into power grids. These systems produce electricity on a large scale through distribution networks as well.

Photovoltaic systems are based on the generation of energy through PV cells. The solar cells convert the solar energy to electrical energy in order to be transferred to the electrical power system, [4]. The well-known solar cell model consists of a current source, an anti-parallel diode, a shunt resistor and a series resistor, [4]. A PV cell can be simulated in Matlab-Simulink, [5]. A unique solar cell generates low energy. As a consequence, an association of solar cells is required to obtain the voltage and current needs. Therefore, the PV cells are connected in series strings and then paralleled to obtain a solar array or module. Usually, the association in series of these solar cells makes a PV module or array that provides more power. The power generated by the solar cell arrays depends on the environmental conditions, such as the temperature and the irradiance. The current – voltage (I – V) and power – voltage (P – V) characteristic curves are obtained from the PV modules to determine where the peak of the curve is located, [6]-[7]. The maximum point in the P – V curve is the maximum power point (MPP) that the PV module can generate and the system should work at this point to achieve the best performance of the PV system. Therefore, there is only one operating point with a maximum power point under particular conditions by each PV module, being the power only maximum for a precise output voltage, [8]. Thus, the MPP changes when the temperature and the irradiance changes as well.

The common grid-connected PV system consists of solar modules, a step-up DC/DC power converter, a DC/AC power converter and a control system, [9], Fig. 1. The PV system (solar modules and the DC/DC converter) can be connected to a load or can be interfaced to the electrical grid using a DC/AC inverter to inject a sinusoidal current in phase with the voltage of the electrical network.

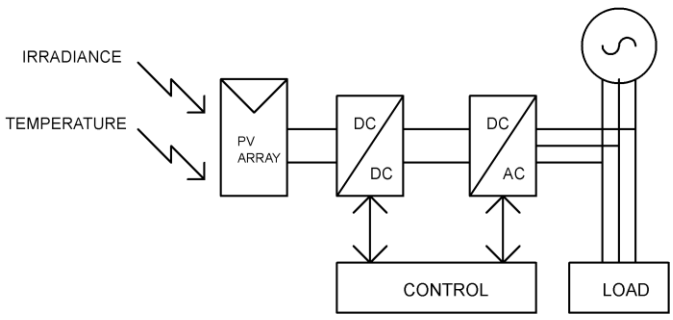

Fig. 1. Grid-connected PV system

The DC/DC power converter aim is to regulate the PV panel output voltage to stay in its maximum power point (MPP), [10]. For that, a DC voltage level variation is achieved through the use and control of the switching devices. The DC/DC converters consist of electronic circuits that control the energy charge and discharge in their storage passive components, i. e. the switching device changes between ON and OFF to accomplish the desired voltage modifying the duty cycle of the DC/DC converter, [11]. There are different topologies of DC/DC power converters, [12]. The most usual types are the buck converter that decreases the output voltage with respect the input voltage, the boost converter that provides an output voltage higher than the input voltage and, the buck-boost converter that it is able to increase or decrease the output voltage. These DC/DC converters can work in two operation modes, the continuous conduction mode (CCM) or the discontinuous conduction mode (DCM), [11]. In CCM, the current flows continuously through the inductor. In DCM, the inductor current is zero for a portion of the switching cycle.

Besides, a control strategy is designed to obtain maximum power transfer under any environmental conditions to operate the PV panel in the MPP. There are different maximum power point tracking (MPPT) algorithms, [13], to reach the MPP, [10]. The algorithms calculate the MPP in each instant of time for any irradiance and temperature. The maximum power point is changing due to the fact that the environmental conditions are continuously modifying. The most used algorithm is the well-known Perturb and Observe (P&O) method, [10], [14]-[15]. The P&O algorithm is based on the variation of the PV output voltage and on the observation of the power obtained to modify the duty cycle of the DC/DC power converter to reach the maximum power. In this case, the output power achieves the equilibrium point (the maximum power) but it has an oscillatory behavior and that point is not always achieved. Therefore, a local maximum could be obtained instead of a global one. Another control technique frequently used is the proportional and integral method (PI), [16]. This control is easy to implement and it has to control the buck-boost converter input voltage to set it at the reference voltage that gives the maximum power. There are several other algorithms; some of them are shown next. The Incremental Conductance, [17]-[19], is based on the fact that the power derivative with respect to the voltage is zero in the maximum power point. This peak can be reached comparing the instantaneous conductance with the incremental conductance. Depending on that result, the duty cycle of the DC/DC power converter is increased or decreased. Similar to the P&O algorithm, this method has an oscillatory behavior in stationary regimen. The Fractional Open Circuit Voltage, [20]-[21], and the Fractional Short Circuit Current, [22]-[23], are two similar techniques. The first one achieves the voltage that supplies the maximum power taking into account that this voltage is proportional to the open circuit voltage under any irradiance and temperature whereas the second algorithm calculates the maximum power point current where this current is proportional to the short circuit current for any environmental conditions. The disadvantages of these methods are that the real MPP are not obtained; only it is achieved approaches and the DC/DC converter has to be disconnected to measure in some points. Another MPPT algorithm used is the Ripple Correlation Control (RCC), [24]-[25], and it relates the power change (the time derivative of the power) with the voltage or current change (voltage or current derivative) to lead the power gradient to zero, obtaining the MPP modifying the duty

cycle of the DC/DC converter. The RCC uses the slight perturbations of high frequency generated by the inherent ripple in any switching power converter. There are also MPP trackers based on Artificial Neural Networks, [26]-[27], and Fuzzy Logic, [28]-[29]. The artificial neuronal network has a better performance but presents an involved structure, whereas fuzzy logic control does not need a mathematical model. It can even be used Neuro-Fuzzy Systems with Fuzzy Logic Controllers MPPT algorithms, [30]-[31]. In this case, the control used a neuro-fuzzy system to find the voltage that supplies the maximum power point and a fuzzy control to achieve the reference voltage given by the neuro-fuzzy system. One of the advantages of this method is that there is no need for mathematical equations and it can work with non-linear systems; however, it is essential to adjust the control after the simulation because the fuzzy logic uses reasoning that are approximates but not exacts. Another technique is the Sliding Mode control, [10], [32]-[33]. A control equation which forces the variables of the system to be in a sliding surface must be implemented. The sliding surface or switching surface is chosen and then a control law should be found in order to guarantee the existence of the sliding mode. This surface regulates the DC/DC converter output voltage adjusting the duty cycle. All these algorithms have different accuracy and complexity, some of them can obtain local maximum instead of global ones and others have involved structures.

Conventional MPPTs are able to reach the maximum power point under standard conditions. However, some problems can appear in PV systems such as mismatch losses that lead to obtain several maxima in P-V curves and the former MPPT algorithms fail to achieve the MPP. The mismatch concern is one of the main causes of losses in the power extraction from PV systems. The mismatch losses are originated from the interconnection of solar cells under different conditions or solar cells that do not have the same properties, [34]. Therefore, the solar cell under the worst condition, i. e. the one that supplies the lowest energy, determines the PV array global output power. There are various types of mismatch losses, such as in short-circuit current or in open-circuit voltage. The most common and damaging kind is the short-circuit current because it is caused by the partial shading of the solar module, [35]-[36]. The reasons of the existence of partial shading are the shadows originated from adjacent buildings, trees, moving clouds or even fast changes in the irradiance. Under partial shading conditions, a PV module is exposed to different values of irradiance and the shaded cells absorb the energy supplied by the unshaded cells that are exposed to higher irradiance leading to highly localized power dissipation and converting this power into heat. Thus, the power generated by the partially shaded modules is much lower than the energy generated by unshaded PV cells. This may be detrimental to the PV modules and the performance of the PV system is seriously deteriorated, being this effect widely studied, [37]-[40]. To solve one of these problems, bypass diodes are connected across the solar modules, [41]-[42], in order to prevent the shaded modules from consuming the power generated by the unshaded PV modules. Therefore, the current flows through an alternative path when there are shaded solar cells. As a consequence of the use of bypass diodes, the PV array I-V and P-V characteristic curves can present multiple power peaks under non-uniform irradiance, complicating the tracking of the maximum power point, [43]-[45]. Therefore, conventional MPPT algorithms are ineffective because they are not able to distinguish local maxima from the global maximum. Lately, different MPPT methods have

been modified in order to improve the tracking of the MPP, [46], such as the Perturb and Observe (P&O) algorithm or hill climbing, [47]-[48], the incremental conductance method, [49], the neural network method, [50]-[52], fuzzy logic controllers, [53]-[54], or the differential evolution of particle swarm optimization (DEPSO), [55]-[56]. Other methods are focused on the measurement of the PV array open-circuit voltage and short-circuit current or the irradiance, [57]-[59], amongst others, [60]-[61].

Grid-connected PV systems require DC/AC converters to connect the system to the power grid, [62]-[64]. The DC/AC power converters or inverters can be three-phase or single-phase. The DC/AC converters aim is to transfer the maximum active power to the network in PV systems. The inverters are controlled to inject nearly sinusoidal currents (to reduce harmonic distortion) in phase with the electrical grid, [65]-[66]. The DC/AC converters consist of a control circuit to calculate the reference current and a power circuit to follow this reference and to inject the final current to the network. The power circuit includes transistors devices to obtain the desired AC output with a specific sequence of transistors commutation. The converter output voltage will be supplied to a load or to the electrical network. In order to inject power to the electrical network, the DC/AC power inverter of the PV system has to be controlled, [67]. The most usual control is the proportional and integral control, [68]. The objective of the inverter control is to inject current co-linear with the voltage in the point of common connection and to keep constant the DC/AC converter input voltage (or the DC/DC converter output voltage). Therefore, a hysteresis current controlled 3-phase inverter (constant power) can be used [69]-[70] to inject all the PV array power into the grid.

When the number of needed PV panels is large, shadowing in some panels strongly reduces the overall power output. Given that individual PV panels usually output a few hundred watts, for most applications it is desirable to seek for a distributed PV architecture in which each PV panel has its own DC/DC converter to locally optimize the MPP even considering partial shadowing, ageing or different operating conditions, [10],[71]. The distributed DC/DC converter outputs are then connected in parallel to feed a load or the grid through one or several distributed inverters (DC microgrid connected to an AC grid). The distributed option ensures higher reliability concerning converter failures or ageing in the converter modules or solar panels, and their smaller individual DC capacitors can be chosen to ensure extended lifetimes. Thus, combining solar modules in series and in parallel creates PV panels able to supply power to help shave midday peaks of grid power consumption of centralized energy as renewable distributed energy resources (DER) using smart-grid-connected PV systems. The distributed energy resource operated within the electrical power self-consumption concept, [72]-[73], where each electricity costumer should be given the possibility to connect a PV system able to produce the energy corresponding to the costumer average consumption. This energy could be used in the producer-consumer (prosumer) site and the short term available surplus injected in the electrical grid. In this case the prosumer receives a payment for the excess electricity generated regarding the amount consumed within a billing period, [74]-[75]. PV systems are advantageous for the smart-grid concept as they can supply or store the extra power during the midday peak power consumption hours, while the prosumer can rely on storage solution or grid electricity during sunless hours, leveling the centralized injected grid power. Therefore, the self-consumption can aid in the

peak-shaving strategy of AC smart-grids. It is well suited for telecommunications applications since telecom apparatus power consumption is roughly constant, [76].

1.2 Objectives

In this work, a PV system containing the PV modules, the DC/DC converter, the DC/AC converter, the load and the control system is modeled in Matlab-Simulink. Once the simulation is validated, then an experimental platform is required to verify the proposed methods.

First of all, the I – V and the P – V curves must be obtained to know the optimum point where the system should operate. Thus, the characteristic curves are achieved in simulation and then they are compared with the experimental curves to prove the validity of the system.

Afterwards, a DC/DC power converter is used in order to control the PV output voltage. A buck-boost (step-up/down) DC/DC converter, [11], connected to the solar modules output is chosen because it converts the DC power from one voltage level to another higher or lower to the input voltage according to the requirements. An adequate control of the DC/DC converter duty cycle allows the converter voltage input to obtain the appropriate value to reach the MPP. In this work, a platform has been designed including a built buck-boost converter to carry out the experiments, using a low-cost microcontroller whereas other works employ acquisition & control commercial boards, [77]-[79].

The buck-boost requires to be controlled to obtain the MPP. Two basic algorithms are developed, the P&O algorithm and the PI control to reach the maximum peak and compare these technique with the proposed algorithm in this work. Another algorithm is developed, the neuro-fuzzy system. The neuro-fuzzy system calculates the reference of PV output voltage and a fuzzy logic control loop reaches the MPP. Then, due to the oscillatory behavior of the P&O method and the required processing time of advanced MPPT algorithms, a non-linear control method is proposed in this work to achieve the maximum power point, the backstepping control, [80]-[81]. The backstepping method guarantees robust operation and asymptotic stability by means of Lyapunov functions. A nonlinear control has been chosen due to the nonlinear, time variant nature and variable structure of the buck-boost converter. Thus a linear control implies a model linearization that is simple but it cannot control the converter in a wide range. In this case, the backstepping controller regulates the PV array output voltage (or the buck-boost input voltage) through the duty cycle of the DC/DC converter so as to reach the maximum power point under any environmental conditions. Besides, an off-line calculated regression plane is used to obtain the PV array output reference voltages that supply the MPPs for different irradiance and temperature values in order to make the control initially faster. Besides, an adaptive backstepping controller is also proposed, [82]. In this case, this control is based on the fact that the values of the inductor and the capacitor of the buck-boost converter are unknown or have variations due to the ageing. The advantage of this method is that the control can be used for buck-boost converters regardless of the parameter values because it has a learning

capacity to solve the model uncertainty by means of an on-line estimation of the unknown or changeable parameters.

In partial shading conditions, a new method using artificial vision to track the maximum power in real time is proposed for the first time to detect the number of solar cells that are affected by partial shading and the intensity of the shadows. Webcams are commonly used in PV power plants as surveillance systems and this new control can take advantage of this use to include them in the PV system. The webcam should point to the solar modules that are series-connected in this work. Artificial vision is commonly used in many real-time applications such as tracking systems to detect vehicles or even people, surveillance, military missions, video communication or videogames, [83]-[85]. In this case, this technique is used to identify the solar cells partial shading in a robust and fast way, detecting the changes of shape and intensity of the shadows in real time.

Regarding the DC/AC power converters, instead of using linear PI compensators to regulate the DC grid voltage at the input of the inverter to inject sinusoidal currents to the grid, [86]-[87], the backstepping method is proposed in this work to generate original and new controllers for the DC/AC converter considering the single-phase converter slow and fast dynamics, [88]-[90]. Dynamics separation is needed as the grid power injected/retrieved by an inverter is not constant during a grid period. The backstepping controller ensures stable and robust operation as an inverter (minimum phase system) or as a rectifier (non-minimum phase system), being also able to cope with the AC grid voltage variations and microgrid operating modes, [91]. Therefore, the advantages of backstepping controllers are related to the use of the converters model direct dynamics, and Lyapunov functions to guarantee the stability and robustness of the system, [92], therefore enhancing the system performance.

In addition, the control of the DC/AC power inverter of the PV system has been also designed to compensate the harmonics, the reactive power and unbalanced loads of the electrical system, [93]-[94], using a strategy based on a modified vectorial theory, [95]. Thus, the global control makes possible to extract the maximum power of the PV system, to compensate the non-linear and unbalanced loads of the electrical system and to regulate the input voltage of the DC/AC power inverter. This way, the Power Quality (PQ) of the electrical network is improved, [96]-[97]. Then, the global system is called PV active power line conditioner. Besides, in the shunt active power filter for the non-linear loads compensation, a switching output reactance has been designed to improve the conditioner tracking when it works with variables non-linear loads. Finally, two quality indices are proved in an experimental distribution network to test the validity of them. The indices are the Load Characterization Index (LCI) that identifies linear and non-linear loads in power systems and the Unbalance Current Ratio (UCR) that assigns responsibility for system unbalance to load and source sides, [98]-[99].

Another application of the system is when there is excess PV energy during sun hours. This energy can also be used to shave the smart-grid consumption peaks in the evening if back-up storage batteries are used. Thus, in this work, the DC/AC converter must operate as an inverter or as a unity power factor rectifier (reversible operation) depending on a telecom load power requirement, on the PV panel power generated and on the

telecom/battery load needs, [100]. During the hours where the telecom application requires more power than the PV system can generate the DC/AC converter works as a rectifier, to complement the PV panel that cannot produce the needed power due to low irradiance levels. At midday hours, the excess power produced by the PV panels can be used to recharge the back-up battery or be injected in the grid after battery recharge, the DC/AC converter working as an inverter. Additionally, if there is a fault in the grid, leading to voltage sag, the PV panel and battery of this hybrid power system will continue to power the load that will not be affected by the sag.

Therefore, the objectives of the thesis are summarized:

- Modeling a grid-connected PV system in Matlab-Simulink.
- Obtaining an experimental platform to validate the performance of the proposed control methods. In this case, a buck-boost converter has been built.
- Obtaining I – V and P – V characteristic curves.
- Designing a non-linear control for the buck-boost converter. In this case, two controllers are proposed, the backstepping controller and the adaptive backstepping controller.
- Designing a MPPT algorithm under partial shading conditions, proposing a novel artificial vision maximum power point tracking method.
- Designing a non-linear control for the DC/AC converter, the backstepping control.
- Obtaining additional applications of the PV system in relation with the power quality: proposing a PV active power line conditioner to transfer the maximum energy and to compensate the non-linear and the unbalanced loads, testing two power quality indices and designing a variable reactance to improve the shunt active filter reference tracking.
- Controlling the DC/AC converter operating as inverter or rectifier when it works under the concept of smart-grid consumption with telecom equipment.

1.3 Organization

This Doctoral thesis is organized according to the directives given by the University of Huelva for a paper compendium thesis. This chapter (Chapter 1) presents the objectives of the proposed research work, the introduction, the state of the art and references. In Chapter 2 is described the photovoltaic system, i. e. the solar modules, the DC/DC converter and the DC/AC converter, the maximum power point tracking algorithms, the experimental platform and the control of PV systems under partial shading conditions. Chapter 3 presents the thesis contributions. The first contribution describes the proposed non-linear backstepping control to track the maximum power point in PV systems to provide energy to a DC load (JCR journal paper, paper 1) in simulation in Matlab-Simulink. The second contribution presents the previous backstepping controller in an experimental platform, with a built buck-boost converter (JCR journal paper, paper 2). The third contribution shows the DC/DC converter and the DC/AC converter controlled using the non-linear backstepping control in an experimental platform (JCR journal paper, paper 3). In this case, a smart grid-

connected distributed photovoltaic system supplies power to telecom equipment. Next contribution number (International conference paper, paper 4) presents the adaptive backstepping control to track the maximum power point of PV systems in a simulation platform whereas contribution number 5 shows a comparative between different MPPT algorithms (International conference paper, paper 5). Another contribution (JCR journal paper, paper 6) shows an assessment of power quality indexes in an experimental distribution network in relation to the future work. Besides, a DC/AC converter operating as inverter and shunt active power filter in PV systems in a simulation platform is presented in contribution number 7 (International conference paper, paper 7). Finally, the last contribution shows the improvement of shunt active power filter compensation through switching output reactances in relation to the power quality work (International conference paper, paper 8). Chapter 4 describes the results and the conclusion and Chapter 5 presents the conclusion and a summary in Spanish.

References:

[1] K. S. Krishna, K. S. Kumar, "A review on hybrid renewable energy systems," *Renewable and Sustainable Energy Reviews*, vol. 52, pp. 907-916, Dec. 2015.

[2] C. L. T. Borges, "An overview of reliability models and methods for distribution systems with renewable energy distributed generation," *Renewable and Sustainable Energy Reviews*, vol. 16, no. 6, pp. 4008-4015, Aug. 2012.

[3] M. B. Shadmand, R. S. Balog, "Multi-objective optimization and design of photovoltaic-wind hybrid system, for community smart DC microgrid," *IEEE Transactions on Smart Grid*, vol. 5, no. 5, pp. 2635-2643, Sept. 2014.

[4] M. Buresch, "Photovoltaic Energy Systems Design and Installation", McGraw-Hill, New York, 1983.

[5] I. H. Altas and A.M. Sharaf, "A Photovoltaic Array Simulation Model for Matlab-Simulink GUI Environment," IEEE ICCEP'07, pp. 341-345, May 2007.

[6] S. S. Inamdar, A. P. Vaidya, "Performance analysis of solar photovoltaic module for multiple varying factors in Matlab/Simulink," *in ICSTM*, pp. 562-567, Chennai, May 2015.

[7] M. L. Florea, A. Baltatanu, "Modeling photovoltaic arrays with MPPT perturbe & observe algorithm," in *2013 8th International Symposium on ATEE*, pp. 1-4, Bucharest, May 2013.

[8] Y. Tian, B. Xia, Z. Xu, W. Sun, "Modified asymmetrical variable step size incremental conductance maximum power point tracking method for photovoltaic systems," Journal *of Power Electronics*, vol. 14, no. 1, pp. 156-164, Jan. 2014.

[9] R. J. Wai, W. H. Wang, "Grid-connected photovoltaic generation system," *IEEE Transactions on Circuits and Systems I: Regular Papers*, vol. 55, no. 3, pp. 953-964, Ap. 2008.

[10] Power Electronics and Control Techniques for Maximum Energy Harvesting in Photovoltaic Systems, Nicola Femia, Giovanni Petrone, Giovanni Spagnuolo, Massimo Vitelli, CRC Press, 2013.

[11] Muhammad Rashid et al, *Power Electronics Handbook*, 3rd, Butterworth Heinemann, Elsevier, 2011.

[12] J. Enrique, E. Durán, M. de-Cardona, J. Andújar, "Theoretical assessment of the 18 maximum power point tracking efficiency of photovoltaic facilities with different 19 converter topologies," *Solar Energy*, vol. 81, no. 1, pp. 31-38, Jan. 2007.

[13] T. Esram, P.L. Chapman, "Comparison of photovoltaic array maximum power point tracking techniques," *IEEE Transactions on Energy Conversion*, vol. 22, no. 2, pp. 439-449, June 2007.

[14] M. A. Elgendy; B. Zahawi; D. J. Atkinson, "Evaluation of perturbe and observe MPPT algorithm implementation techniques," in *PEMD*, pp. 1-6, 2012.

[15] J. Ahmed, Z. Salam, "An improved perturb and observe (P&O) maximum power point tracking (MPPT) algorithm for higher efficiency," *Applied Energy*, vol. 150, pp. 97-108, July 2015.

[16] T. Y. Sea, J. S. Ka, C. U. Lee, D. H. Chung, "MPPT performance improvement of PV system using Hybrid-PI controller", in *13th ICCAS*, pp. 434-436, Oct. 2013.

[17] P. Sivakumar, A. A. Kader, Y. Kaliavaradhan, M. Arutchelvi, "Analysis and enhancement of PV efficiency with incremental conductance MPPT technique under non-linear loading conditions," *Renewable Energy*, vol. 81, pp. 543-550, Sep. 2015.

[18] H. Kumar, R. K. Tripathi, "Simulation of variable incremental conductance method with direct control method using boost converter," in *SCES*, pp. 1-5, Uttar Pradesh, Mar. 2012.

[19] K. Visweswara, "An investigation of incremental conductance based maximum power point tracking for photovoltaic system," *Energy Procedia*, vol. 54, pp. 11-20, 2014.

[20] Y. P. Huang, "A rapid maximum power measurement system for high-concentration photovoltaic modules using the fractional open-circuit voltage technique and controllable electronic load," *IEEE Journal of Photovoltaics*, vol. 4, no. 6, pp. 1610-1617, Nov. 2014.

[21] A. Ramasamy, N. S. Vanitha, "Maximum power tracking for PV generating system using novel optimized fractional order open circuit voltage – FOINC method," in *ICCCI*, pp. 1-6, Coimbatore, Jan. 2014.

[22] H. A. Sher, A. F. Murtaza, A. Norman, K. E. Addoweesh, K. Al-Haddad, M. Chiaberge, "A new sensorless hybrid MPPT algorithm bases on fractional short-circuit current measurement and P&O MPPT," *IEEE Transactions on Sustainable Energy*, vol. 4, no. 6, pp. 1-9, July 2015.

[23] A. Sandali, T. Oukhoya, A. Cheriti, "Modeling and design of PV grid connected system using a modified fractional short-circuit current MPPT," in *IRSEC*, pp. 224-229, Ouarzazate, Oct. 2014.

[24] T. Esram, J.W. Kimball, P.T. Krein, P.L. Chapman, P. Midya, "Dynamic maximum power point tracking of photovoltaic arrays using ripple correlation control," *IEEE Transactions on Power Electronics*, vol. 21, no. 5, pp. 1282-1291, Sept. 2006.

[25] C. Barth, R. C. N. Pilawa-Podgurski, "Dithering digital ripple correlation control for photovoltaic maximum power point tracking," *IEEE Transactions on Power Electronics*, vol. 30, no. 8, pp. 4548-4559, Aug. 2015.

[26] R. Ramaprabha, B. L. Mathur, M. Sharanya, "Solar Array Modeling and Simulation of MPPT using Neural Network ," in *Int. Conf. on Control, Automation, Communication and Energy Conservation*, pp. 1-5, 2009.

[27] M. A. Islam, M. A. Kabir, "Neural network based maximum power point tracking of photovoltaic arrays," in *IEEE TENCON*, pp. 79-82, Bali, Nov. 2011.

[28] A. El Khateb, N. A. Rahim, J. Selvarai, M. N. Uddin, "Fuzzy-logic-controller-based SEPIC converter for maximum power point tracking," *IEEE Transaction on Industry Applications*, vol. 50, no. 4, pp. 2349-2358, July 2014.

[29] B. Bendib, F. Krim, H. Belmili, M. F. Almi, S. Boulouma, "Advanced fuzzy MPPT controller for a stand-alone PV system," *Energy Procedia*, vol. 50, pp. 383-392, 2014.

[30] A. Chaouachi, R. M. Kamel, K. Nagasaka, "A novel multi-model neuro-fuzzy based MPPT for three-phase grid-connected photovoltaic system," *Solar Energy*, vol. 84, no. 12, pp. 2219-2229, Dec. 2010.

[31] A. A. Kulaksiz, O. Aydogdu, "ANN-based maximum power point tracking of photovoltaic system using fuzzy controller," in *INISTA*, pp. 1-5, Trabzon, July 2012.

[32] E. Bianconi, J. Calvente, R. Giral, E. Mamarelis, G. Petrone, C. A. Ramos-Paja, G. Spagnuolo, M. Vitelli, "A fast current-based MPPT technique employing sliding mode control," *IEEE Transactions on Industrial Electronics*, vol. 60, no. 3, pp. 1168-1178, Mar. 2013.

[33] E. Mamarelis, G. Petrone, G. Spagnuolo, "Design of a sliding-mode-controlled SEPIC for PV MPPT applications," *IEEE Transactions on Industrial Electronics*, vol. 61, no. 7, pp. 3387-3398, July 2014.

[34] A. Mäki, S. Valkealahti, "Power losses in long string and parallel-connected short strings of series-connected silicon-based photovoltaic modules due to partial shading conditions," *IEEE Transactions on Energy Conversion*, vol. 27, no. 1, pp. 173-183, March 2012.

[35] E. V. Paraskevadaki, S. A. Papathanassiou, "Evaluation of MPP voltage and power of mc-Si PV modules in partial shading conditions," *IEEE Transactions on Energy Conversion*, vol. 26, no. 3, pp. 923-932, Sept. 2011.

[36] R. Ramaprabha, B. L. Mathur, "Impact of partial shading on solar PV module containing series connected cells," *International Journal of Recent Trends in Engineering*, vol. 2, no. 7, pp. 56-60, Nov. 2009.

[37] M. Z. S. El-Dein, M. Kazerani, M. M. A. Salama, "Optimal photovoltaic array reconfiguration to reduce partial shading losses," *IEEE Transactions on Sustainable Energy*, vol. 4, no. 1, pp. 145-153, Jan. 2013.

[38] P. Bakas, A. Marinopoulos, B. Stridh, "Impact of PV module mismatch on the PV array energy yield and comparison of module, string and central MPPT," in *38th IEEE PVSC*, Austin, Tx., 2012, pp. 1393-1398.

[39] M.C. Alonso-García, J.M. Ruiz, F. Chenlo, "Experimental study of mismatch and shading effects in the I–V characteristic of a photovoltaic module," *Solar Energy Materials & Solar Cells*, vol. 90, no. 3, pp. 329-340, Feb. 2006.

[40] J. D. Bastidas, C. A. Ramos-Paja, E. Franco, G. Spagnuolo, G. Petrone, "Modeling of photovoltaic fields in mismatching conditions by means of inflection voltages," in *WEA*, Bogota, 2012, pp. 1-6.

[41] S. Silvestre, A. Boronat, A. Chouder, "Study of bypass diodes configuration on PV modules," *Applied Energy*, vol. 86, no. 9, pp. 1632-1640, Sept. 2009.

[42] H. Zhenga, S. Lia, R. Challoob, J. Proanoa, "Shading and bypass diode impacts to energy extraction of PV arrays under different converter configurations," *Renewable Energy*, vol. 68, pp. 58-66, Aug. 2014.

[43] H. Patel, V. Agarwal, "MATLAB-based modeling to study the effects of partial shading on PV array characteristics," *IEEE Transactions on Energy Conversion*, vol. 23, no. 1, pp. 302-310, March 2008.

[44] Y. Yi, J. Sheng-lan, G. Hai-qin, C. Juan, "Simulation study on characteristics of photovoltaic array under partial shading," in *33rd Chinese Control Conference*, Nanjing, 2014, pp. 6992-6997.

[45] K. Ding, X. G. Bian, H. H. Liu, T. Peng, "A MATLAB-Simulink-based PV module model and its application under conditions of nonuniform irradiance," *IEEE Transactions on Energy Conversion*, vol. 27, no. 4, pp. 864-872, Dec. 2012.

[46] Y. H. Liu, J. H. Chen, J. W. Huang, "A review of maximum power point tracking techniques for use in partially shaded conditions," *Renewable and Sustainable Energy Reviews*, vol. 41, pp. 436-453, Jan. 2015.

[47] K. Chen, S. Tian, Y. Cheng, L. Bai, "An improved MPPT controller for photovoltaic system under partial shading condition," *IEEE Transactions on Sustainable Energy*, vol. 5, no. 3, pp. 978-985, July 2014.

[48] X. Weidong, W. G. Dunford, "A modified adaptive hill climbing MPPT method for photovoltaic power systems," in *IEEE PESC*, 2004, vol. 3, pp. 1957–1963.

[49] K. S. Tey, S. Mekhilef, "Modified incremental conductance algorithm for photovoltaic system under partial shading conditions and load variation," *IEEE Transactions on Industrial Electronics*, vol. 61, no. 10, pp. 5384-5392, Oct. 2014.

[50] S. A. Rizzo, G. Scelba, "ANN based MPPT method for rapidly variable shading conditions," *Applied Energy*, vol. 145, pp. 124-132, May 2015.

[51] K. Punitha, D. Devaraj, S. Sakthivel, "Artificial neural network based modified incremental conductance algorithm for maximum power point tracking in photovoltaic system under partial shading conditions," *Energy*, vol. 62, pp. 330-340, Dec. 2013.

[52] M. Karakose, M. Baygin, K. S. Parlak, "A new real-time reconfiguration approach based on neural network in partial shading for PV arrays," in *3rd ICRERA*, Milwakuee, pp. 633-637, 2014.

[53] C. Cecati, F. Ciancetta, and P. Siano, "A multilevel inverter for photovoltaic systems with fuzzy logic control," *IEEE Transactions on Industrial Electronics*, vol. 57, no. 12, pp. 4115–4125, Dec. 2010.

[54] P. C. Sekhar, S. Mishra, "Takagi-Sugeno fuzzy-based incremental conductance algorithm for maximum power point tracking of a photovoltaic generating system," *IET Renewable Power Generation*, vol. 8, no. 8, pp. 900-914, Nov. 2014.

[55] K. Ishaque, Z. Salam, A. Shamsudin, M. Amjad, "A direct control based maximum power point tracking method for photovoltaic system under partial shading conditions using particle swarm optimization algorithm," *Applied Energy*, vol. 99, pp. 414-422, Nov. 2012.

[56] M. Seyedmahmoudian, R. Rahmani, S. Mekhilef, A. M. T. Oo, A. Stojcevski, T. K. Soon, A. S. Ghandhari, "Simulation and hardware implementation of new maximum power point tracking technique for partially shaded PV system using hybrid DEPSO method," *IEEE Transactions on Sustainable Energy*, vol. 6, no. 3, pp. 850–862, July 2015.

[57] A. A. Bayod-Rujula, J. A. Cebollero-Abian, "A novel MPPT method for PV systems with irradiance measurement," *Solar Energy*, vol. 109, pp. 95-104, Nov. 2014.

[58] S. Silvestre, S. Kichou, A. Chouder, G. Nofuentes, E. Karatepe, "Analysis of current and voltage indicators in grid connected PV (photovoltaic) systems working in faulty and partial shading conditions," *Energy*, vol. 86, pp. 42-50, June 2015.

[59] M. E. Nezhad, B. Asaei, S. Farhangi, "Modified analytical solution for tracking photovoltaic module maximum power point under partial shading condition," in *13th EEEIC*, Wroclaw, 2013, pp. 182-187.

[60] N. A. Ahmed, M. Miyatake, "A novel maximum power point tracking for photovoltaic applications under partially shaded insolation conditions," *Electric Power System Research*, vol. 78, pp. 777–784, May 2008.

[61] N. Hashim, Z. Salam, S. M. Ayob, "Maximum power point tracking for stand-alone photovoltaic system using evolutionary programming," *IEEE 8th International PEOCO*, pp. 7-12, Langkawi, Mar. 2014.

[62] X. Yu, C. Cecati, T. Dillon, and M.G. Simões, "The new frontier of smart grids: an industrial electronics perspective," *IEEE Industrial Electronics Magazine*, vol. 5, no. 3, pp. 49-63, Sep. 2011.

[63] P. P. Dash, M. Kazerani, "Dynamic modeling and performance analysis of a grid-connected current-source inverter-based photovoltaic system," *IEEE Transactions on Sustainable Energy*, vol. 2, no. 4, pp. 443-450, May 2011.

[64] G.-K. Hung, C.-C. Chang, C.-L. Chen, "Automatic phase-shift method for islanding detection of grid-connected photovoltaic inverters," *IEEE Transactions on Energy Conversion*, vol. 18, no. 1, pp. 169-173, Mar. 2003.

[65] J. M. Shen, H. L. Jou, J. C. Wu, K. D. Wu, "Five-level inverter for renewable power generation system," *IEEE Transactions on Energy Conversion*, vol. 28, no. 2, pp. 257-266, June 2013.

[66] N. Lekgamheng, Y. Kumsuwan, "Power analysis of single-phase grid-connected photovoltaic systems based on two-stage current source converters," in *ECTICON*, pp. 1-4, Phetchaburi, May 2012.

[67] A. Luo, Y. Chen, Z. Shuai, C. Tu, "An improved reactive current detection and power control method for single-phase photovoltaic grid-connected DG system," *IEEE Transactions on Energy Conversion*, vol. 28, no. 4, pp. 823-831, Dec. 2013.

[68] S. Minaei, E. Yuce, S. Tokat, O. Cicekoglu, "Simple Realizations of Current-Mode and Voltage-Mode PID, PI and PD Controllers," in *ISIE*, vol. 1, pp. 195-198, June 2005.

[69] R. Davoodnezhad, D. G. Holmes, B. P. McGrath, "A novel three-level hysteresis current regulation strategy for three-phase three-level inverters," *IEEE Transactions on Power Electronics*, vol. 29, no. 11, pp. 6100-6109, Nov. 2014.

[70] N. Prabhakar, M. K. Mishra, "Dynamic hysteresis current control to minimize switching for three-phase four-leg VSI topology to compensate nonlinear load," *IEEE Transactions on Power Electronics*, vol. 25, no. 8, pp. 1935-1942, Aug. 2010.

[71] A. Maki, S. Valkealahti, "Effect of photovoltaic generator components on the number of MPPs under partial shading conditions," *IEEE Transactions on Energy Conversion*, vol. 28 no. 4, pp. 1008-1017, Dec. 2013.

[72] R. Luthander, J. Widen, D. Nilsson, J. Palm, "Photovoltaic self-consumption in buildings: A review," *Applied Energy*, vol. 142, pp. 80-94, Mar. 2015.

[73] M. Castillo-Cagigal, A. Gutierrez, F. Monasterio-Huelin, E. Caamaño-Martin, D. Masa, J. Jimenez-Leube, "A semi-distributed electric demand-side management system with PV generation for self-consumption enhancement," *Energy Conversion and Management*, vol. 52, no. 7, pp. 2659-2666, July 2011.

[74] SELF CONSUMPTION OF PV ELECTRICITY - Position Paper, July 2013, Epia org, http://www.epia.org/fileadmin/user_upload/Position_Papers/Self_and_direct_consumption_-_position_paper_-_final_version.pdf.

[75] Enabling The European Consumer To Generate Power For Self-Consumption, SunEdison, November 2011, http://www.sunedison.com/wps/wcm/connect/35bfb52a-ec27-4751-8670-fe6e807e8063/SunEdison_PV_Self-consumption_Study_high_resolution_%2813_Mb%29.pdf?MOD=AJPERES.

[76] X. Ren, Z. Tang, X. Ruan, J. Wei, and G. Hua, "Four switch buck-boost converter for telecom DC/DC power supply applications," *in 23rd Annual IEEE APEC*, pp. 1527-1530, Feb. 2008.

[77] J. Zeng, W. Qiao, L. Qu, "A single-switch isolated DC/DC converter for photovoltaic systems," in *ECCE*, pp. 3446-3452, 2012.

[78] P. Pichlik, J. Zdenek, "Converter regulation of stand-alone photovoltaic system at low solar radiation," in *AE*, pp. 207-210, 2012.

[79] A. Daoud, A. Midoun, "Simulation and Experimental Study of Maximum Power Point Tracker Based on a DC/DC Buck Converter," *Int. Review of Electrical Engineering*, vol. 5, no. 2, pp. 514-520, Ap. 2010.

[80] K. Ezal, Z. Pan, P. V. Kokotovic "Locally optimal and robust back-stepping design," *IEEE Transactions on Automatic Control*, vol. 45, no. 2, pp. 260-271, Feb. 2000.

[81] R.A. Freeman, P. V. Kokotovic, "Tools and procedures for robust control of nonlinear systems," in *33rd IEEE Conference on Decision and Control*, vol. 4, pp. 3458-3463, Nov. 2003.

[82] M. Krstic, I. Kanellakopoulos, P. V. Kokotovic, "Nonlinear design of adaptive controllers for linear systems," *IEEE Transactions on Automatic Control*, vol. 39, no. 4, pp. 738 -751, Ap. 1994.

[83] S. L. Ching, M. Sabudin, "Website image colour transformation for the colour blind," in *2nd ICCTD*, Cairo, 2010, pp. 255-259.

[84] F. Y. Shih, H. Wu, "Decomposition of geometric-shaped structuring elements using morphological transformations on binary images," in *11th Annual International Phoenix Conference on Computers and Communications*, Scottsdale, AZ, 1992, pp. 356-363.

[85] T. B. Nguyen, S. T. Chung, "An improved real-time blob detection for visual surveillance," in *2nd International CISP*, Tianjin, 2009, pp. 1-5.

[86] M. T. Benchouia, I. Ghadbane, A. Golea, K. Srairi, M. E. H. Benbouzid, "Implementation of adaptive fuzzy logic and PI controllers to regulate the DC bus voltage of shunt active power filter," *Applied Soft Computing*, vol. 28, pp. 125-131, Mar. 2015.

[87] A. A. A. Radwan, Y. A. R. I. Mohamed, E. F. El-Saadany, "Assessment and performance evaluation of DC-side interactions of voltage-source inverters interfacing

renewable energy systems," *Sustainable Energy, Grids and Networks*, vol. 1, pp. 28-44, Mar. 2015.

[88] B. R. Lin, S. C. Tsay, M. S. Liao, "Integrated power factor compensator based on sliding mode controller," *IEE Proceedings Electric Power Applications*, vol. 148, no. 3, pp. 237-244, May 2001.

[89] DC/AC Converters, N. Patin, Power Electronics Applied to Industrial Systems and Transports, vol. 2, pp. 35-100, 2015.

[90] S. K. Mazumder, A. H. Nayfeh, D. Boroyevich, "An investigation into the fast-and-slow-scale instabilities of a single phase bidirectional boost converter," *IEEE Transactions on Power Electronics*, vol. 18, no. 4, pp. 1063-1069, July 2003.

[91] X. Lu, J. M. Guerrero, K. Sun, J. C. Vasquez, R. Teodorescu, L. Huan, "Hierarchical Control of Parallel AC-DC Converter Interfaces for Hybrid Microgrids," *IEEE Transactions on Smart Grid*, vol. 5, no. 2, pp. 683-692, Mar. 2014.

[92] M. W. McConley, B. D: Appleby, M. A. Dahleh, E. Feron, "A computationally efficient Lyapunov-based scheduling procedure for control of nonlinear systems with stability guarantees," *IEEE Transactions on Automatic Control*, vol. 45, no. 1, pp. 33-49, Jan. 2000.

[93] H. Akagi, "Active harmonic filters," in *Proceedings of the IEEE*, vol. 93, no. 12, pp. 2128-2141, Dec. 2005.

[94] J.P. Macken, K. Vanthournout, J. Van den Keybus, G. Deconinck, R.J.M. Belmans, "Distributed control of renewable generation units with integrated active filter," *IEEE Transactions on Power Electronics*, vol. 19, no. 5, Sep. 2004.

[95] S. Khani, S. H. Hosseini, L. Mohammadian, "Application of the vectorial theory in PV-AF system for load supply and harmonic compensation with unbalanced and distorted supply voltages," in *ICEE*, pp. 1-6, Tehran, May 2011.

[96] S. Mekhilef, M. Tarek, N. A. Rahim, "Single-phase hybrid active power filter with adaptive notch filter for harmonic current estimation," *IETE Journal of Research*, vol. 57, no. 1, pp. 20-28, Jan. 2011.

[97] D. Masand, S. Jain, G. Agnihotri, "Control strategies for distribution static compensator for power quality improvement," *IETE Journal of Research*, vol. 54, no. 6, pp. 421-428, Nov. 2008.

[98] R. S. Herrera, J. R. Vazquez, "Identification of unbalanced loads in electric power systems," *International Transactions on Electrical Energy Systems*, vol. 24, no. 9, Sep. 2014.

[99] R. S. Herrera, P. Salmeron, "Harmonic disturbance identification in electrical systems with capacitor banks," *Electric Power System Research*, vol. 82, no. 1, pp. 18-26, Jan. 2012.

[100] X. Yizhe, Y.M. Chen, A. Q. Huang, "Five-level bidirectional converter for renewable power generation system," in *40th Annual Conference of the IEEE IECON*, pp. 5514-5519, Dallas, Oct. 2014.

[101] J. Muñoz, E. Lorenzo, "Capacitive load based on IGBTs for on-site characterization of PV arrays," *Solar Energy*, vol. 80, no. 11, pp. 1489–1497, 2006.

[102] Y. Shi, X. Yang, "Wide range soft switching PWM three-level DC-DC converters suitable for industrial applications," *IEEE Transactions on Power Electronics*, vol. 29, no. 2, pp. 603-616, Feb. 2014.

[103] G. Mallesham, S. Mishra, A. N. Jha, "Maiden application of Ziegler-Nichols method to AGC of distributed generation system," *IEEE PES PSCE'09*, pp. 1-7, Mar. 2009.

[104] M. I. El Adawy, M. E. Aboul-Wafa, H. A. Keshk, M. M. El Tayeb, "A SOFT-backspropagation algorithm for training neural networks," *19th National Radio Science Conference*, pp. 397-404, 2002.

[105] H. K. Khalil, Nonlinear systems, 3rd edition, Prentice Hall Upper Saddle River, NJ, 2002.

[106] R. Soler-Bientz, F. Gómez-Castro, L. Omar-Ricalde, "Developing a computational tool to assess shadow pattern on a horizontal plane, preliminary results," *35th IEEE PVSC*, pp. 2312-2317, June 2010.

[107] M. Cardador, "Maximum power point tracker of grid connected photovoltaic systems using matrix converters," M. S. EEC thesis, Universidade de Lisboa, Instituto Superior Técnico, June 2011.

[108] Electrónica Industrial, Fernando A. Silva, Fundaçao Calouste Gulbenkian, 2ª Ediçao, 2013.

[109] R. W. Wall, "Simple methods for detecting zero crossing," IEEE IECON, vol. 3 , pp. 2477-2481, Nov. 2003.

2 PV System and MPPT Algorithm

2.1 Introduction

A grid-connected PV system consists of PV modules, a DC/DC power converter, a DC/AC power converter, loads and a control system. The PV array is connected to the DC/DC converter to regulate the voltage level. Then, the DC/DC converter is connected to and inverter to transfer the energy to the electrical network. AC loads can be connected at the DC/AC converter output or DC loads can be connected between the DC/DC converter and the inverter. All of the devices that form the PV system are presented in this Chapter.

2.2 PV system

2.2.1 Solar Cell Model

A photovoltaic cell turns the light into electrical energy depending on the environmental conditions such as the irradiance and the temperature. That conversion is called the photovoltaic effect, which generates electromotive force when the solar cell surface is exposed to the sun light. A solar cell is basically a $p - n$ junction made with semiconductor material, such as silicon. This kind of material has an energy band where an electron can be excited to make it move to the conduction band or n region, creating a gap in the valence band or p region. Thus, an electric field is created joining two chemically treated silicon regions because one of the surfaces is doped to turn it into *n* region and the substrate is still a *p* region. The sun light is appropriate for the creation of the electron-hole pairs and when it is introduced into the solar cell, the photons break the pairs. Therefore, a potential difference is originated between the upper and bottom part of the solar cell and a current is generated.

The voltage provided by a photovoltaic cell is around 1 V and it is necessary to connect solar cells in series to create PV panels or modules to generate higher voltages. These modules can be connected in series and parallel to obtain the suitable power according to the needs of the users.

The equivalent electric circuit that represents a photovoltaic cell is shown in Fig. 2. Its model has a current source I_l that represents the current generated by the photons, in A. This value is constant when the irradiance and the temperature do not change. It also has an anti-parallel diode D_1 represented by saturation current I_o and the ideal factor η. Besides, two resistors have been added to include the losses. The series resistance R_s, in Ω, models the ohmic losses when the current goes through the semiconductor material and its value is increased by the number of solar cells connected to the system. The shunt electrical resistance R_{sh}, in Ω, represents the current leakage and its value is high. If an ideal photovoltaic cell is considered, R_s is zero and R_{sh} becomes infinite.

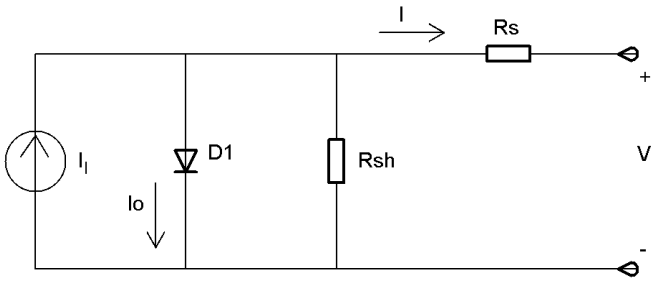

Fig. 2. PV cell equivalent circuit

The equation that relates I, the solar cell output current in A, to V, the solar cell output voltage, in V, is shown in (1).

$$I = I_l - I_o\left(e^{\frac{V+R_s I}{\eta V_T}} - 1\right) - \frac{V + R_s I}{R_{sh}} \tag{1}$$

I_l is the light generated current, in A, (2), and it is calculated using the surface of the cell in cm^2, the density of the short-circuit current J_{sc}, in A/cm^2, the working temperature T, in ºC, the temperature factor α_{JSC} in A/ºC cm^2 and the irradiance G in W/cm^2.

$$I_l = Area \cdot \left(J_{SC}\frac{G}{1000} + \alpha_{Jsc}(T - 27)\right) \tag{2}$$

I_o, (3), is the cell reverse saturation current, in A, where V_t is the thermal voltage, in V, the gap energy is E_g, in eV, the open circuit voltage is V_{oc}, in V and T_k is the temperature measured in K.

$$I_o = \frac{J_{SC} \cdot Area \cdot {T_k}^3 e^{-\frac{E_g}{V_t}}}{\left(e^{\frac{V_{oc}}{\eta V_t'}} - 1\right) 300^3 e^{-\frac{E_g'}{V_t'}}} \tag{3}$$

V_t is defined in equation (4), where K is the Boltzmann's constant, in J/K, and its value is 1.38×10^{-23}J/K and q is the charge of an electron, in C, with a value of 1.6×10^{-19} C. This equation is characterized for a temperature of 0 ºC, V_t'.

$$V_t = \frac{kT_k}{q}, \quad V_t' = V_t\big|_{T_k=300} \tag{4}$$

The gap energy, (5), depends, amongst other factors, on the temperature coefficient α_{gap} and the value of β_{gap}, for the characterized equation at 0 ºC for E_{go}, which is the gap

energy at 0 ºC and E_g' at 300K. The temperature coefficients are given by the percentage of change per temperature degree.

$$E_g = E_{go} - \frac{\alpha_{gap} T_k^{\,2}}{\beta_{gap} + T_k}, \quad E_g' = E_g\big|_{T_k=300} \tag{5}$$

In order to obtain the Kelvin temperature, (6), is used.

$$T_k = T + 273 \tag{6}$$

Some data provided by the manufacturers of the solar cells are required to characterize the photovoltaic modules under standard conditions. The parameters used for modeling the solar cells are shown in Table 1.

Table 1. Solar cell parameters

Parameter	**Value**
Area	39 cm^2
R_s	$10.5e^{-3}$ Ω
R_{sh}	1e4 Ω
V_{oc}	0.61 V
η	1.18
E_{go}	1.16 eV
α_{gap}	$7e^{-14}$ eV/K
β_{gap}	1100 K
J_{sc}	$28.16e^{-3}$ A/cm^2
α_{Jsc}	$30e^{-6}$ A/K cm^2

The method to accomplish the characteristic curves of the PV solar cells is the capacitive method. It must be taken into account that the capacitor that it is used as the load should have a high value because the loading time is directly proportional to the PV modules open circuit voltage and to its capacitance. Besides, it is inversely proportional to the short-circuit current and therefore the capacitance value must be high enough to let the capacitor discharge to obtain the characteristic curves of the PV system, current – voltage (I – V) and power – voltage (P – V). At the beginning of the measurement, the capacitor must be discharged and then it is charged. Then, the current decreased and the voltage increased while the capacitor is charging. Then, when the capacitor is charged, the PV cells output current is zero and it is obtained an open-circuit voltage. The value of the capacitor is related with the required measurement speed. Thus, if a high measurement speed is needed, the value of the capacitor should be lower.

2.2.2 PV Modules

Due to the low voltage that generates a unique solar cell, it is required to connect various PV cells depending on the voltage and current requirements of the electrical system where it is connected. The association of these solar cells makes a PV module. It is essential to connect solar cells in series and in parallel in a suitable way in order to achieve the maximum power point. To get a desired value of the PV module output voltage, the solar cells must be connected in series whereas the cells have to be connected in parallel to obtain a desired PV array output current. The most used connection is the combination of solar cells in series and in parallel to achieve the power required.

The equivalent model of a photovoltaic module is very similar to the model of a solar cell. The only changes that must be done are the voltage and current values. The voltage is obtained multiplying the voltage of a photovoltaic cell by the number of solar cells in series and the current is calculated multiplying the current of a solar cell by the number of cells in parallel that contains the photovoltaic module, as it is shown in (7) and (8). The shape of the characteristic curves for the combination of cells in series and parallel is the same as the one photovoltaic cell but it is obtained higher values. The curves are modified by the environmental conditions, such as the temperature and the irradiance.

$$V_{PV} \Rightarrow \begin{cases} V_{PV} = \sum_{i=1}^{ns} V_{PVi} \\ V_{PV} = n_S * V_{PVi} \end{cases} \tag{7}$$

$$I_{PV} \Rightarrow \begin{cases} I_{PV} = \sum_{i=1}^{np} I_{PVi} \\ I_{PV} = n_P * I_{PVi} \end{cases} \tag{8}$$

Looking at the equations, they imply that if there is only a combination of cells in series, the PV module total output current is the same as the one solar cell whereas if the connection of the cells is only in parallel, the PV panel output voltage is the voltage of a solar cell.

The current – voltage (I – V) and power – voltage (P – V) characteristic curves must be determined to analyze appropriately the behavior of the solar modules as well as to obtain the open circuit voltage, V_{oc}, without load and when the current is zero and this voltage will be the maximum voltage extracted. The short-circuit current, I_{sc}, is also obtained with a load in short-circuit, when the voltage is zero, thus this current will be the maximum that can provide the PV module.

Once that the characteristic curves are defined, the maximum power point (MPP) can be obtained. The MPP is the only working point that provides the maximum power of the solar module. If the system works at this point, the global PV system will get a higher efficiency. The MPP changes when the temperature and the irradiance changes as well.

Thanks to the (1) to (8), the solar modules can be simulated using Matlab–Simulink in this work in order to obtain the I–V and P–V characteristic curves under different environmental conditions and for different combination of solar cells in series and in parallel.

2.2.2.1 PV Array Simulation

From the mathematical model previously described and from the PV cell equivalent circuit in Fig. 2, the photovoltaic generator module has been implemented in Simulink, as it is shown in Fig.3.

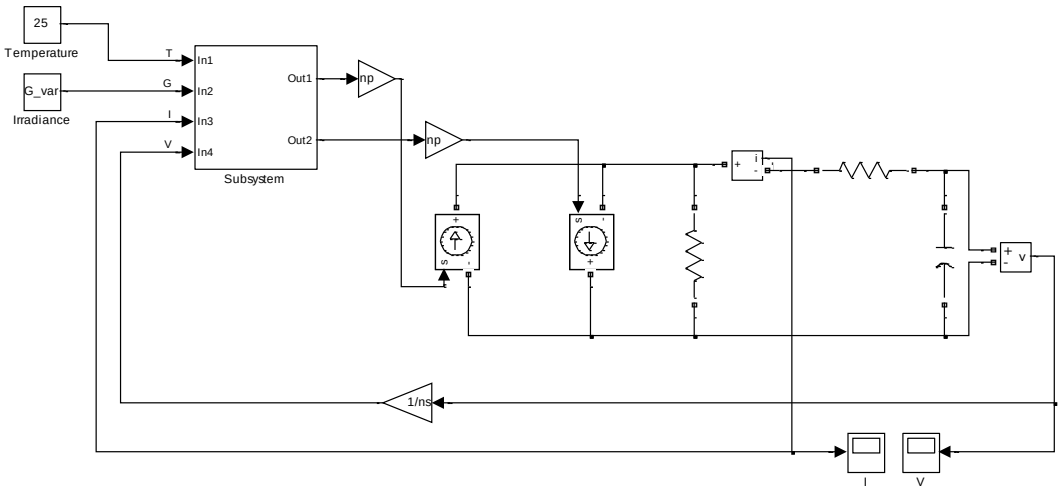

Fig.3. PV modules in Matlab-Simulink

The capacitor shown in Fig.3 is the capacitor used to obtain the characteristic curves. Then, the resistors and the current-dependant sources simulate the solar cell equivalent circuit of Fig. 2. Besides, the subsystem includes equations from (1) to (6). The system inputs are the irradiance and the temperature as well as the output current and the output voltage. In order to describe a PV module with more than one PV cell, the gain symbols represent the number of solar cells in series and in parallel. Finally, there are some measurement devices.

Initially, a solar cell has been simulated. After that, photovoltaic cells in series and in parallel have been added to define the PV system. The input parameters of the system are the environmental conditions, i. e. the temperature T, in ºC and the irradiance G, in W/m^2, because the PV output voltage and current are based on those parameters. In addition to the environmental conditions, the solar modules output voltage and current are feedback parameters because they are used in the model equations.

Accounting for the standard values provided by the manufacturer, the simulations are carried out for a solar cell and after that, the PV modules simulations are done. The I – V and P – V characteristic curvesare obtained with the simulations as well as the open circuit voltage, the short-circuit current and the maximum power that can be extracted.

Firstly, the characteristic curves for a solar cell are obtained. For that, there are some methods and in this case the curves are measured through a capacitive load, [101], as it is

shown in Fig.3, where a capacitor has been included in the photovoltaic cell model. This method has been selected because due to the solar cell behavior, that ranges from a zero voltage or short-circuit to the maximum voltage or open circuit and the capacitor allows the system to go from short-circuit to open voltage. When the capacitor is charging, the current decreases whereas the voltage is increasing. When the capacitor is charged, the solcar cell current is zero. The photovoltaic cell provide electric power along all the points of the curves with the exception of the open voltage point and the short-circuit point.

Therefore, the characteristic curves for a solar cell under the standard conditions, 25 ºC and 1000 W/m^2 are presented in Fig. 4 and Fig. 5.

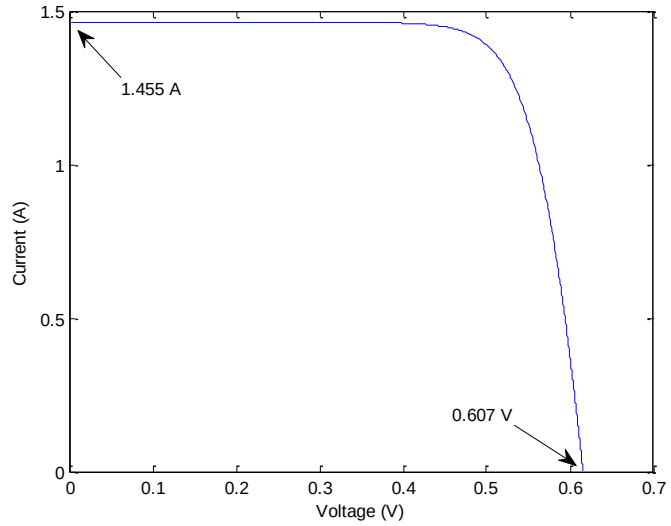

Fig. 4. Solar cell I – V curve

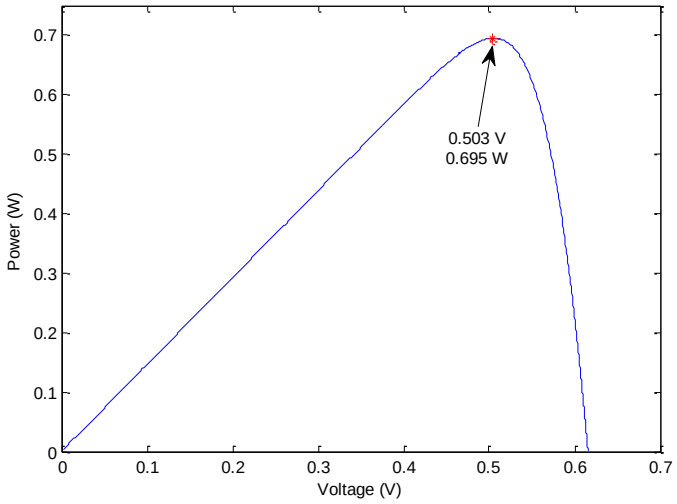

Fig. 5. Photovoltaic cell P – V curve

Fig. 4 shows the I – V characteristic curve where the open circuit voltage V_{oc} is 0.607 V and the current is zero for an only solar cell. The short-circuit current is 1.455 A when the voltage is zero. Fig. 5 presents the maximum power point obtained with a photovoltaic cell. The MPP, in this case 0.695 W, is reached when the voltage is 0.503 V under standard conditions. This power is the maximum power that a solar cell can supply and for that

reason it is required the combination of solar cells in series and in parallel to make this power increase to the desired level.

Then, the electrical parameters of the photovoltaic cell can be obtained, Table 2.

Table 2. PV cell electrical parameters

Parameter	Value
Maximum power	0.695 W
Voltage for the MPP	0.503 V
Current for the MPP	1.401 A
Open circuit voltage	0.607 V
Short-circuit current	1.455 A

The number of solar cells in series is increased in order to check that the photovoltaic output voltage increases as well. This simulation has been made using the standard conditions, 25ºC y 1000 W/m^2, taking into account that one solar module has 36 solar cells in series.

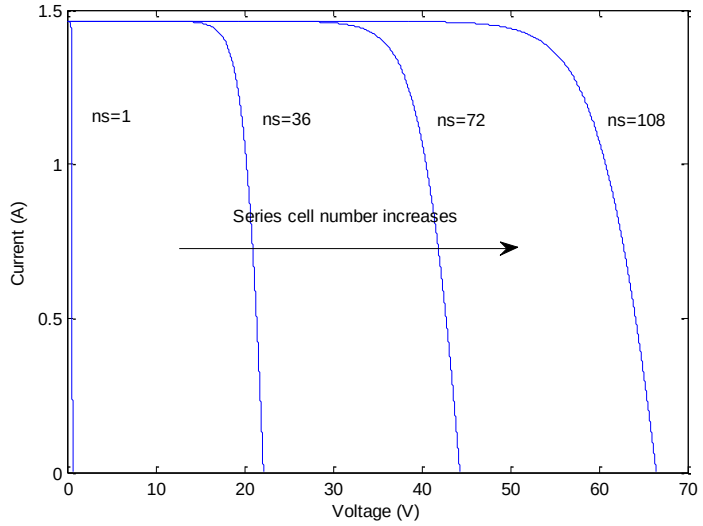

Fig. 6. I–V curve with a range of solar cells in series

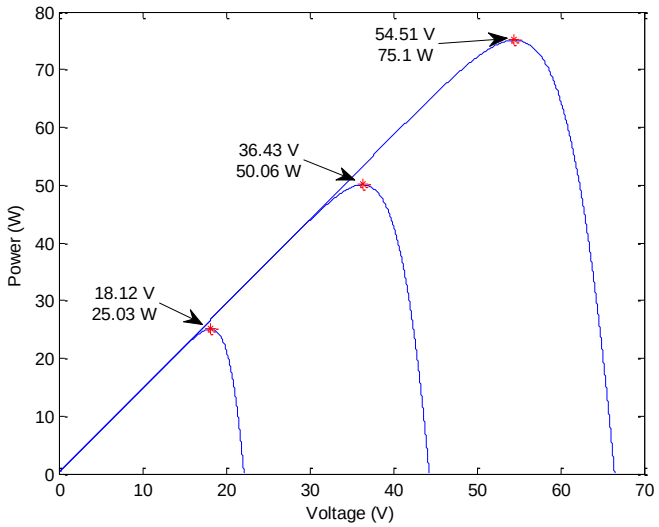

Fig. 7. P–V curve with a range of solar cells in series

It can be confirmed that the open circuit voltage for each of the modules fulfills the equation 2.8. For example, if 36 solar cells are considered, the voltage must be calculated multiplying 0.607x36, obtaining a voltage of 21.85 V, that it is the similar to the obtained in the simulation, as it is shown in Fig. 6 and Fig. 7.

The photovoltaic array used in this work consists of solar modules of 36 solar cells in series connected to other PV modules in series. The solar modules can also be connected in parallel, obtaining Fig. 8 and Fig. 9.

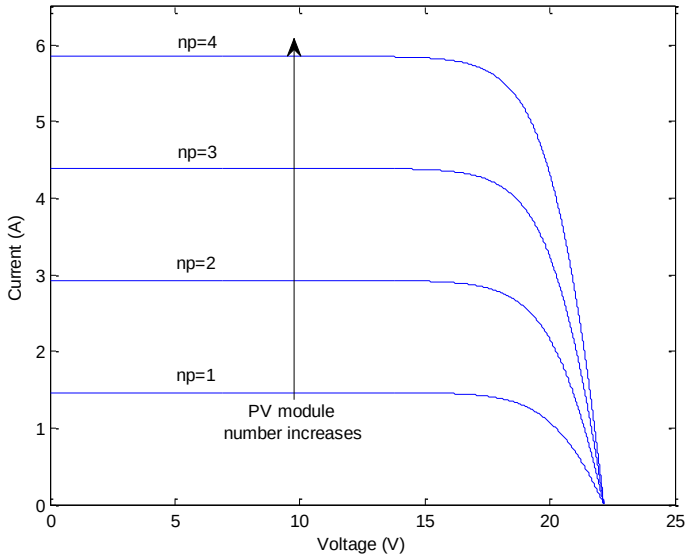

Fig. 8. I–V curve with different number of PV modules in parallel

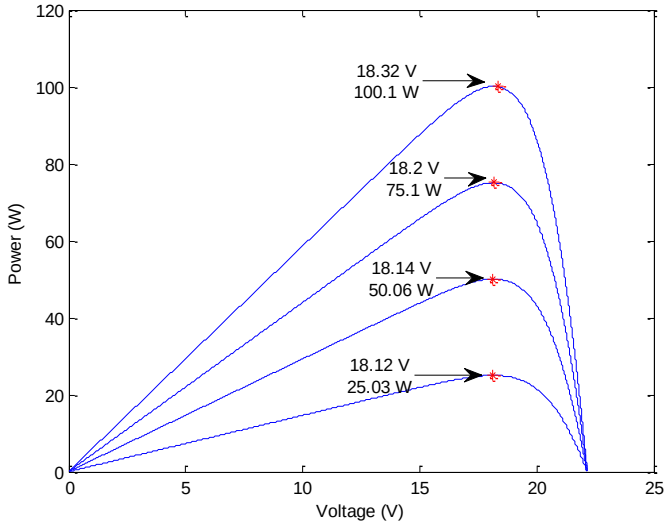

Fig. 9. P–V curve with different number of PV modules in parallel

The characteristics curves of a PV module with 36 solar cells in series are shown in Fig. 10 and Fig. 11.

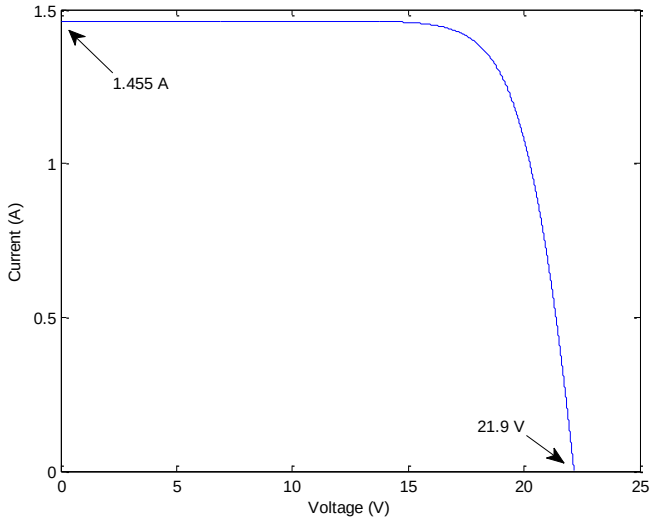

Fig. 10. PV module I–V characteristic curve

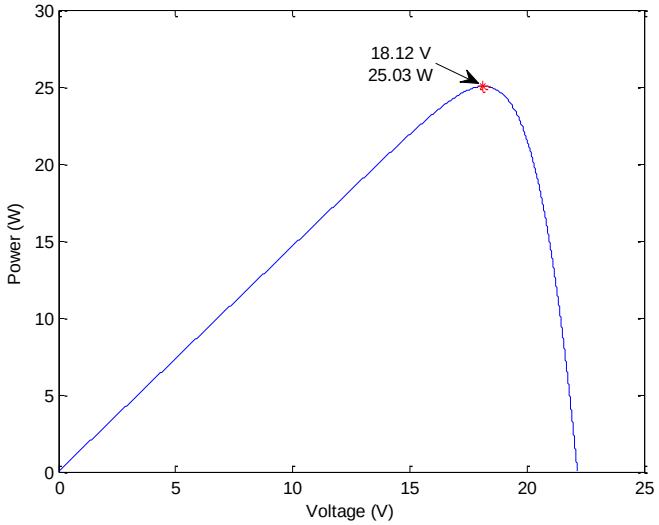

Fig. 11. PV module P–V characteristic curve

The characteristic curves I – V and P – V are presented for a temperature of 25 ºC and different values of irradiance in Fig. 12 and Fig. 13.

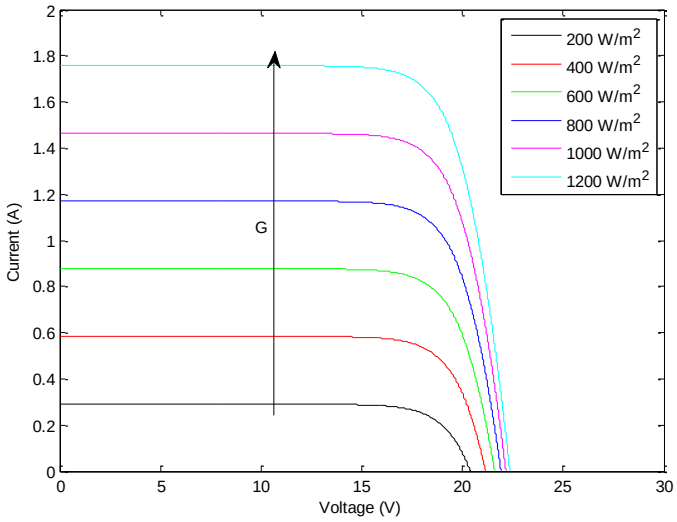

Fig. 12. I–V curves under different values of irradiance

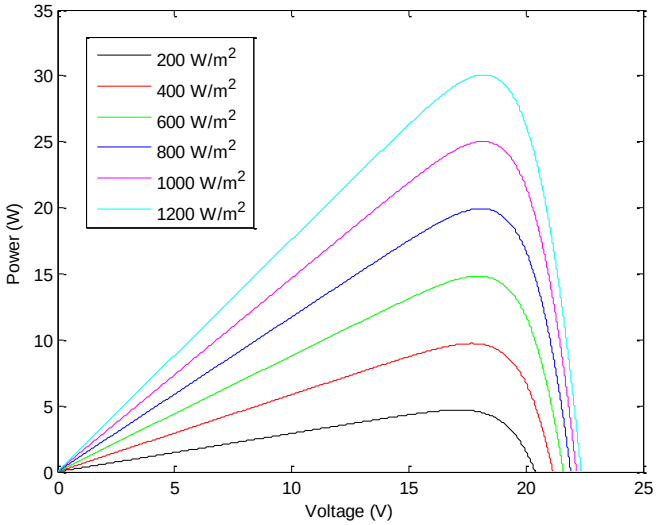

Fig. 13. P–V curves under different values of irradiance

As it can be seen in Fig. 13, there is only one point where the PV module output power is maximum under certain working conditions. The maximum power points for each of the modeled irradiance are detailed in Table 3.

Table 3. MPPs with different irradiances

Irradiance (W/m^2)	**MPP (W)**
200	4.71
400	9.9
600	14.98
800	19.98
1000	25.03
1200	30.05

When the irradiance that comes from the solar light increases, the extracted power increases as well.

The characteristic curves are presented in Fig. 14 and Fig. 15 when the irradiance keeps constant, with a value of 1000 W/m^2, and when the temperature changes from 0ºC to 80 ºC.

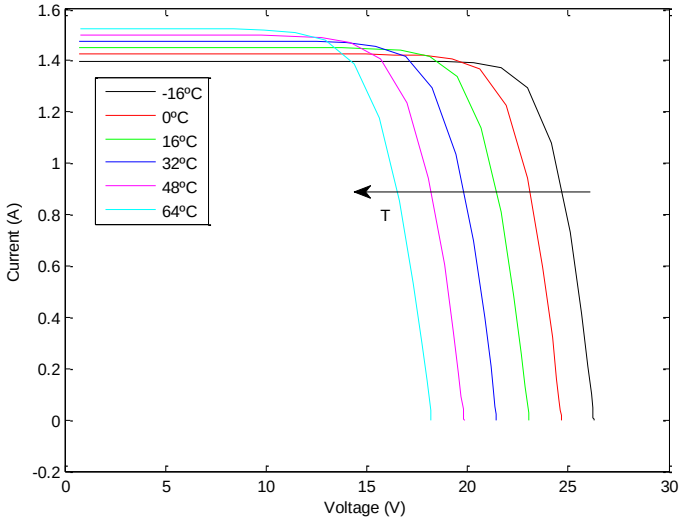

Fig. 14. I–V curves under different values of temperature

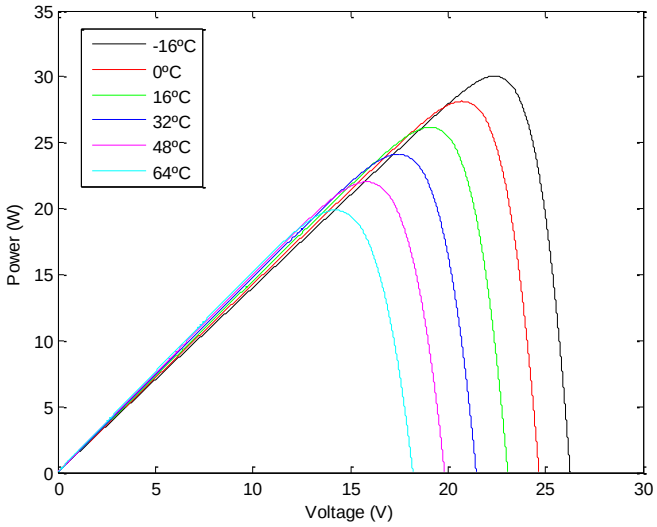

Fig. 15. P–V curves under different values of temperature

Contrarily to the previous case, when the temperature decreases, the power increases. Therefore, the optimum conditions to extract the maximum power point from the photovoltaic systems are the highest irradiance and the lowest temperature.

Fig. 16 shows a surface with the maximum power points depending on the temperature and the irradiance.

Looking at the previous figure, the maximum power is obtained with the minimum temperature, 0 ºC, and the maximum irradiance, 1000 W/m^2 whereas the lowest power is extracted by the solar modules when the irradiance has its lowest values, 200 W/m^2, and the highest temperature, 100 ºC.

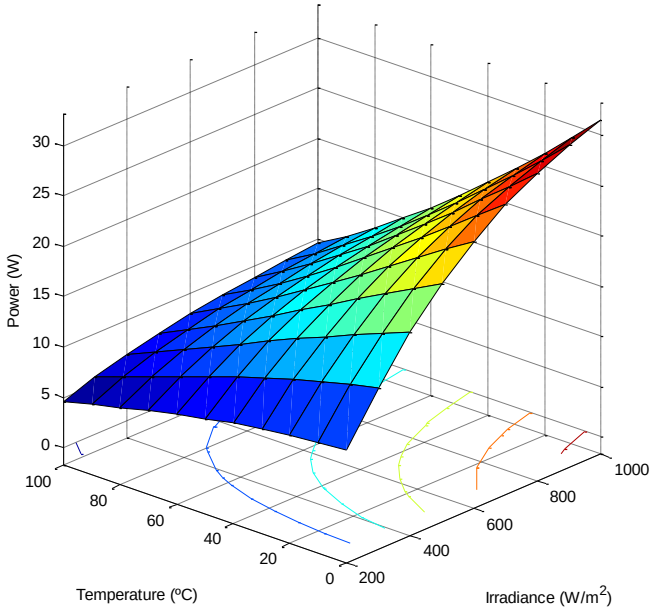

Fig. 16. Maximum power depending on the irradiance and the temperature

2.2.3 DC/DC Converter

At the PV array output is required to include a DC/DC power converter to set the solar modules output voltage at the desired value in order to track the maximum power point.

The DC/DC power converters are the devices most used in the industrial applications, [102]. The three topologies more common are the buck, boost and buck-bost power converters. They are circuits that control the energy charge and discharge in their storage passive components, such as the inductors and the capacitors. The three topologies are non-isolated because the DC/DC converter input and output voltages share a common ground. These topologies have different properties depending on the interconnection between their devices.

The buck converter or step-down power stage is a DC/DC converter that supplies an output voltage lower or the with the same value than its input voltage. It has two storage components, a capacitor and an inductor, a power switch and a diode as shown Fig. 17.

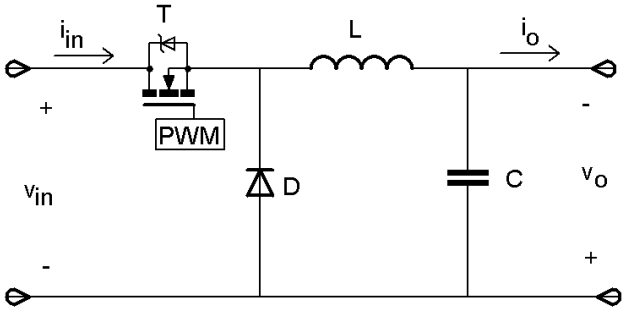

Fig. 17. Buck converter topology

The boost converter or step-up power stage is a DC/DC converter that provides an output voltage higher or equal to the input voltage. It also has two storage electrical components as well as the power switch and the diode but in this case they are connected as shown in Fig. 18.

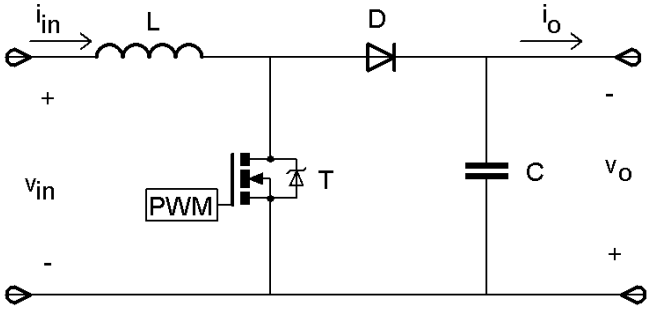

Fig. 18. Boost converter topology

The parameters used in Fig. 17 and Fig. 18 are i_{in}, the input current, v_{in}, the input voltage, i_o, the output current, and v_o, the output voltage.

The buck-boost converter or sometimes called step-up/down power stage is located between the PV array and the DC/AC power converter or between the PV modules and a DC load. It can increase or decrease the buck-boost converter output voltage in relation to the input voltage. This converter can be obtained from the connection in cascade of the buck converter and the boost converter. Fig. 19 depicts the buck-boost converter topology, showing the interconnection of the different components.

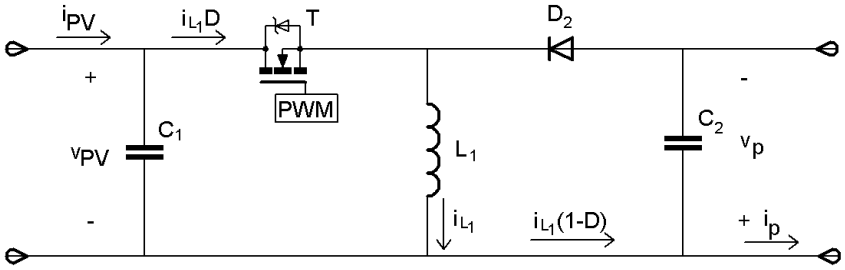

Fig. 19. Buck-Boost converter with input filtering capacitor

γ is the buck-boost converter duty cycle, v_p is the buck-boost converter output voltage, v_{pv} is the DC/DC converter input voltage or the PV array output voltage, i_{L1} is the current through the inductor and i_{PV} is the solar modules current. The voltages are measured in V and the currents in A. Parameters L_1, C_1 and C_2 represent the values of the inductor and the capacitors respectively. Besides, it is essential to select a power semiconductor able to work with the voltages and currents flowing through the buck-boost converter. In this case, a metal-oxide-semiconductor field-effect transistor (MOSFET) is used as a power switch, T, and an output Schottky diode for loss minimization is chosen, D_2. The MOSFETs do not need a continuous flow if drive current to remain in the ON state and they can offer higher switching speeds compared with other transistors. Besides, they have low switching power losses and thermal runaway.

2.2.3.1 Buck-Boost Converters

In this work, a buck-boost has been used and built. The buck-boost performance is based on the regulation of the temporary energy storage. Then, the energy is transferred to a load or to the DC/AC converter in a specific period of time. Thus, a DC voltage level change is obtained by means of the use and control of the switching devices. Therefore, the control aim is to make the buck-boost converter work in a stable way regulating the PV array output voltage. This solar module output voltage should remain constant in a certain value, close to the reference voltage. The reference voltage is fixed by the voltage that supplies the maximum power to extract the maximum power from the PV system. The power transfer through the DC/DC converter is regulated adjusting the buck-boost duty cycle.

The buck-boost converter is able to supply an output voltage higher (boost power stage) or lower (buck power stage) than the input voltage. Besides, the buck-boost converter output voltage is opposite in polarity from the DC/DC converter input voltage.

The buck-boost converter operation principle is based on a binary signal responsible for the change of the switch between on and off, i. e. the MOSFET is on when the binary signal γ is 1 and it is off when γ is 0. These on-times and off-times are controlled by a PWM (Pulse-Width-Modulation) control that determines the switch position as a function of time. The switching action causes a train of pulses due to the MOSFET, the diode and the inductor. When the diode is conducting, a L/C output filter is formed to filter the train pulses that generate the buck-boost converter output voltage.

This DC/DC converter operation can be divided into two types of operations: when the switch is closed ($\gamma = 1$) and when the switch is open ($\gamma = 0$).

Fig. 20 shows the working of the buck-boost converter when the MOSFET is closed. When $\gamma = 1$, the switch is active during a time t_{ON} while the diode is inversely polarized. Thus, the load is isolated from the source and the current does not flow by the diode. Then, the source is connected to the inductor supplying the input current to the inductor. This way, the value of the inductance increases lineally and is able of storing energy.

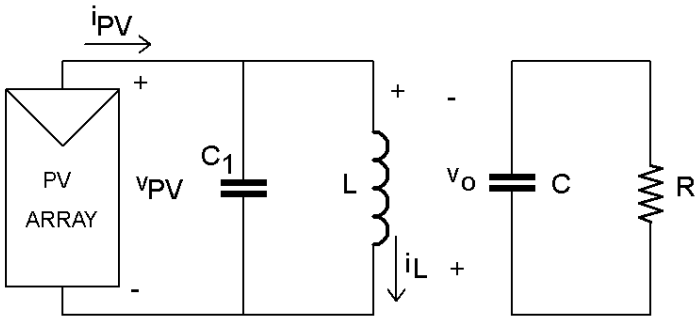

Fig. 20. Buck-boost converter when the MOSFET is ON

Fig. 21 depicts the working of the DC/DC converter when the switch is open. Once the time t_{ON} is over, the switch is open during the interval time t_{OFF}, preventing the source from the energy supply. The diode now provides a way to the inductor current. Thus, the previously stored energy in the inductor is transferred to rest of the circuit. When the time

that the switch is open is over, the switch is closed again during the period of time t_{ON} and this process is repeated.

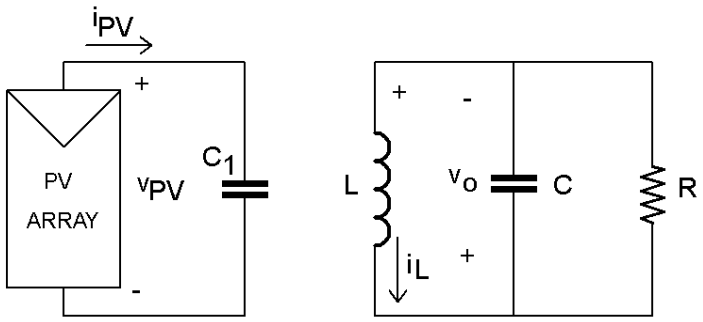

Fig. 21. Buck-boost converter when the MOSFET is OFF

A buck-boost converter can operate in continuous conduction mode (CCM) or discontinuous conduction mode (DCM) depending on the inductor current, i. e. if the current flowing through the inductor is zero or not in the operation time, *t*, due to the fact that the time when the switch is close is related to the time that the inductor requires to transfer all the stored energy. Thus, the current is flowing continuously through the inductor when the buck-boost is working in CCM during the entire switching in steady-state operation whereas the inductor current is zero for a portion of the switching cycle when the buck-boost converter is working in DCM. In this case, the value of the inductor current starts at zero, then it obtains a maximum to return later to zero.

Thus, in discontinuous conduction mode the inductor current is zero for a portion of the switching cycle if the output load current is decreased below a critical current level. Therefore, the current is zero for a moment in the period of time when the switch is OFF because t_{OFF} exceeds the time that the inductor can transfer energy. As a consequence, the next switching cycle will start from a current of zero value due to the fact that the inductor has been discharged completely. The buck-boost converter working in DCM has three states per switching cycle. The ON state is when the MOSFET is ON and the diode is OFF. The OFF state is when the MOSFET is open and the diode is closed. Finally, the idle state is when the MOSFET and the diode are OFF. In this case, the power stage is at the boundary between continuous and discontinuous mode.

In this work, the buck-boost converter will work in continuous conduction mode, guaranteeing the current is continuously flowing through the load and it will never be zero. In contrast to the DCM, the CCM assumes two states during each switching cycle, the ON state when the MOSFET is closed and the diode is open and the OFF state when the MOSFET is OFF and the diode is ON. The CCM allows the photovoltaic system to change from zero voltage or short-circuit to open circuit voltage. This way, the I – V and P – V characteristics curves of the photovoltaic modules can be obtained because the buck-boost provides a DC/DC converter output impedance that varies from zero to infinite.

In CCM, the duty cycle γ is calculated dividing the time that the switch is closed by the total time of a cycle, (9).

$$\gamma = \frac{t_{ON}}{t_C} \tag{9}$$

where t_c is the addition of t_{ON}, the time when switch is closed, plus t_{OFF}, the time when the MOSFET is open. The buck-boost converter is driven by a fixed frequency Pulse Width Modulation (PWM) duty cycle generator with duty cycle γ, $\gamma \in]\,0,\,1[$.

There is a relation between the buck-boost converter output voltage and the buck-boost converter input voltage or the PV array output voltage, (10).

$$\frac{v_p}{v_{PV}} = \frac{\gamma}{1-\gamma} \tag{10}$$

Then, the power supplied by the photovoltaic modules has to be the same that the power supplied to the load when there are no losses in the buck-boost converter components, (11).

$$P_{PV} = P_O \Rightarrow v_p = \left(v_{PV} \cdot i_{PV}\right) / i_p \tag{11}$$

The aim of the inductor is to temporarily store energy as current to achieve its transfer in two directions. The inductor value requires to be calculated to guarantee that the buck-boost converter is working in continuous conduction mode.

The input power of the real buck-boost converter should remain constant and be equal to the DC/DC converter output power in the case when there are no losses. In the real model, the electric component losses have been added and the power transfer does not remain constant between the input and the output. The efficiency of the buck-boost is calculated taking into consideration the converter output power in relation with the input power in order to know the losses of the different elements of the converter.

The buck-boost converter is defined by their characteristic equations. The equations that determine the circuit when the power switch is closed are (12), (13) and (14).

$$i_{PV} = -C_1 \frac{dv_{PV}}{dt} + i_{L1} \Rightarrow \frac{dv_{PV}}{dt} = \frac{i_{PV}}{C_1} - \frac{i_{L1}}{C_1} \tag{12}$$

$$v_{PV} = v_{L1} = L_1 \frac{di_{L1}}{dt} \Rightarrow \frac{di_{L1}}{dt} = \frac{v_{PV}}{L_1} \tag{13}$$

$$i_{C2} = -C_2 \frac{dv_p}{dt} = \frac{v_p}{R} \Rightarrow \frac{dv_p}{dt} = -\frac{v_p}{RC} \tag{14}$$

Then, the equations that model the buck-boost converter when the power switch is open are (15), (16) and (17).

$$i_{PV} = C_1 \frac{dv_{PV}}{dt} \Rightarrow \frac{dv_{PV}}{dt} = \frac{i_{PV}}{C_1} \tag{15}$$

$$v_p = v_{L1} = L_1 \frac{di_{L1}}{dt} \Rightarrow \frac{di_{L1}}{dt} = -\frac{v_p}{L_1} \tag{16}$$

$$i_{C2} = C_2 \frac{dv_p}{dt} = i_{L1} - i_p = i_{L1} - \frac{v_p}{R} \Rightarrow \frac{dv_p}{dt} = \frac{i_{L1}}{C_2} - \frac{v_p}{RC} \tag{17}$$

The equations that define the converter regardless of the power switch position are (18), (19) and (20). They use the parameter γ with two values, 0 and 1. γ is 1 when the power switch is ON and γ is 0 when the MOSFET is OFF. In this case, the state averaging method is used.

$$\frac{dv_{PV}}{dt} = \frac{i_{PV}}{C_1} - \frac{\gamma i_{L_1}}{C_1} \tag{18}$$

$$\frac{di_{L_1}}{dt} = \frac{\gamma v_{PV}}{L_1} - \frac{(1-\gamma)v_p}{L_1} \tag{19}$$

$$\frac{dv_p}{dt} = \frac{i_{L_1}(1-\gamma)}{C_2} - \frac{v_p}{RC_2} \tag{20}$$

One of the advantages of selecting the buck-boost converter is that there are no limits on the input resistor to track the maximum power with the changeable environmental conditions. The DC/DC converter input voltage is varying due to the fact that it depends on the temperature and irradiance incident on the photovoltaic modules. Thus, the control should be able to change the duty cycle to achieve the maximum power. Another benefit of using this converter is the small number of components required to work. Besides, the buck-boost converter can supply voltages in the different ranges, obtaining output voltages equal to the input voltage or even lower or higher than the input levels.

Once the buck-boost converter is implemented, it is necessary to design a controller to regulate its input voltage in order to track the maximum power point.

2.2.3.2 Buck-Boost Converter Simulation

The buck-boost converter has been implemented in a simulation platform in Matlab-Simulink from the described model in Fig. 19 as shown in Fig. 22.

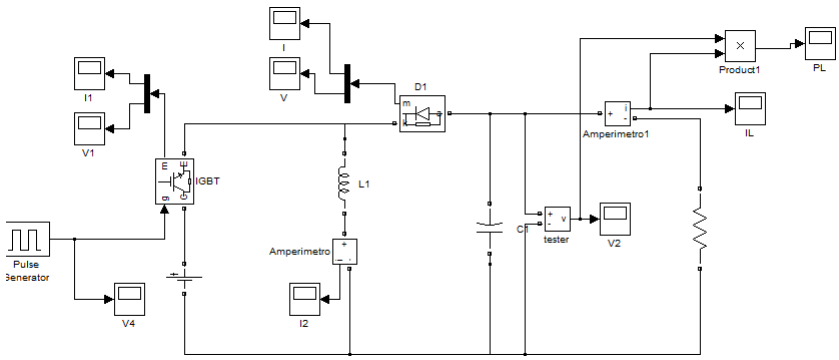

Fig. 22. Buck-boost converter simulated in Matlab-Simulink

The electrical parameters are shown in Table 4.

Table 4. Buck-boost converter electrical parameters

Parameter	Value
Inductor (L)	20 mH
Capacitor (C_1)	1000 μF
Capacitor (C_2)	5700 μF

Taking into consideration (10), the relation between the buck-boost converter output voltage and its input voltage depends on the duty cycle γ. When the duty cycle is 50%, the converter input voltage is the same as the output voltage. From 50% on, the output voltage starts to increase its value regarding the input voltage. If the duty cycle is lower than 50%, then the output voltage is lower than the input voltage. Fig. 23 depicts the obtained results from the buck-boost converter simulation for a range of values of the duty cycle, from 10% to 90%, i. e. from γ = 0.1 to γ = 0.9. In this case, the buck-boost input voltage is 10 V. This converter works as a buck converter when the duty cycle is lower than 50% (γ = 0.5) because the output voltage is lower than 10 V. Thus, the output voltage is the same as the input voltage when the duty cycle is 50%. From γ = 0.5 on the buck-boost works as a boost converter, achieving output voltages higher than the input voltages.

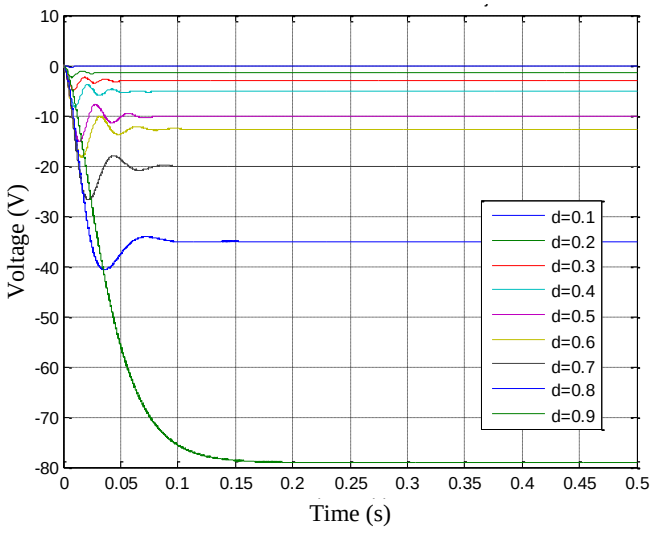

Fig. 23. Output voltage variation depending on the duty cycle

2.2.4 DC/AC Converter

The grid-connected photovoltaic systems are connected to the electrical network through DC/AC power converters. The DC/AC converters are known as inverters. There are two main types of inverters, the single-phase inverters and three-phase inverters. The DC/AC power converter input can be connected at the output of the DC/DC converter and the output of the inverter is connected to the electrical network with an AC load. There is also another way to connect the inverter when the PV system is designed for self-consumption with a telecom load. In this case, the DC/AC converter input is connected to the output of a DC load (or telecom load connected between the DC/DC converter and the inverter) and then the inverter output is connected to the grid. The aim of the inverter is to change the DC input voltage to an AC output voltage with the desired magnitude and frequency. The inverter consists of a control circuit and a power circuit. The power circuit is formed by electronic power components or power switches.

2.2.4.1 Single-Phase Inverter

In this work, a single-phase full bridge inverter or single-phase H-bridge inverter is used. This topology guarantees lower distortion compared to the single-phase half-bridge topology. Fig. 24 presents the single-phase inverter. It is built with four power switches, in this case insulated-gate bipolar transistors (IGBTs). Each IGBT has connected an anti-parallel diode to make the return reactive current flows to the voltage source, i.e. the diodes are required to make possible a bidirectional switching in currentwhen the transistors are OFF.

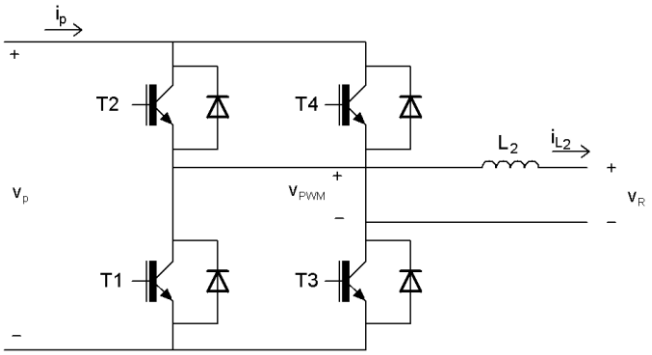

Fig. 24. Single-Phase DC/AC Inverter

The single-phase DC/AC converter input voltage and current are the buck-boost converter output voltage v_p and the DC/DC converter output current, i_p. v_p is controlled by the DC/AC converter to keep it almost constant. i_{L2} is the alternating output current and v_R is the electrical network voltage. The inverter is driven using a three level PWM sinusoidal modulator that will be explain in control section. At the inverter output there is an inductor to filter the current. The DC/AC converter generates a voltage square waveform across the load.

The inverter output voltage has three different levels. It can be $+v_p$, $-v_p$ and zero, depending on the power switches state. Table 5 presents the possible combinations of the ON and OFF transistor states.

Table 5. ON/OFF transistor states combination

On state	Output voltage
T2 & T3	$+v_p$
T4 & T1	$-v_p$
T2 & T4	0
T1 & T3	0

It is essential to know that T1 and T2 should not be closed at the same time and T3 and T4 cannot either be closed at the same time to prevent causing a short-circuit on the DC source. Therefore, to guarantee the transistors are never ON simultaneously a small time delay is added to the gate signal. Real switches do not turn ON and OFF instantaneously and this has to be taken into consideration to design the power switches control. Thus, it is necessary to include a blanking time to avoid the short-circuit caused by the commutations.

The single-phase DC/AC converter dynamics (21) and (22) can be written in strict-feedback form as:

$$C_2 \frac{dv_p^2}{2dt} = i_p v_p - i_{L_2} v_R \tag{21}$$

$$L_2 \frac{di_{L_2}}{dt} = \beta v_p - v_R \tag{22}$$

Equation (21) represents the energy transfer through the inverter, considering it is conservative and operates at unity power factor. In equation (22), the sinusoidal modulation waveform β is the function that converts the DC/AC converter switched voltage, v_{PWM}, to the fundamental sinusoidal voltage. Equations (21) and (22) will be used to define the DC/AC converter slow and fast dynamics respectively in the backstepping control presented later. The inverter has been controlled to inject nearly sinusoidal currents in order to reduce harmonic distortion in phase with the low voltage AC grid.

One of the advantages of this DC/AC converter is that it can work as an inverter or as a unity power factor rectifier, transferring power to the electrical network or from the grid. In the case there is a telecom load between the DC/DC converter and the DC/AC converter and the PV system works within the self-consumption concept, this converter has dual role. The DC/AC converter operation will depend on the telecom load power needs, on the power generated by photovoltaic modules and on the telecom load or battery requirements.

At midday hours, when the sun can supply more sun light, the PV system can generates more power than the required by the load and the excess power can be used to recharge the back-up battery or be injected in the electrical network after battery recharge. In

this case, the DC/AC converter is working in inverter mode. Another benefit of using this type of hybrid power system is if there is a fault in the grid leading to voltage sag, the photovoltaic modules and the battery remain providing power to the load regardless of the sag. As it will be seen later, the DC/AC converter working as an inverter must inject a nearly sinusoidal current to prevent harmonic distortion in phase with the network voltage. The inverter is connected to grid through a step-down transformer.

The DC/AC converter works in rectifier mode at night or during the hours where the telecom application needs more power than the power delivered by the PV modules. Thus, the rectifier sinks power from the electrical network. In this case, the grid complements the photovoltaic panels when they cannot produce more power due to low irradiance levels. In the rectifier mode, the AC current should have opposite phase relative to the network voltage.

2.2.4.2 Three-Phase Inverter

The three-phase bridge DC/AC converter is formed by six power switches, in this case six IGBTs, Fig. 25. Each transistor is inversely connected to a diode to make the return reactive current flow to the voltage source. Thus, the power siwtches operate either in the cut off or in the saturation region within a specific commutation sequence to achieve the desired output voltages. The power circuit is a voltage source inverter (VSI) and the inverter works as a voltage source.

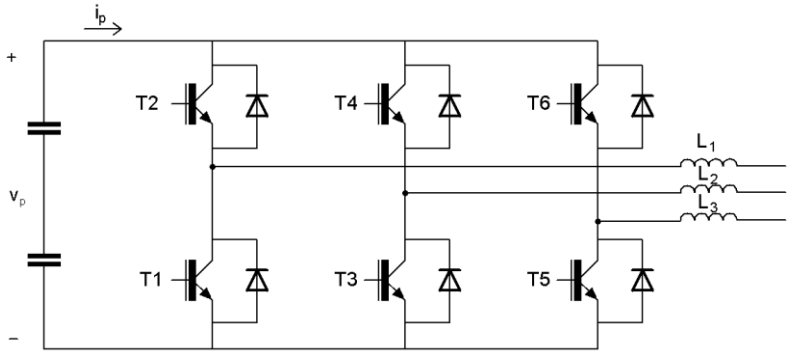

Fig. 25. Three-phase DC/AC converter

The three-phase inverter connected to the grid consists of the input capacitor, the three-phase bridge formed by the power switches and a filter. In this case, inductors are used to attenuate harmonics. The output voltage achieved in this type of inverters is $v_o/2$ and $-v_o/2$.

Like the single-phase inverter, the three-phase inverter has also a control circuit. This circuit generates ON and OFF signals to commute the semiconductors. The energy transfer from the DC side to the AC side is obtained with an appropriate commutation of the transistors. There can be three or two active components at the same time in this type of DC/AC converters. In the first case, with three active elements, the operation is 180 degree conduction mode whereas in the second case the inverter operation is 120 degree conduction mode.

In this work, the 180 degree conduction mode is used. Therefore, there is three power switches conducting at the same time, one of each branch, otherwise there would be a shortcircuit in the DC source. Each transistor conducts 180º changing the phase of the control signals appropriately to achieve that three of the power switches conduct in any time. Thus, when the IGBT T1 is ON the IGBT T2 is OFF, if the power switch T3 is conducting, the switch T4 is not conducting and finally the semiconductor T5 is closed if the semiconductor T6 is open, and vice versa.

The DC/AC converters are essential to connect the PV systems to the electrical network. The energy that it is injected to the grid has specific features in order to be transferred to three-phase systems because the frequency is imposed by the grid. The current amplitude depends on the energy level supplied by the photovoltaic system.

2.3 Maximum Power Point Tracking Algorithm

The maximum power point tracking is essential to reach the maximum power under any environmental conditions. This control is required due to the fact that the solar cells has low efficicency when they convert the incident solar energy. Therefore, the exploitation of the generated maximum power is needed. The most used method to track the MPP is the conventional Perturb and Observe (P&O). This algorithm is based on the variation of the buck-boost converter duty cycle to find the maximum power.

The power supplied by the photovoltaic generator depends on the temperature and the incident irradiance. The MPPT algorithm calculates the maximum power point in each instant of time regardless of the system environmental conditions. The MPP changes all the time, sometimes it varies rapidly because of fast changes in the environmental conditions although other times the MPP can remain constant.

In this work, the P&O algorithm and a PI control are implementedin order to compare them with the proposed method. A neuro-fuzzy controller is also designed to reach the MPP and finally the non-linear backstepping control is the method proposed in the thesis.

2.3.1 Perturb and Observe Algorithm

The advantage of this method is that it is simple and easy to implement. The P&O is based on the variation of the PV modules output voltage controlling the DC/DC converter duty cycle, and comparing the power supplied by the solar cells in the current instant of time with the power obtained in the previous instant of time. If the power of the current cycle is greater than the previous one, the voltage must be modified in the same way, increasing or decreasing it, whereas if the power is lower than the previous power, then the voltage must be varied in the opposite way, increasing or decreasing it as well. When the MPP is reached, the control algorithm oscillates around the maximum power. The flowchart of the P&O method is shown in Fig. 26, describing what it has been explained previously. ΔP is the incremental power and it represents the difference between the current power and the power

in the previous instant of time whereas ΔV is the PV panels incremental voltage and it is the difference between the voltage in the current instant of time and the previous voltage.

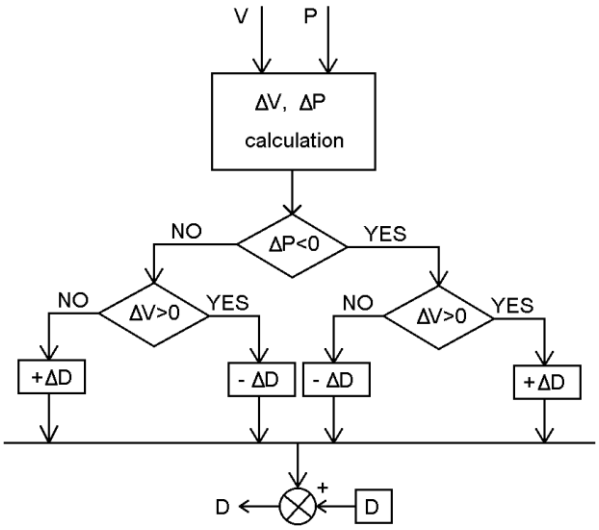

Fig. 26. P&O control flowchart

There are four different cases where the photovoltaic array must obtain the maximum efficiency and the control signal must be calculated.

- ΔP > 0 and ΔV > 0: in this case, the voltage variation should continue, i. e. the PV array output voltage should carry on increasing until the maximum power point is reached, Fig. 27. For that, the buck-boost converter duty cycle is decreased.

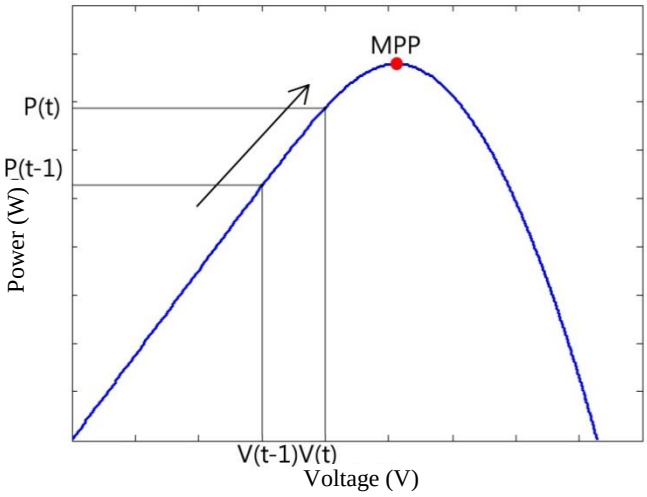

Fig. 27. P-V curve where ΔP > 0 and ΔV > 0

- ΔP > 0 and ΔV < 0: similar to the first case, the voltage variation should continue but the PV modules output voltage should carry on decreasing to reach the maximum power, Fig. 28. Thus, the DC/DC converter duty cycle is increased.

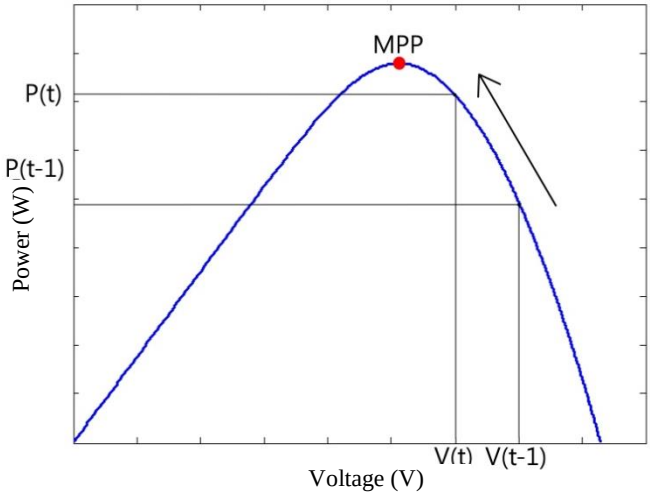

Fig. 28. P-V curve where $\Delta P > 0$ and $\Delta V < 0$

- $\Delta P < 0$ and $\Delta V < 0$: in this case, the voltage should change in the opposite way to the previous cycle. Therefore, the solar panels output voltage should be increased to achieve the maximum power point decreasing the buck-boost converter duty cycle, Fig. 29.

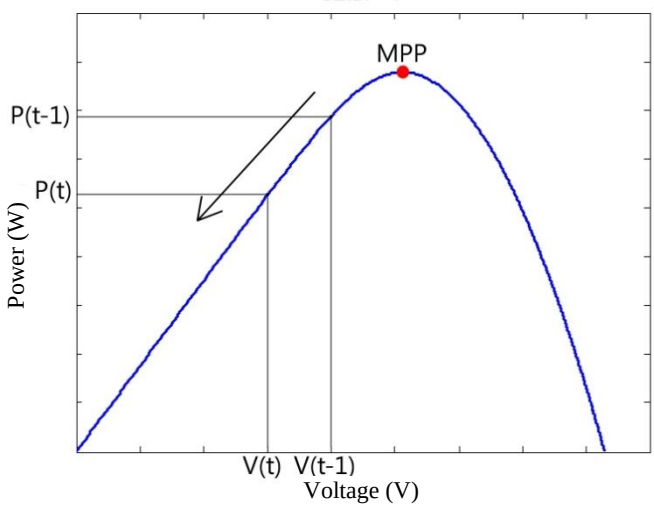

Fig. 29. P-V curve where $\Delta P < 0$ and $\Delta V < 0$

- $\Delta P < 0$ and $\Delta V > 0$: the PV generator output voltage should vary in the opposite way to the previous cycle as well to obtain a decrease in the PV array voltage to reach the MPP, Fig. 30. In this case, the DC/DC converter duty cycle should be increased.

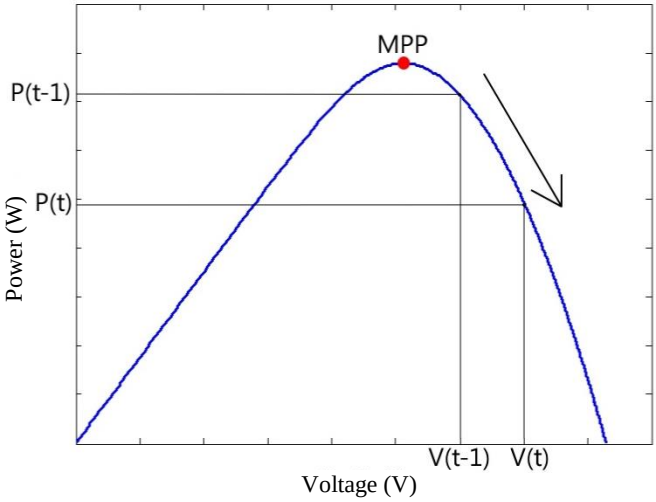

Fig. 30. P-V curve where $\Delta P < 0$ and $\Delta V > 0$

The disadvantage of this technique is energy losses due to the oscillation around the MPP even when the maximum power is achieved, reducing the efficiency of the PV system. Another drawback is the slow response of the system under this control technique. Besides, the control can sometimes reach a local maximum instead of a global maximum.

Fig. 31 shows the changeable irradiance used for the test. Then, Fig. 32 depicts the PV modules output voltage achieved under the P&O method. The irradiance is initially 1000 W/m^2 and then it changes to 400 W/m^2, to 800 W/m^2 and finally to 1000 W/m^2 again. In all the cases the voltage that provides the maximum power point is achieved except when the irradiance is 1000 W/m^2 from 0.15 s to 0.25 s because it reaches a local maximum instead a global maximum. Besides, the voltage ripple of the P&O algorithm is greater than the ripple with other techniques. Thus, the ripple leads to power losses in steady state.

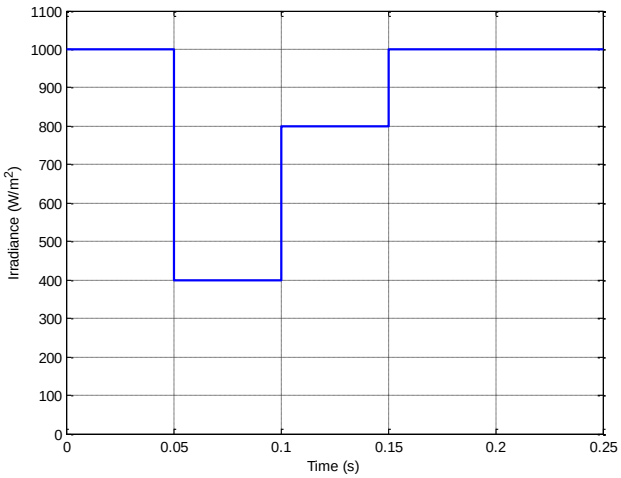

Fig. 31. Changeable irradiance

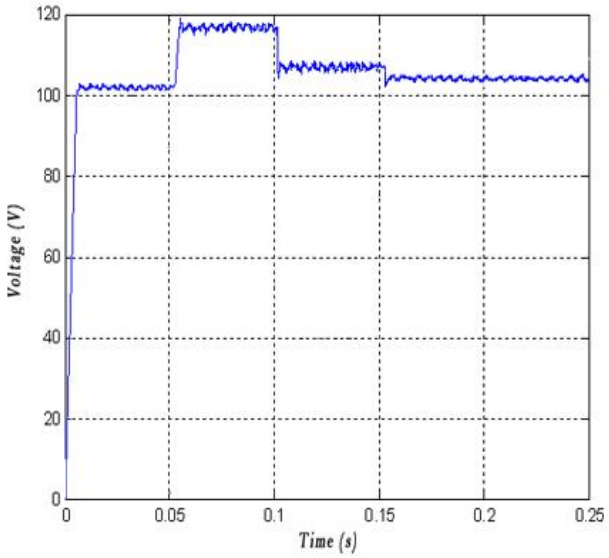

Fig. 32. PV array output voltage under changeable irradiance

Fig. 33 presents the power extracted by the PV modules under the same conditions of the previous test to obtain the response. The maximum power points are obtained from the P-V curves. The MPP is 1520 W when the irradiance is 1000 W/m^2, although 1450 W is reached. For 400 W/m^2, the maximum power is 760 W and for an irradiance of 800 W/m^2 the maximum power point is 1370 W. The P&O method fails to reach the MPP from 0.15 s on because it obtains 1380 W due to the fact that a local maximum is reached. The When the MPP is reached, there is an oscillation around the maximum point in steady state.

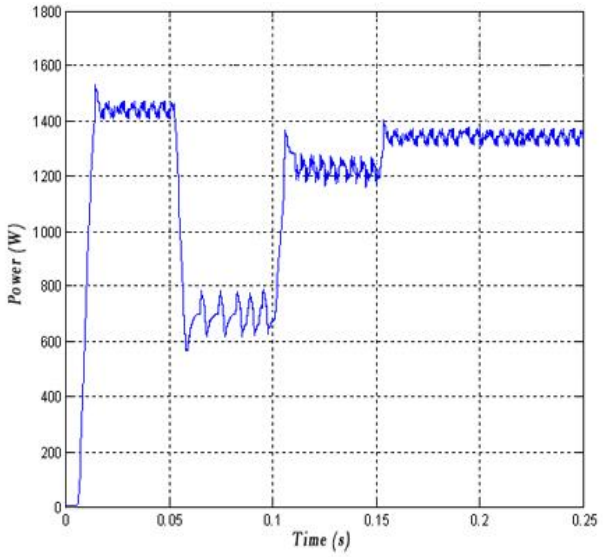

Fig. 33. PV array output power under changeable irradiance

These problems are solved using other algorithms, such as the PI control, the neuro-fuzzy controllers amongst others, or the proposed backstepping control as it will be presented in chapter 3.

2.3.2 PI Control

The PI control is thoroughly used and a well-known technique. In this case, it is applied to the buck-boost converter to make its input voltage track the reference voltage. The reference voltage should be reached by the PI control by means of the commutation of the DC/DC converter switch. The reference is the voltage that provides the maximum power, being calculated depending on the environmental conditions, the temperature and the irradiance.

In this work, the PI parameters are adjusted by the Ziegler-Nichols method, [103]. It is based on the system measurements using a linear model in open-loop. This method can obtain the PI parameters empirically close to the optimal values in a region of convergence. The parameters are obtained using a reaction curve and applying (23) and (24) .

$$K = 0.9\frac{T}{L} \tag{23}$$

$$K_i = \frac{0.3}{L} \tag{24}$$

where $L = t_1 - t_o$ and $T = t_2 - t_1$.

The system is modeled using a first order transfer function, (25).

$$G(s) = \frac{K_o e^{-s\tau_O}}{1 + s\gamma_o} \tag{25}$$

with $\gamma_o > 0$ and the parameters are (26), (27) and (28).

$$L = \tau_O = t_1 - t_0 \tag{26}$$

$$T = \gamma_O = t_2 - t_1 \tag{27}$$

$$K_o = \frac{y_1 - y_0}{u_1 - u_0} \tag{28}$$

To use this method, a step signal is applied to the system (the PV generator connected to the buck-boost converter) when it is stabilized in an operation point and the behavior of the system in open-loop must fulfill first order system requirements. The step signal is 0.2 in 0.06 s. The input (the duty cycle) is modified from $u_0 = 0.6$ to $u_1 = 0.4$. The response of the system is shown in Fig. 34.

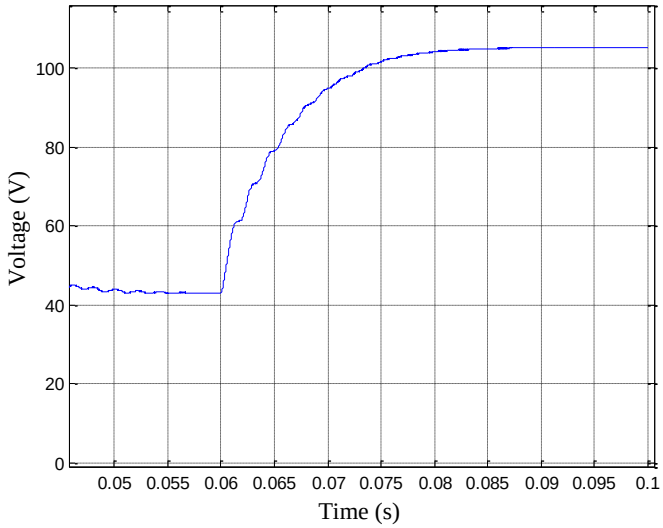

Fig. 34. System response under a step signal

The reaction curve is similar to the curve used by Ziegler-Nichols method. Thus, this technique can be applied. Then, the values are identified from the curve, as Fig. 35 depicts.

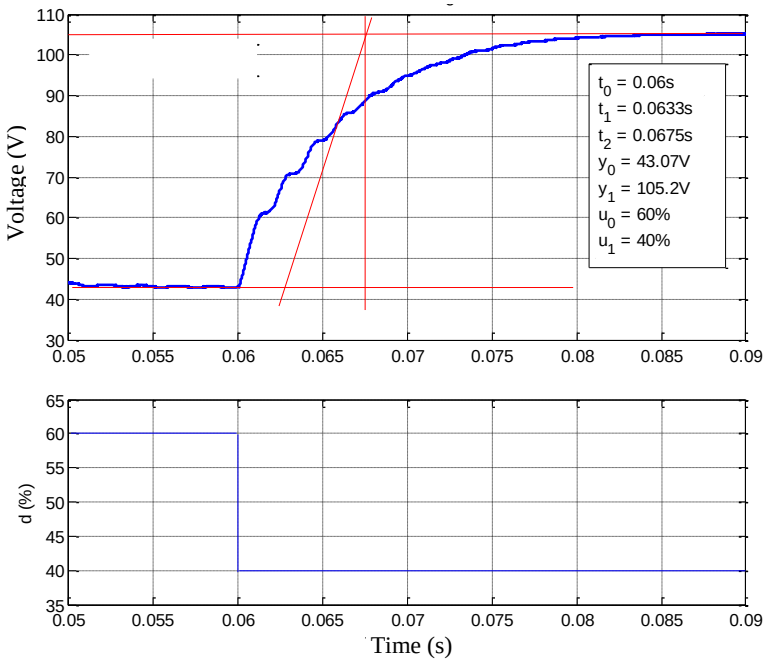

Fig. 35. Values obtained using Ziegler-Nichols method

t_o is the time when the step signal is applied, t_1 is the time when the line of maximum gradient and the constant value of the voltage before applying the step intersect whereas t_2 represents the time where the line of maximum gradient intersects with the stabilized voltage after the step. y_o is the constant value of the voltage before applying the step and y_1 is the new operation point of the system. Finally, u_o represents the initial input signal and u_1 the new input signal.

These parameters need to be validated. For that, different reference voltages are given in order to verify the performance of the system using the Ziegler-Nichols method changing the values of the temperature and irradiance, Fig. 36. Then, the values are checked with the values obtained in the I-V and P-V curves.

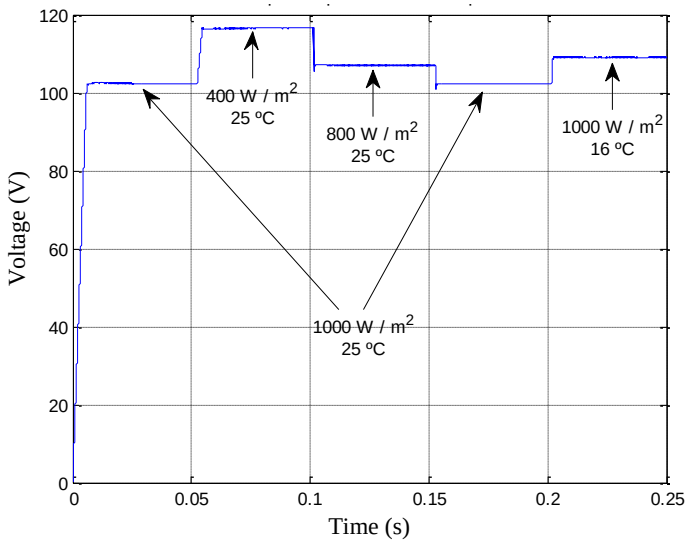

Fig. 36. Reference voltage obtained by Ziegler-Nichols method

As Fig. 36 shows, the reference voltages are achieved in all the cases without oscillations and the reference value is obtained faster than using the P&O algorithm. Thus, the maximum power is accomplished under changeable environmental conditions, as Fig. 37 depicts.

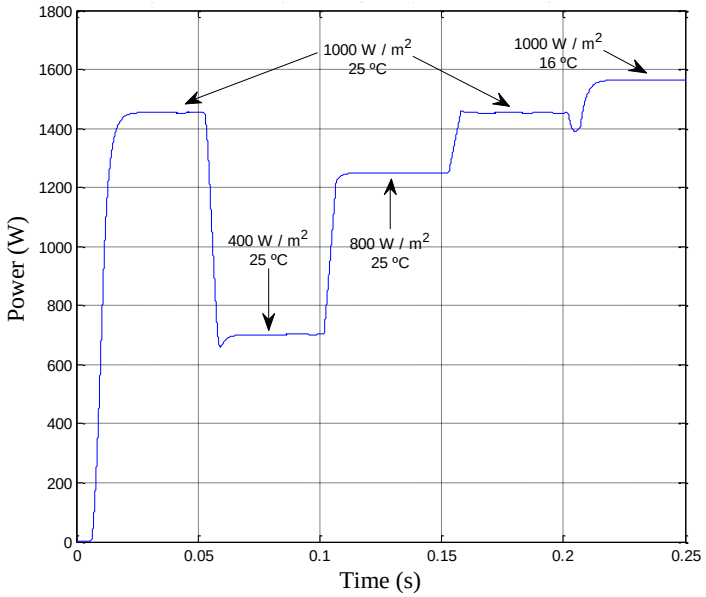

Fig. 37. Maximum power under changeable temperature and irradiance

The characteristic curves provide the maximum power without considering the buck-boost converter losses.

2.3.3 Neuro-Fuzzy System and Fuzzy Logic Controller

The same as the PI control, the buck-boost converter input voltage should track the reference voltage, but in this case a neuro-fuzzy system is used to calculate the reference voltage, the voltage that provides the maximum power. In order to make the PV module output voltage tracks the reference voltage, a fuzzy logic control has been designed. One of

the advantages of this method is that there is no need for mathematical equations and it can work with non-linear systems although after the simulation it is essential to adjust the control because the fuzzy logic uses reasoning that are approximates but not exacts. Fig. 38 presents the structure of the control.

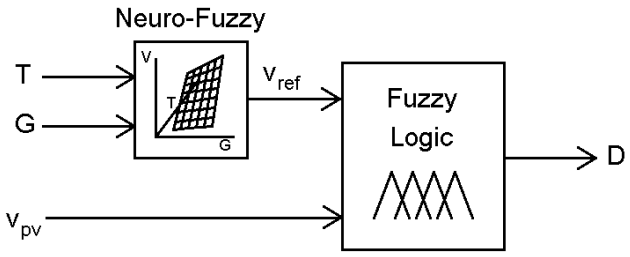

Fig. 38. Neuro-fuzzy and fuzzy control

The input data for the neuro-fuzzy system are the temperature and the solar radiation and the output data are the DC/DC converter input voltages that generate the maximum power, i.e. the reference voltage. Then, a fuzzy logic controller is used to obtain the buck-boost converter duty cycle comparing the reference voltage with the measured voltage.

2.3.3.1 Neuro-Fuzzy Fystem

Thus, the neuro-fuzzy system is used to know the optimum voltage which will be used as reference voltage. Fuzzy logic is based on rules and membership functions to relate inputs to outputs. GENFIS3, a function from Matlab, has been used to determine these rules and functions where data inputs are the irradiation and the temperature, and the data output is the PV array output voltage that supplies the maximum power. Fig. 39 depicts the reference voltages.

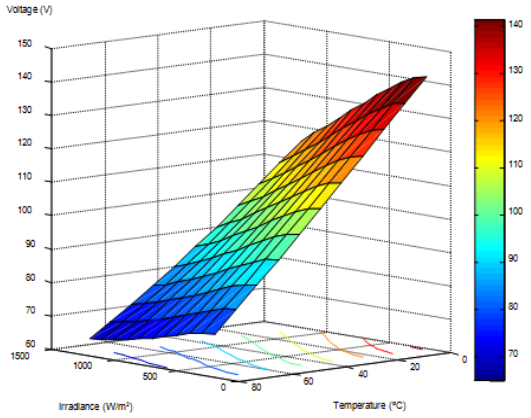

Fig. 39. Reference voltage of the MPP depending on the irradiance and temperature

Fig. 40 presents the membership functions for the input data. In this case, Gaussians curves have been used.

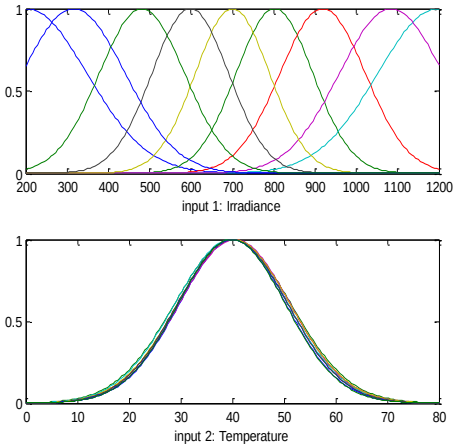

Fig. 40. Membership functions; inputs are temperature and irradiation

Then, to create a trained system with the membership functions and rules, an adaptive neuro-based fuzzy inference system (ANFIS) is used to achieve the required voltage in order to control the system using the MPPT algorithm. ANFIS generates from the fuzzy rules, the input data (irradiance and temperature) and the output data (the reference voltage) a trained system using a backpropagation algorithm used in the neural network, [104]. Thus, the system can learn from the provided data.

2.3.3.2 Fuzzy Logic Controller

The neuro-fuzzy system provides the reference voltage at the DC-DC power converter input. In this work, the control loop to keep constant that voltage has been implemented using fuzzy logic. Thus, the Matlab fuzzy graphical tool has been used to create membership functions and rules, where the input is the error between the theoretical voltage and the PV array output measured voltage whereas the output is the duty cycle of the DC-DC power converter.

Fig. 41 depicts the input data. Gaussian curves are used. The input and output data are defined. The input data are:

- Low: when the PV array voltage is lower than the reference voltage.
- Perfect: when the PV array voltage is the same as the reference voltage.
- High: when the PV array voltage is higher than the reference voltage.

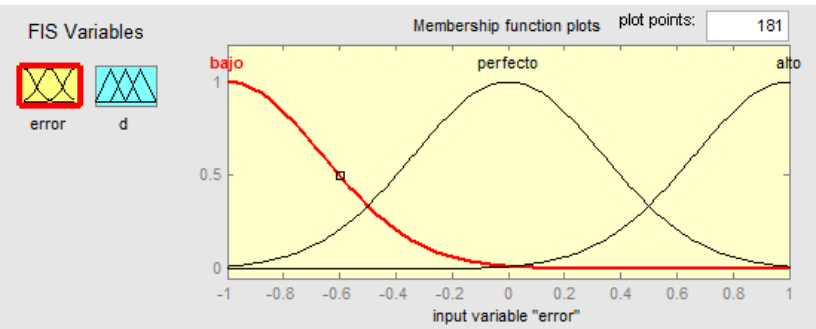

Fig. 41. Input membership functions

Then, the output data are:

- Less_D: the buck-boost converter duty cycle must be decreased.
- Hold_D: the buck-boost converter duty cycle must be kept constant.
- More_D: the buck-boost converter duty cycle must be increased.

Fig. 42 depicts the output data. In this case, Triangular functions are used.

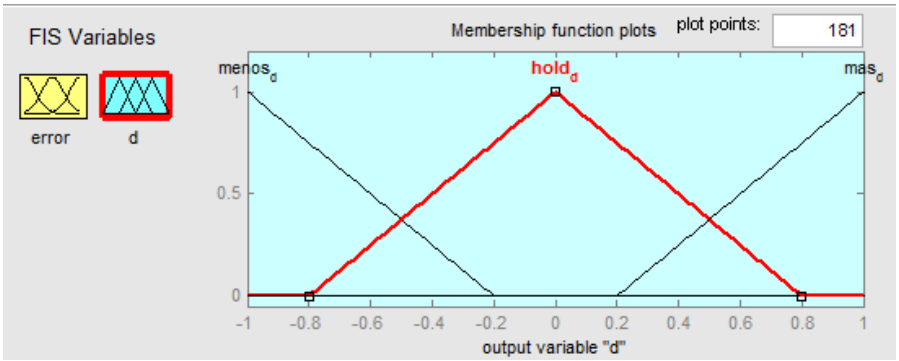

Fig. 42. Output membership functions

Then, a combination of rules is created:

- If "Low" then "Less_D": it is required to reduce the duty cycle to increase the PV array output voltage.
- If "Perfect" then "Hold_D".
- If "High" then "More_D": it is necessary to increase the duty cycle to decrease the PV array output voltage.

In order to validate the proposed method, Fig. 43 and Fig. 44 show the evolution of the PV output voltage and power, respectively, with the designed control under irradiance changes. Considering the results obtained from the characteristic curves, the voltages that supply the maximum power point and the maximum power are obtained.

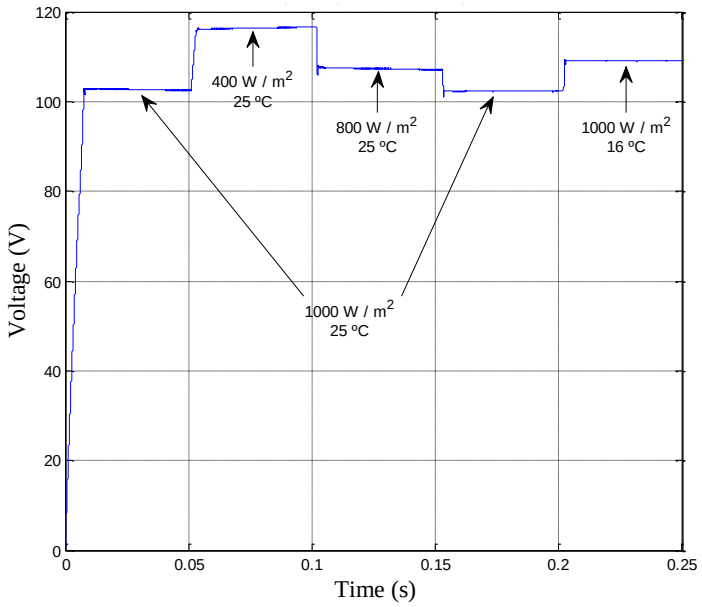

Fig. 43. Voltage that provides the MPP obtained

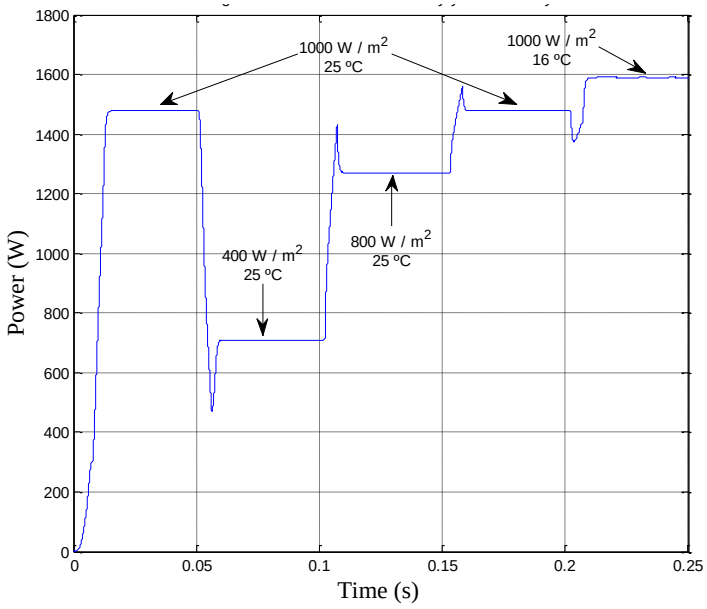

Fig. 44. Maximum power under changeable irradiance and temperature

The maximum power is obtained in all the cases without oscillations, although a peak appears during the transition between different irradiances. In order to improve these results, a backstepping controller is proposed in this work.

2.3.4 Backstepping Control

A non-linear backstepping approach is used to obtain the control laws for the DC/DC converter and the DC/AC converter. This proposed control has been used to track the maximum power point of the PV modules under changeable environmental conditions. It is applied to the buck-boost converter to regulate the solar cells output voltage. Another backstepping controller has been proposed for the DC/AC converter to inject sinusoidal current in phase with the electrical network voltage to reduce the harmonic distortion when the solar system injects power to an AC load. Besides, this control must allow the converter to work as an inverter or as a rectifier, depending on the power requirement of the DC load when the PV system has to supply energy to a telecommunication load for self-consumption.

The nonlinear backstepping method, [80], first calculates the fictitious or virtual control input to stabilize the lower order subsystem (18) at the origin, and then finds a way to calculate γ the control signal to enforce the dynamics in (19) necessary to track value required to stabilize (18). The algorithm steps backward from (19) until the ultimate control γ is obtained. Compared to linear controllers, better results can be obtained since backstepping applies a recursive methodology to the model direct dynamics and Lyapunov functions to guarantee the system stability and robustness.

2.3.4.1 Buck-Boost Converter Backstepping Control

The aim of this control is to extract the maximum power. In order to do this, a nonlinear backstepping controller is designed to control the duty cycle of the buck-boost converter switch. This way, the output voltage of the PV modules can be regulated to track the reference voltage.

Usually, a buck-boost converter is controlled so that its output v_p voltage presents a constant reference value. However, in this self-consumption PV system the purpose of the buck-boost backstepping controller is to define the converter duty cycle so that the converter regulates its input voltage to enforce the PV panel operation at the MPP. To accomplish this, the backstepping input v_{PV} voltage outer loop defines the inductor current reference value $i_{L_1 ref}$ to control the inductor i_{L1} current, and a recursively obtained inner current loop defines the needed duty cycle to track $i_{L_1 ref}$.

To apply the backstepping method, [105], and stabilize the buck-boost to the origin (zero error), first the tracking error e_{PV} is defined to enforce the buck-boost input voltage v_{PV} to track the PV array MPP reference voltage v_{PVref} (zero tracking error), (29).

$$e_{PV} = v_{PV} - v_{PVref} \tag{29}$$

Using the model equation (18), to calculate the time derivative of e_{pv} in (29), (30) is received.

$$\dot{e}_{PV} = i_{PV} / C_1 - (i_{L_1} \gamma) / C_1 - \dot{v}_{PVref} \tag{30}$$

In this equation i_{L1} can be determined to be the stabilizing control input (or the virtual control law [80]) and the current reference for the inner loop. Now, a Lyapunov function globally positive-definite and radially unbounded for all e_{PV} is selected, (31).

$$V_v = e_{PV}^2 / 2 \tag{31}$$

To guarantee the solution is globally asymptotically stable, the time derivative of the Lyapunov function $\dot{V}_v$ must be globally negative-definite for all $e_{PV,}$ [105]. Therefore $e_{PV}\dot{e}_{PV} < 0$, a condition that can be enforced using (32).

$$\dot{e}_{PV} = -k_{PV} e_{PV} \Rightarrow i_{PV}/C_1 - \left(i_{L_1}\gamma\right)/C_1 - \dot{v}_{PVref} = -k_{PV} e_{PV} \tag{32}$$

If k_{PV} in (32) is constant and positive then $\dot{V}_v < 0$ is verified. Supposing zero tracking error, the reference current i_{L1ref}, for the virtual control law i_{L1} (stabilizing function), obeys $i_{L1ref} = i_{L1}$, and can be obtained from (32), since $0<\gamma<1$.

$$i_{L_1 ref} = \left(C_1 k_{PV} e_{PV} + i_{PV} - C_1 \dot{v}_{PVref}\right)/\gamma \tag{33}$$

The reference current for the inner loop ($i_{L_1 ref} \neq 0$) is a function of the buck-boost modulator duty cycle γ. To define this duty-cycle a second feedback loop enforcing $i_{L1} = i_{L_1 ref}$ is needed. The inductor current i_{L1} should equal $i_{L_1 ref}$ to achieve a zero tracking error defined as $e_{i_{L1}} = i_{L1} - i_{L_1 ref}$. Its time derivative is (34).

$$\dot{e}_{i_{L1}} = \dot{i}_{L_1} - \dot{i}_{L_1 ref} \tag{34}$$

The i_{L1ref} time derivative, $i_{L_1 ref}$, is obtained from (33) using $\dot{e}_{pv}$ from (30) while considering that $i_{L_1} = e_{i_{L1}} + i_{L_1 ref}$, yielding (35).

$$\dot{i}_{L_1 ref} = -k_{PV} e_{i_{L1}} - \frac{C_1 k_{PV}^2}{\gamma} e_{PV} + \frac{1}{\gamma} \dot{i}_{PV} - \frac{C_1}{\gamma} \ddot{v}_{PVref} - i_{L_1 ref} \frac{\dot{\gamma}}{\gamma} \tag{35}$$

Consequently, the $e_{i_{L1}}$ time derivative in (34) is written as (36), taking into account (19) and (35).

$$\dot{e}_{i_{L1}} = -\frac{v_p}{L_1} + \frac{v_{PV} + v_p}{L_1} \gamma - \left(- k_{PV} e_{i_{L1}} - \frac{C_1 k_{PV}^2}{\gamma} e_{PV} + \frac{1}{\gamma} \dot{i}_{PV} - \frac{C_1}{\gamma} \ddot{v}_{PVref} - i_{L_1 ref} \frac{\dot{\gamma}}{\gamma} \right) \tag{36}$$

Taking into account the input voltage Lyapunov function (31), a recursively defined composite Lyapunov function (37), [105], with similar properties to (31), is considered for the inductor current.

$$V_i = e_{PV}^2 / 2 + e_{i_{L1}}^2 / 2 \tag{37}$$

Considering (30), (34) and (36), the Lyapunov function (37) time derivative is (38).

$$\begin{aligned} \dot{V}_i = & -k_{PV} {e_{PV}}^2 + e_{i_{L1}} \left[\frac{-v_p}{L_1} + \frac{v_{PV} + v_p}{L_1} \gamma + e_{PV} \left(\frac{C_1 {k_{PV}}^2}{\gamma} - \frac{\gamma}{C_1} \right) \right. \\ & \left. - k_{PV} e_{i_{L1}} + \frac{C_1}{\gamma} \ddot{v}_{PVref} - \frac{1}{\gamma} \dot{i}_{PV} + i_{L_1 ref} \frac{\dot{\gamma}}{\gamma} \right] = -k_{PV} {e_{PV}}^2 - k_{i_L} {e_{i_{L1}}}^2 \end{aligned} \tag{38}$$

To guarantee stability, the $\dot{V}_i$ value must obey $\dot{V}_i = -k_{PV} e_{PV}{}^2 - k_{i_L} e_{i_{L1}}{}^2$, thus the constant k_{i_L} must be positive, so that the $\dot{V}_i$ function is negative. Thus, equating the term relative to $e_{i_{L1}}$ (within the square brackets) to $-k_{i_L} e_{i_{L1}}{}^2$, the controller $\dot{\gamma}$ in (39) is received.

$$\dot{\gamma} = \frac{1}{i_{L_1 ref}} [\frac{v_p}{L_1}\gamma - \frac{v_{PV} + v_p}{L_1}\gamma^2 - e_{PV}(C_1 k_{PV}{}^2 - \frac{\gamma^2}{C_1}) + e_{i_{L1}}(k_{PV} - k_{i_L})\gamma - C_1 \ddot{v}_{PVref} + \dot{i}_{PV}] \qquad (39)$$

The time integral of this equation returns the duty cycle that controls the DC/DC converter to obtain the maximum power regulating the DC/DC converter input voltage. As expected, the back-stepping technique provided a virtual control $\dot{\gamma}$ and the controller has to go back through an integrator.

Fig. 45 depicts a flow chart in order to summarize the design and implementation of the backstepping controller in the dsPIC.

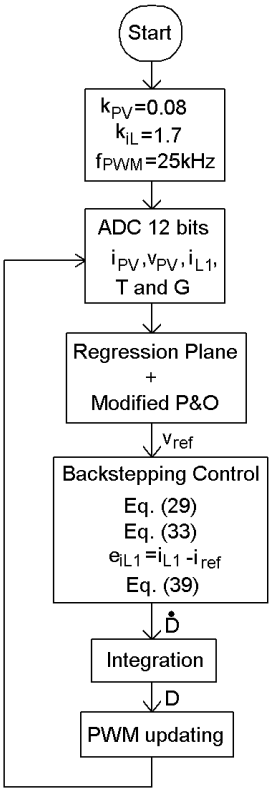

Fig. 45. DC/DC converter backstepping implementation flow chart

The sampling time for the control loop is 10 ms and the PWM frequency is 25 kHz with a 10 bits PWM resolution. Besides, the duty cycle change rate is 10 ms and it is updated with the sampling time. The integrated development environment (IDE) is MPLAB and the programming language is C. The PWM frequency and k_{PV} and k_{iL} constant values are defined. Then, the analogical digital converter reads the value of the PV module output current and voltage, the inductor current, the temperature and the irradiance. After that, the regression plane and the modified P&O algorithm are applied to obtain the reference voltage that should be reached to achieve the maximum power. Once the reference voltage is known,

the backstepping control calculates the time derivative of the buck-boost converter duty cycle and then this value is integrated. Finally, the PWM is updated in each control loop.

2.3.4.2 Adaptive Backstepping Control

The proposed adaptive backstepping controller is a modification of the backstepping control. The objective is also to control the duty cycle of the DC/DC converter switch, regulating the output voltage of the PV modules so as to track the reference voltage. It is based on the fact that the inductor and the capacitor of the buck-boost converter are unknown or have variations. It has a learning capacity to solve the model uncertainty by means of an on-line estimation of the unknown or changeable parameters. Thus, the capacitor is renamed as $\theta = C_1$ and the inductor as $\phi = 1/L$. Another parameter is used to make the calculations easier, $\psi = 1/C_1$. Then, the backstepping steps should be followed again, defining the voltage error and obtaining the virtual control input i_{L1ref}. After that, the same Lyapunov function to the backstepping control is proposed, obtaining the same stabilization function or reference current. Then, the current error is defined and another Lyapunov function is proposed (the same as the backstepping control, (38)), (40).

$$\begin{aligned} \dot{V}_i &= -k_{PV} {e_{PV}}^2 + e_{iL1}\Big[v_p\phi + (v_{PV} - v_p)\gamma\phi + \\ & e_{PV}\Big(\frac{{k_{PV}}^2}{\gamma}\theta - \gamma\psi\Big) - k_{PV} e_{iL1} + \frac{\ddot{v}_{PVref}}{\gamma}\theta - \\ & \frac{1}{\gamma}\dot{i}_{PV} + \hat{\dot{i}}_{L1ref}\frac{\dot{\gamma}}{\gamma}\Big] = -k_{PV} {e_{PV}}^2 - k_{iL} {e_{iL1}}^2 \end{aligned} \tag{40}$$

From that, the controller (41) is obtained.

$$\dot{\gamma} = \frac{1}{\hat{\dot{i}}_{L1ref}}[-v_p\gamma\hat{\phi} - (v_{PV} - v_p)\gamma^2\hat{\phi} - e_{PV}({k_{PV}}^2\hat{\theta} - \gamma^2\hat{\psi}) + e_{iL1}(k_{PV} - k_{iL})\gamma - \ddot{v}_{PVref}\hat{\theta} + \dot{i}_{PV}] \tag{41}$$

where $0 < \gamma < 1$, $i_{L1ref} \neq 0$ and $\hat{\theta}$, $\hat{\phi}$ and $\hat{\psi}$ are the estimated parameters and their errors are (42), (43) and (44).

$$\tilde{\theta} = \theta - \hat{\theta} \tag{42}$$

$$\tilde{\phi} = \phi - \hat{\phi} \tag{43}$$

$$\tilde{\psi} = \psi - \hat{\psi} \tag{44}$$

Now, replacing (41) in (40) and the estimation parameters by their errors, yields (45).

$$\dot{V}_i = -k_{PV} e_{PV}{}^2 + e_{iL1}[v_p\tilde{\phi} + (v_{PV} - v_p)\gamma\tilde{\phi} + \frac{e_{PV} k_{PV}{}^2}{\gamma}\tilde{\theta} - e_{PV}\gamma\tilde{\psi} - k_{iL} e_{iL1} + \frac{\ddot{v}_{PVref}}{\gamma}\tilde{\theta}] \quad (45)$$

In order to achieve the parameter adaptation laws for $\hat{\theta}$, $\hat{\phi}$ and $\hat{\psi}$, different Lyapunov functions are defined, (46), (47) and (48).

$$V_3 = \frac{1}{2}\xi^{-1}\tilde{\phi}^2 \quad (46)$$

$$V_4 = \frac{1}{2}\Delta^{-1}\tilde{\theta}^2 \quad (47)$$

$$V_5 = \frac{1}{2}\Gamma^{-1}\tilde{\psi}^2 \quad (48)$$

The time derivatives of this Lyapunov functions are (49), (50) and (51), replacing the time derivative of the errors by the time derivative of the parameters, which is zero, minus the time derivative of the estimated parameters.

$$\dot{V}_3 = -\xi^{-1}\tilde{\phi}\dot{\hat{\phi}} \quad (49)$$

$$\dot{V}_4 = -\Delta^{-1}\tilde{\theta}\dot{\hat{\theta}} \quad (50)$$

$$\dot{V}_5 = -\Gamma^{-1}\tilde{\psi}\dot{\hat{\psi}} \quad (51)$$

where γ, Δ and Γ are constants and positive.

Finally, the Lyapunov function is (52).

$$\begin{aligned}\dot{V} = \dot{V}_2 + \dot{V}_3 + \dot{V}_4 + \dot{V}_5 = -k_{PV} e_{PV}{}^2 - k_{iL} e_{iL1}{}^2 \\ + [(v_p(1-\gamma) + v_{PV}\gamma)e_{iL1} - \frac{1}{\xi}\dot{\hat{\phi}}]\tilde{\phi} + \\ [e_{iL1}(\frac{e_{PV}}{\gamma}k_{PV}^2 + \frac{\ddot{v}_{PVref}}{\gamma}) - \frac{1}{\Delta}\dot{\hat{\theta}}]\tilde{\theta} + \\ [-e_{PV}\gamma e_{iL1} - \frac{1}{\Gamma}\dot{\hat{\psi}}]\tilde{\psi}\end{aligned} \quad (52)$$

Thus, in order to make the state vector vanish asymptotically, the terms with the estimation parameters must be cancelled, (53), (54) and (55).

$$\dot{\hat{\phi}} = \xi[v_p(1-\gamma) + v_{PV}\gamma]e_{iL1} \tag{53}$$

$$\dot{\hat{\theta}} = \Delta\left[\frac{e_{PV}}{\gamma}k_{PV}^2 + \frac{\ddot{v}_{PVref}}{\gamma}\right]e_{iL1} \tag{54}$$

$$\dot{\hat{\psi}} = -\Gamma e_{PV}\gamma e_{iL1} \tag{55}$$

2.3.4.3 DC/AC Power Converter Control

The backstepping method is proposed in this work to generate original and new controllers for the DC/AC converter considering the single-phase converter slow and fast dynamics, [88]-[90]. Dynamics separation is needed as the grid power injected/retrieved by an inverter is not constant during a grid period. The backstepping controller ensures stable and robust operation as an inverter (minimum phase system) or as a rectifier (non-minimum phase system).

In the DC/AC inverter/rectifier, the control objective for the backstepping controller is to regulate the inverter input voltage, so that a telecom load can be supplied, as well as to source or sink AC sinusoidal current from the grid. The backstepping controller also needs two loops, an inner fast dynamics AC current loop and an outer slow dynamics DC voltage loop. In order to keep the DC voltage nearly constant, from (21) the square of the input voltage must track a reference voltage squared to guarantee the energy balance within a grid voltage period, transferring the PV array excess power, if available, to the grid side, or sinking power from it in sunless or shadowing conditions. To source (or sink) AC current to the grid, the inductor current should track a sinusoidal reference current to ensure low harmonic injection into the electrical network ensuring low harmonic distortion.

To apply the backstepping method, the error of the outer loop voltage v_p must be defined as the difference between the square of voltage average value v_p^2 at the converter DC side and the square of its reference v_{pref}^2 value. This reference must be reached by the control to enforce v_{pref}^2 to v_p^2 to make any deviation vanish, (56).

$$e_{v_p^2} = v_{pref}^2 - v_p^2 \tag{56}$$

The time derivative of the input voltage error, $\dot{e}_{v_p^2}$ considering (21), is (57).

$$\dot{e}_{v_p^2} = \dot{v}_{pref}^2 - 2(i_p v_p - i_{L_2} v_R)/C_2 \tag{57}$$

As in the DC/DC converter, a similar Lyapunov function for the inverter input voltage is chosen and its time derivative is (58).

$$\dot{V}_{vp} = e_{v_p^2}\, \dot{e}_{v_p^2} = -k_{vp}\, e_{v_p^2}^2 \tag{58}$$

$\dot{V}_{vp}$ is negative if k_{vp} is constant and positive. Taking into account this derivative and (57), a stabilizing function, I_{L_2}, can be obtained, (59).

$$I_{L_2} = (2i_p v_p - C_2 k_{vp} e_{v_p^2} - C_2 \dot{v}_{pref}^2)/(2v_R) \tag{59}$$

To separate the converter dynamics, this stabilizing function must relate the systems energy balance to the amplitude value I_{L2} of the i_{L2} current. Since I_{L2RMS} is the control parameter for the inner AC current loop, the fast dynamics trajectory can be foreseen considering that $i_{L_2 ref}$ must be a sinusoidal current in phase with v_R for $I_{L_2} > 0$, or with opposite phase for $I_{L_2} < 0$. This sinusoidal current reference can be written as $i_{L_2 ref} = I_{L_2} v_{Rpu} = I_{L_2} v_{Rpu}$, v_{Rpu} being a grid synchronized unity amplitude sinusoid. To track this reference, the loop error is (60).

$$e_{i_{L2}} = i_{L_2 ref} - i_{L_2} \tag{60}$$

A control law must be obtained using the time derivative of the error in (60).

$$\dot{e}_{i_{L_2}} = \dot{i}_{L_2 ref} - (\beta v_p - v_R)/L_2 \tag{61}$$

The Lyapunov function for the DC/AC converter inductor current is (62).

$$\dot{V}_{i_{L2}} = e_{i_{L_2}} \dot{e}_{i_{L_2}} = -k_{i_{L2}} e_{i_{L2}}^2 \tag{62}$$

$\dot{V}_{i_{L2}}$ will be negative if $k_{i_{L2}}$ is constant and positive. Taking into account this derivative and (61), the modulation waveform β is obtained.

$$\beta = (L_2 \dot{i}_{L_2 ref} + v_R + k_{i_{L2}} L_2 e_{i_{L_2}})/v_p \tag{63}$$

where $v_p \neq 0$.

2.4 Partial Shading Conditions

Maximum power point tracking algorithms should track the maximum power point from photovoltaic generators under any environmental condition. Nevertheless, most of conventional MPPT methods fail when the solar cells are affected by partial shading conditions due to the fact that multiple peaks appear in the P-V characteristic curve. Besides, some problems can appear in PV systems such as mismatch losses that lead to several maxima in the P-V curves.

The mismatch concern is one of the main causes of losses in the power extraction. They are originated from the interconnection of solar cells under different conditions or properties. Therefore, the solar cell under the worst condition determines the PV array global output power. The most common and damaging type of mismatch losses is the short-circuit current because it is caused by the partial shading of the solar modules.

The partial shading existence is originated from adjacent buildings, trees, moving clouds or even fast changes in the irradiance. A PV module is exposed to different values of irradiance under partial shading conditions and the shaded cells absorb the energy supplied by the unshaded cells that are exposed to higher irradiance leading to highly localized power dissipation and converting this power into heat. The power generated by the partially shaded modules is much lower than the energy generated by unshaded PV cells. This may be detrimental to the PV modules and the performance of the PV system is seriously deteriorated.

To solve one of these problems, bypass diodes are connected across the solar modules to prevent the shaded modules from consuming the power generated by the unshaded PV modules. Therefore, the current flows through an alternative path when there are shaded solar cells. As a consequence, the I-V and P-V characteristic curves present multiple power peaks under non-uniform irradiance, complicating the MPP tracking.

Former MPPT algorithms are ineffective because they are not able to distinguish local maxima from global ones. Different MPPT methods have been modified to improve the tracking (the P&O, the incremental conductance, neuro-fuzzy controllers or DEPSO).

In this thesis a new method using artificial vision to track the maximum power in real time is proposed. Many methods are able to detect pattern of shadows previously studied, [43], [106]. In this case, the PV systems used to have cameras to monitor the solar power plants and the same camera can be used to detect the solar cells affected by partial shading, identifying the changes of shape and intensity of the shadows in real time. The used PV system is presented in Fig. 46. It shows series-connected PV modules and they are supervised by a webcam the PV system consists of PV panels, buck-boost converters, DC/AC converters and loads.

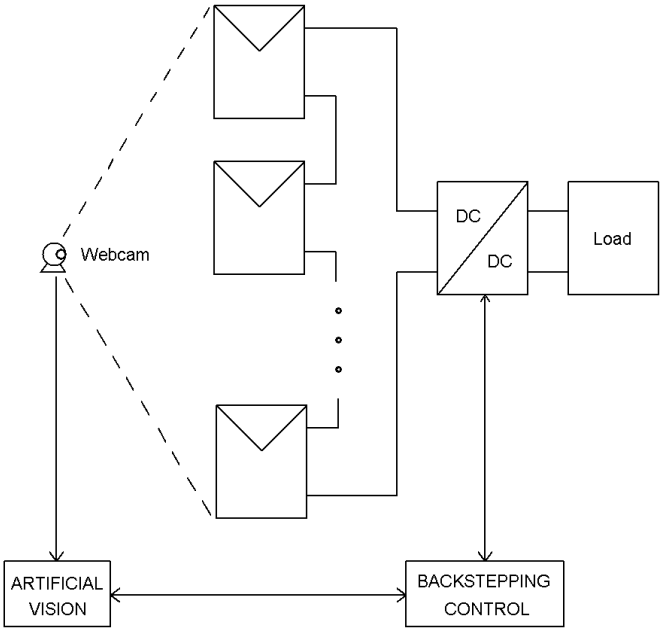

Fig. 46. PV system with webcam to detect shadows

The main problem of the series-connected modules is a significant power drop when a solar cell or a group of cells are affected by the slightest shadow. To solve this, bypass diodes, $D_{bi,}$ to reduce the impact of mismatch losses are connected in anti-parallel with each solar module, as shown in Fig. 47. Thus, the current flows through these diodes when the PV panel is shaded.

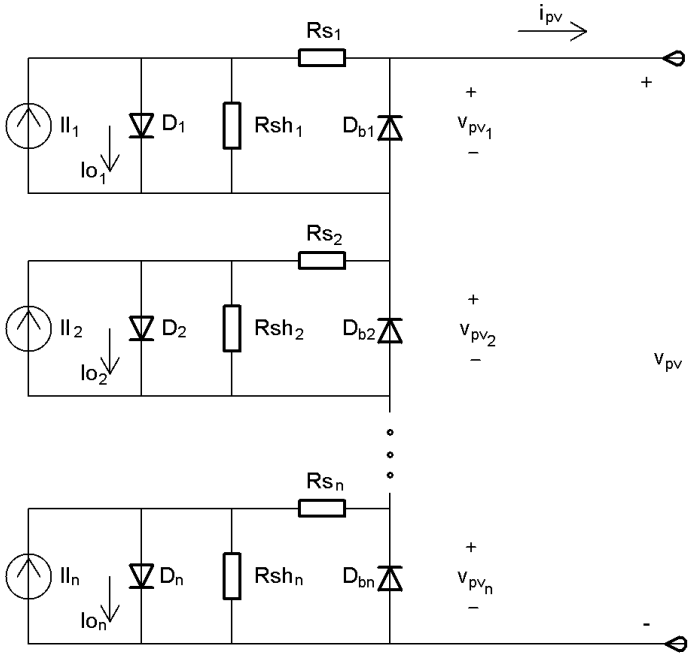

Fig. 47. PV solar cells equivalent circuit with bypass diodes

When the PV array is under a unique value of irradiance, the P-V curves behave similar to Fig. 9, with only one peak. However, if there are non-uniform conditions, the P-V curves have multiple peaks, as shown Fig. 48.

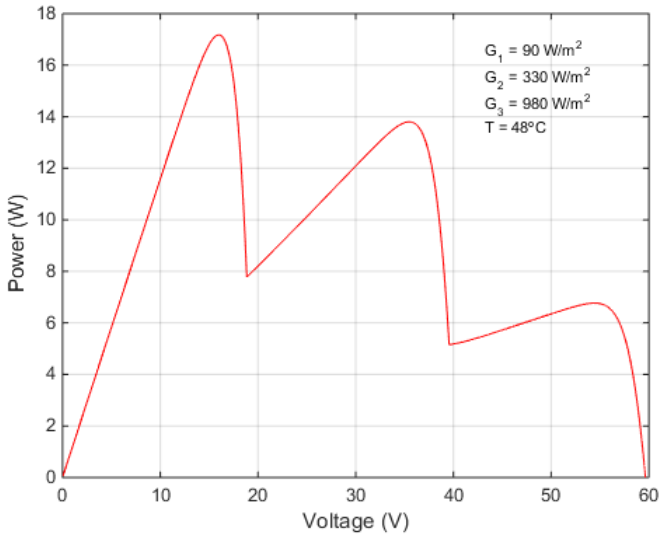

Fig. 48. P-V curve under non-uniform irradiance

The proposed method to find and track the MPP is based on the artificial vision with a backstepping control. The artificial vision identify the solar cells affected by the partial shading and the intensity of the shadows providing the backstepping control the reference voltage that supplies the maximum power whereas the non-linear control regulates the PV array output voltage.

Now, the artificial vision algorithm is described. Firstly, the each PV module image should be selected (the images are the region of interest, ROI). Afterward, the image is converted to another color format, in this case Hue-Saturation-Value (HSV), [83] because this format can achieve a robust color thresholding. Then, it is essential the image thresholding to choose the color range related to the shadows and remove the information that it is not required. Thus, a binary image is obtained. After that, a morphological transformation is needed to filter the noise. Next, the closed region of adjacent pixels with similar properties should be identified in the blob detection. An area filtering is used to select the shadow minimum size to be taken into account. Finally, the intensity of the shadows is obtained using an estimated irradiance $\hat{G}$, and the reference voltage is calculated using the sensor measurements T, v_{PV} and, i_{PV}.

The estimated irradiance is obtained from a regression plane built with the PV array output voltage and current measurements and the temperature. This plane provides the estimated irradiance required to calculate the irradiance of each PV panel or also called shadow irradiance, G_s. The images received by the webcam supply the area of the shaded solar cells and the shadow intensity, I_s. I_s the mean value of the gray level of the pixels contained in the blob (0 is the value when there is no shadow and 255 is the value for the maximum level of darkness) and it is expressed as the gray percentage. The shadow irradiance is empirically calculated using the shadow intensity in several experiments under non-uniform conditions. G_s is an attenuation of each PV module irradiance. When there is no shadow, the shadow irradiance is the estimated irradiance.

Once G_s is obtained, the reference voltage that supplies the maximum power can be achieved. For that, a theoretical voltage is calculated from the shadow irradiance and the

temperature using a regression plane to lead the MPPT method where the maximum is located, guaranteeing the peak of the P-V curve is found. Afterwards this voltage is adjusted to achieve the reference voltage needed by the backstepping control to regulate the PV array output voltage.

2.5 Additional Application: PV Active Power Line Conditioner

Apart from using the DC/AC converter to transfer energy and convert DC voltage to AC output voltage, the inverter used in the grid-connected PV systems are able to operate as power line conditioners in the point of common connection. Therefore, the conditioning stage could be removed. The main disadvantage of this stage is the high cost and using the PV system inverter brings a savings in devices and cost. Thus, a distributed global compensation in the electrical network is achieved taking into consideration the different connection points in the systems based on renewable energy.

The ideal DC/AC power converter output voltage waveforms are sinusoidal whereas in real inverters the signals has harmonics and the voltage waveforms are not sinusoidal. The connection of non-linear and unbalanced loads in the power electrical systems can lead to a disruption of the electrical wave quality because a high level of harmonic distortion is originated causing disturbance in the transport, distribution and consumption of electrical energy. This can originate problems in the electrical network and the connected loads.

One conventional solution to the harmonic compensation problem is the use of tuned passive filter. The filter is tuned with the harmonic that needs to be removed. The drawback of this technique is that the compensation is fixed and it can produce resonance in the grid.

Other devices able to improve the electrical wave quality are the active power line conditioner (APLC) or also so-called active power filter (APF). These conditioners, connected in series or in parallel with the system loads, allow the compensation of harmonics, reactive power, unbalance, etc. The devices consist of two stages, the controls stage and the power stage. The control stage calculates the reference current or voltage that the APLC should supply to the system to obtain the desired compensation. The power stage includes a DC/AC power converter to generate the real compensation signal. The main disadvantage of using conditioners is the high cost of acquiring them.

Thus, one of the aims of the active filters is to remove harmonics, creating harmonics components to cancel the load components that require to be compensated. Besides, these devices can also compensate reactive power, negative sequence current, balancing currents that flow by the phases if the loads are unbalanced. This way, the current by the neutral is decreased (if there is neutral) and the conditioners can reduce the voltage harmonics as well. Therefore, the filters are able to make the grid current be sinusoidal and the voltage provided to the load have the same waveform. Another benefit is that the active conditioners can adapt themselves to the changes that appear in the electrical network and the load harmonics, reducing the possibility of resonance compared to passive filters. The conditioners are connected in the point of common connection (PCC) of the system in order to not allow the current harmonics flow by the whole system.

Series active power filters provide the required compensation voltage to obtain sinusoidal voltage. Apart from canceling harmonic voltages, they can balance and regulate the load and line voltage. There are also hybrid conditioners. They consist of an active and a passive filter. One of their objectives is to compensate harmonics avoiding resonance problems as well as reducing cost.

In PV systems, a DC/AC converter transfers the power to the electrical network and it is the responsible for the compensation of the harmonic current, the current reactive component and the inverse sequence current when it operates as active power line conditioner connected in parallel with the load. The filter insulates the voltage harmonics between the distribution system and the load, it regulates the voltage, cancel harmonics, correct the power factor, balance the line currents when the load is unbalanced and cancel the neutral current. Besides, the conditioner balances the voltage in the PCC.

Ideally, the APLC in parallel behaves as a controlled current source. The active conditioner injects harmonic currents of the load in the point of common connection in counter-phase to cancel them. Thus, the filter obtains a sinusoidal waveform for the source current. The system with the PV conditioner is shown in Fig. 49. The total PV conditioner current, i_T, has two components. The first one is i_{PV}, which transports the active power generated by the PV array. The second one is i_C, the current needed to compensate the non-active power of the electrical loads. The current supplied by the conditioner should cancel the harmonic currents of the load, i_L.

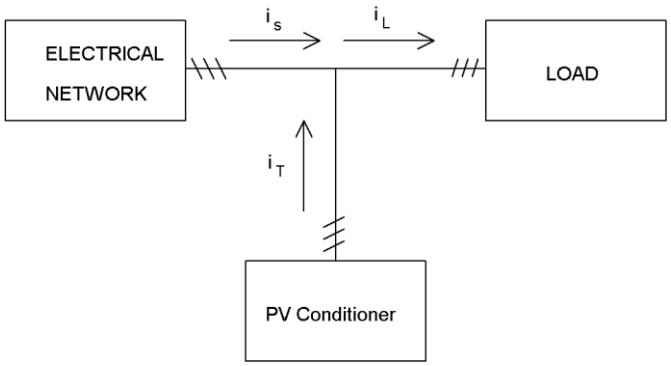

Fig. 49. System with the PV active power line conditioner connected

This is achieved by means of the power stage, the control stage and a closed control loop for the compensation current. The control circuit calculates the compensation current that should be injected by the conditioner from the voltage and current measurements of the load. Using an appropriate control strategy is possible to guarantee that the source current is sinusoidal, balanced, it is direct sequence and in phase with the fundamental component of the source voltage. Thus, the filter supplies the reactive component required to cancel the harmonics.

The reference current calculated by the control circuit is achieved from the load current and voltage. A PWM technique is used to switch the components of the inverter to reconstruct the waveform required. Therefore, the filter output current needs to be measured to obtain the reference current.

The control strategy is the responsible for obtaining the harmonic compensation using a calculating algorithm from the voltage and current measurements. In this work, a sinusoidal compensation is proposed to achieve a sinusoidal, balanced, positive sequence grid current and in phase with the positive sequence fundamental component of the source voltage. A modification of the vectorial theory, [95], is used to calculate the reference current. It fulfills the objectives for three-phase non-linear and unbalanced loads with a reduction of computation time compared with other methods. Besides, the hysteresis band modulation is used. Apart from that, the control must include the injection of the generated PV active power.

To determine the i_c, the load active current i_a has to be calculated, (64). The shunt active conditioner will supply the difference between the load current and its active component. The current i_a depends on the active power, P in W, and on the voltage.

$$i_a = \frac{P}{V_{1+}^2} v_{1+} = G_1 v_{1+} \tag{64}$$

where v_{1+} is the fundamental direct sequence voltage at the PCC in V, G_1 is the equivalent conductance of the load 1/Ω and P is the active power consumed by the load in W.

The compensation current $i_{c,}$ (65), is the difference between the load current and its active component. The conditioner must follow this current, that it is the reference current.

$$i_C = i_L - G_1 v_{1+} \tag{65}$$

Additionally, to achieve the maximum power extraction from the PV system, the input voltage of the inverter must be adjusted because the voltage in the capacitor has to be constant. A parameter ρ is added to the conductance that depends on the error between the capacitor voltage and the reference voltage. These parameters allow a proportional control to guarantee a constant DC voltage.

$$i_C = i_L - (G_1 \pm \rho) v_{1+} \tag{66}$$

The total reference current of the PV conditioner is in (67).

$$i_T = i_{PV} + i_C = i_L - K v_{1+} \tag{67}$$

where K is $G_1 - G_1' \pm \rho$, being K an adjustment parameter. If the error between this reference current and the inverter output current is higher than a hysteresis band, the state of semiconductors will change to follow the reference.

2.6 Experimental Set-up

An experimental platform containing a subset of devices is designed to validate the proposed methods. The platform includes commercial PV modules to convert the light into electrical energy (or a PV simulator in some experiments to obtain the conditions required to carry out sets of experiment), a built buck-boost converter to transfer the energy from one voltage level to another, a commercial DC/AC power converter to trasnfer the energy to the electrical network, loads that need power, a PC to supervise the tests and a commercial webcam to make the shadow detection possible.

2.6.1 PV Array

The electrical features of the commercial PV modules are described in Table 6. A PV module has 36 solar cells in series. A PV module is used in the papers where the backstepping control is explained for the buck-boost converter whereas three series connected PV modules are used in the submitted paper where the PV system is under partial shading conditions. In the paper where the backstepping control for the inverter is detailed, a PV simulator is used. The PV module is depicted in Fig. 50.

Table 6. Electrical Parameters of a Commercial PV Module

Parameter	Values
Maximum Power	20 W
Maximum Power Voltage	17.5 V
Maximum Power Current	1.15 A
Open-circuit Voltage	21.6 V
Short-circuit Current	1.28 A

Fig. 50. Commercial PV module with 36 solar cells in series

2.6.2 Buck-Boost Power Converter

The required experimental plaftorm to validate the proposed control methods requires a DC/DC converter connected at the output of the photovoltaic array.

In this case, a buck-boost converter has been built taking into consideration the power that can be generated by the PV modules. The buck-boost converter operates in continuous conduction mode and for that it is required to calculate the inductor and capacitor needed to fulfill this mode. First of all, the inductor should be designed, (68), to make the DC/DC converter works in CCM once the switching frequency is known, 25 KHz.

$$L_{\min} = \frac{(1-D)^2 v_0}{2 I_{0\min} f_s} \tag{68}$$

According to the system electrical parameters and considering the minimum value of the duty cycle, the minimum value of the inductor to accomplish CCM is 10 mH.

Besides, it is essential to calculate the capacitor value. Its aim is to provide the buck-boost converter output current in the switching cycle in the conduction period and it works as an output filter. The worst condition for the capacitor is when the DC/DC converter output current and the duty cycle have maximum values and it should fulfill (69).

$$C_{\min} = \frac{I_{0\max} D}{\Delta V_0 f_s} \tag{69}$$

In this case, the duty cycle is has the maximum value. The capacitor must have a value high enough to absorb all the energy and filter the voltage without exceeding the ripple voltage limits, where the buck-boost converter output voltage ripple is ΔV_o. The minimum value of the capacitor is 146.4 µF in the worst case.

The current has also a ripple. Thus, a high commutation frequency and a high inductor value can be used in order to decrease it. In this case, the two capacitors have values of 1000 µF and 5700 µF whereas the inductor is 20 mH.

Then, LEM, LA25-NP and LV25-P, sensors are added to measure the currents and voltages at the input and output of the converters. Another sensor is used to measure the temperature, a LM35. For that, the voltage and current probes have resistors that required to be calculated. The voltage sensor LEM LV 25-P with the resistors is presented in Fig. 51, where R_M is the LEM probe and R_1 is the resistor in the primary.

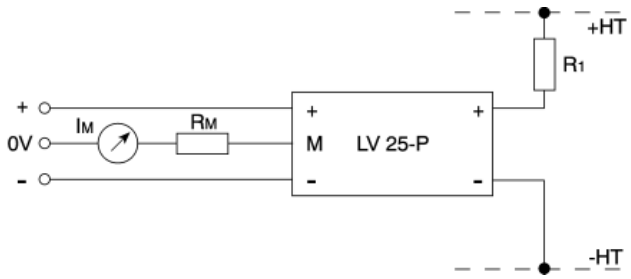

Fig. 51. LEM LV 25-P sensor connection

R_1 is achieved depending on the rms current that flows for the primary. This current is 10 mA and the voltage V_{+HT_-HT} is 100V.Thus, the resistor is calculated applying the Ohm's law, obtaining a value of 10 kΩ.

$$R_1 = \frac{V_{+HT\_-HT}}{I_{\mathrm{P}rms}} \tag{70}$$

The resistor in the voltage probe should be calculated to obtain the maximum range of measurement at the output, 5 V, when the input voltage is 100 V. It is 5 V because the ADC readings use unipolar channels from 0 to 5 V. Thus, the secondary has a value of the rms current that flows at the probe output when the primary has a value of 10 mA. That current is 25 mA. Then, the resistor is obtained using Ohm's law and the value achieved is 200 Ω.

$$R_M = \frac{V_M}{I_{Srms}} \tag{71}$$

The same process using the Ohm's law is repeated with the current sensor. In this case, the R_M is calculated. Fig. 52 shows the resistor in the current probe.

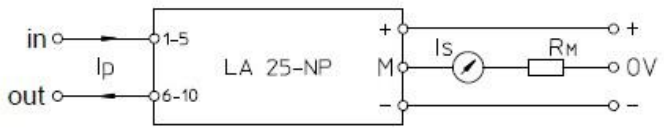

Fig. 52. LEM LA 25-NP sensor connection

The secondary rms current is 25 mA and the reading through a bipolar channel is from -10 V to 10 V. then, applying Ohm's law, the resistor is obtained, achieving a value of 200Ω.

$$R_M = \frac{V_M}{I_{Srms}} \tag{72}$$

With the obtained values, a board is designed to measure the buck-boost converter input and output voltages and the buck-boost converter output, input and inductor current, as shown Fig. 53.

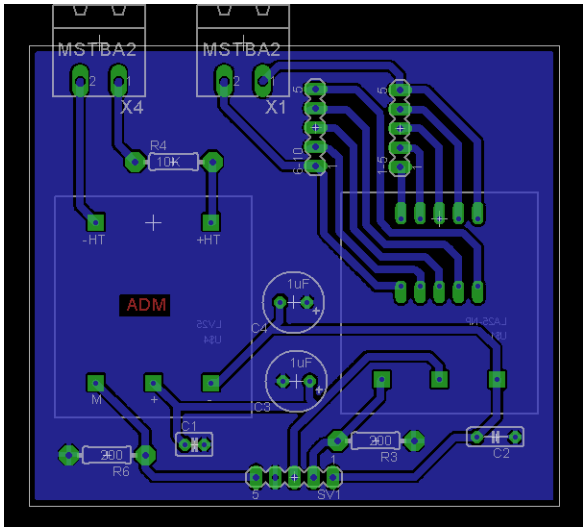

Fig. 53. LEM LA 25-NP and LEM LV 25-P sensors connection

Fig. 54 shows the buck-boost converter with current and voltage sensors required and a low-cost microcontroller. The PV array feeds the converter using a MOSFET CSD19536KCS driven by FOD3180 driver and a diode MBR10200. The microcontroller used is the dsPIC30F3013. In the DC/DC converter backstepping control, the equations implemented in the microcontroller are (29), (33) and (39).

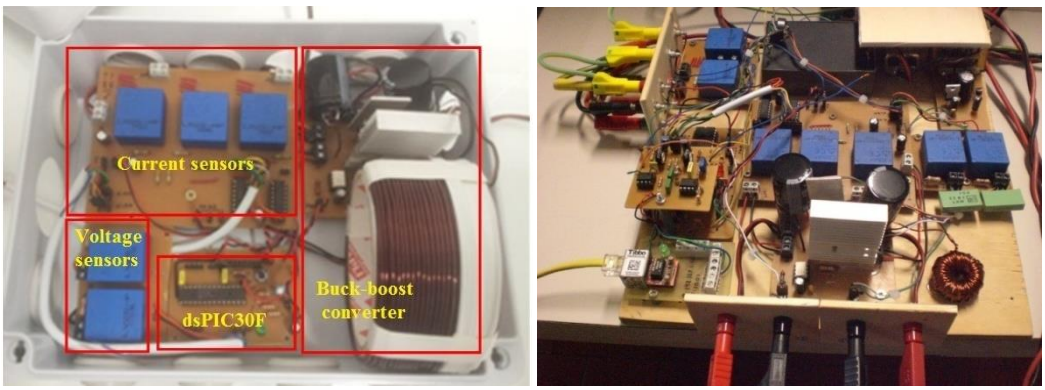

Fig. 54. Sensors, dsPIC and buck-boost converter

Fig. 55 depicts the proposed design of the buck-boost power converter including the isolated MOSFET switching signal using the FOD3180 driver whereas Fig. 56 shows the control board to control the buck-boost converter, the sensors and communication with the PC and to send the data in real-time.

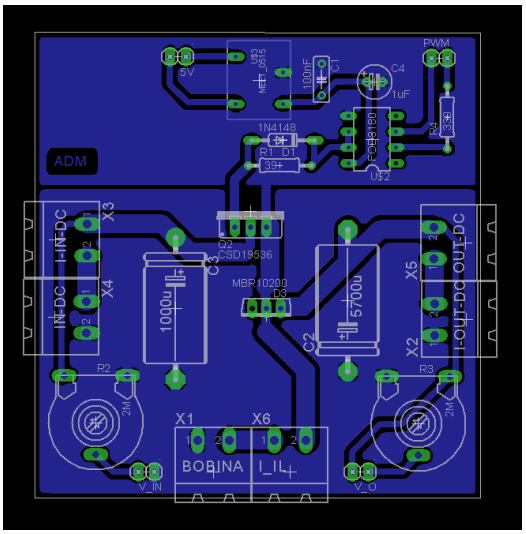

Fig. 55. Buck-boost converter PCB

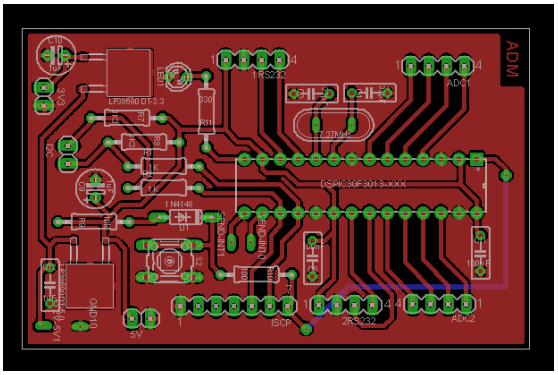

Fig. 56. dsPIC PCB

In the cases where the irradiance measure is necessary, a pyranometer or a compensated calibrated cell is used. The buck-boost converter input voltage range is 10 V – 70 V whereas the maximum DC/DC converter output voltage is 100 V. The maximum power that can be transferred by this converter is 70 W. Finally, the output voltage ripple is 0.5 % of v_p. The sampling time for the control loop is 10 ms, and the PWM frequency is 25 kHz with a 10 bits PWM resolution.

2.6.3 Experimental Platform 1

In the first part of this work, an experimental platform has been designed. It is consists of a commercial solar array (PV module), a built buck-boost converter with the dsPIC and the voltage and current sensors in a box, a resistive load and a PC to supervise the control parameters, as it is shown in Fig. 57.

Fig. 57. Experimental system supervised by PC

In order to compare the simulation results with the real curves, a PV module has been tested outdoor in the platform. The PV array output is connected to the DC/DC converter input and the buck-boost converter output is connected to the resistive load. Fig. 58 shows the I-V and P-V curves of the simulated PV model and the characteristic curves of the used PV module in order to prove the accuracy between them under different environmental conditions.

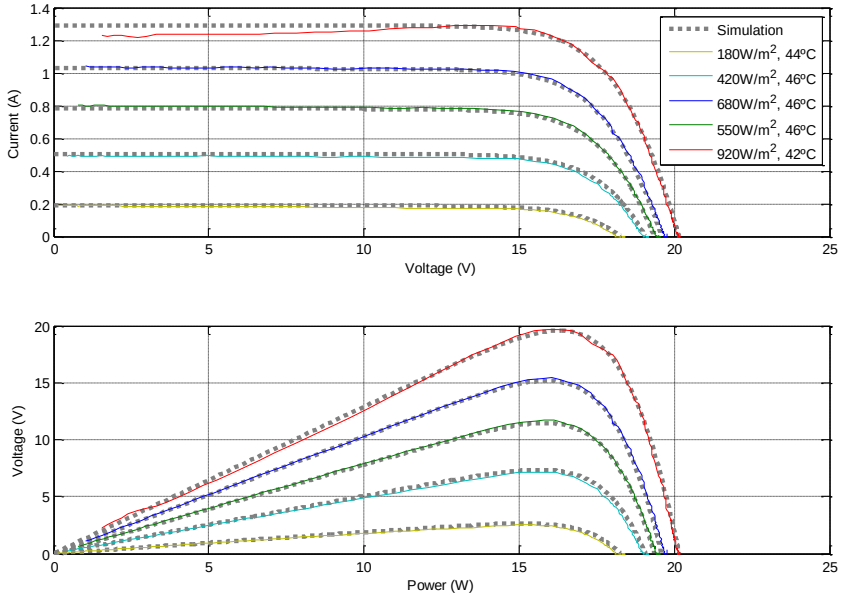

Fig. 58. Comparison between I-V and P-V curves of the simulated PV model and the real PV module

As it can be seen, the simulated curves and the experimental curves are very similar. The obtained values coincide until 99% in the worst cases.

Then, this experimental platform has been used to test the validity of the backstepping controller for the buck-boost converter.

2.6.4 DC/AC Power Converter

A DC/AC converter is required to transfer the energy to the electrical network. It is connected at the buck-boost converter output or at the output of a DC load. Then, the inverter output is connected to the grid or/and to an AC load.

In the experimental platform, a single-phase full-bridge inverter is used to check the performance of the backstepping control. It is a commercial inverter, the 4 CT60M-18F driven by IR2130 with an output inductance of L_2=13.1 mH. A transformer has been included between the DC/AC converter output and the weak load voltage 230V, 50Hz grid due to the use of the telecom load when the load is connected between the DC/DC converter and the DC/AC converter. The telecom equipment has usually a nominal voltage of 48 V, although it can range from 36 V to 75 V, and it needs a transformer to adapt the inverter AC output voltage to the grid voltage. The used inverter is depicted in Fig. 59.

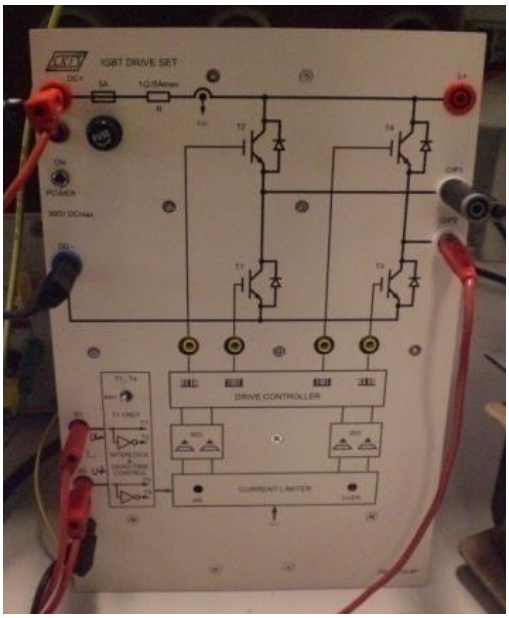

Fig. 59. DC/AC power converter

The dsPIC was programmed to implement the constant frequency buck-boost modulator, the 3 level DC/AC converter modulator, the sampling of the voltages v_{PV}, v_p, v_R and currents i_{L1}, i_{L2}, 10kHz, the grid synchronization, and the calculations needed in equations (59) and (63). The values of the controller gains are $k_{PV}=5$, $k_{i_L}=75$, $k_{vp}=4.7$ and $k_{i_{L2}}=4600$.

The dsPIC is supervised, via a local internet connection using a EM203 serial-to-Ethernet module, by a pc computer where a virtual instrument has been programmed using Visual Basic, to monitor the PV system operation and to generate the MPP reference voltage v_{PVref}.

Fig. 60 presents the design implemented to detect the zero-crossing in order to obtain the grid synchronization. A comparator with dynamic hysteresis is used, [108]-[109].

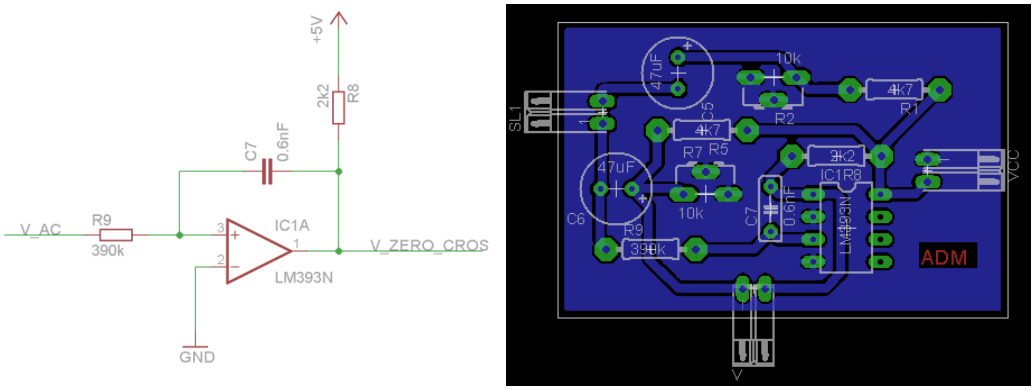

Fig. 60. Zero-crossing detector for synchronization

2.6.5 Experimental Platform 2

Apart from the commercial PV modules, a PV simulator, [107], is used to obtain a variety of irradiances. In this case the PV simulator includes a KC50TPV panel simulator. At nominal irradiance the KC50T simulator outputs nearly 54W and their electrical parameters are listed in Table 7.

Table 7. Electrical Parameters of Solar Module Simulator at 1000W/m^2

Parameter	Values
Maximum power(P_{max}), in W	54 (+10%/-5%)
Maximum power voltage (V_{MPP}), in V	18.2
Maximum power current (I_{MPP}), in A	3
Open-circuit voltage (V_{OC}), in V	21.7
Short-circuit current (I_{SC}=I_1), in A	3.31
Equivalent series resistance R_s in Ω	0.2
Equivalent shunt resistance R_{sh} in Ω	200

The panel simulator used in some experiments is shown in Fig. 61, [107].Then, the PV array feeds a buck-boost converter built, as it is shown below.

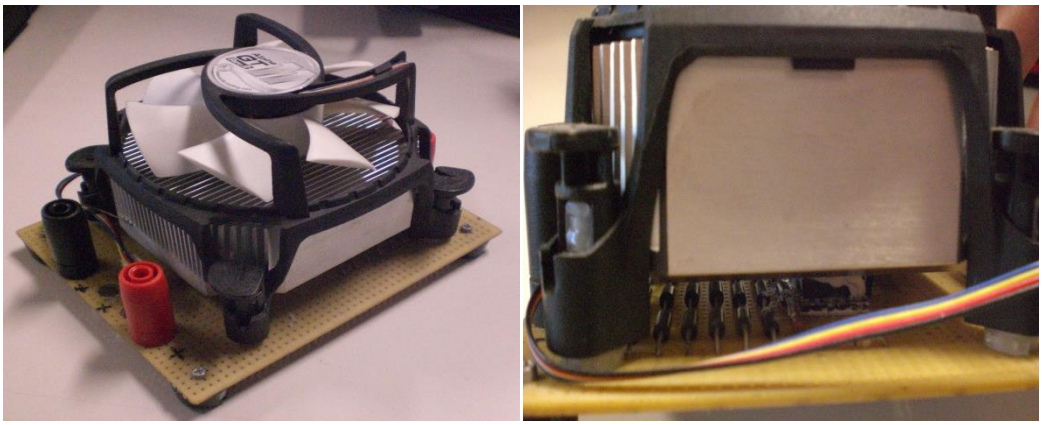

Fig. 61. PV simulator used for the experimental tests

The experimental platform is designed to verify the performance of the backstepping controls in the buck-boost converter and in the DC/AC converter, as Fig. 62 shows.

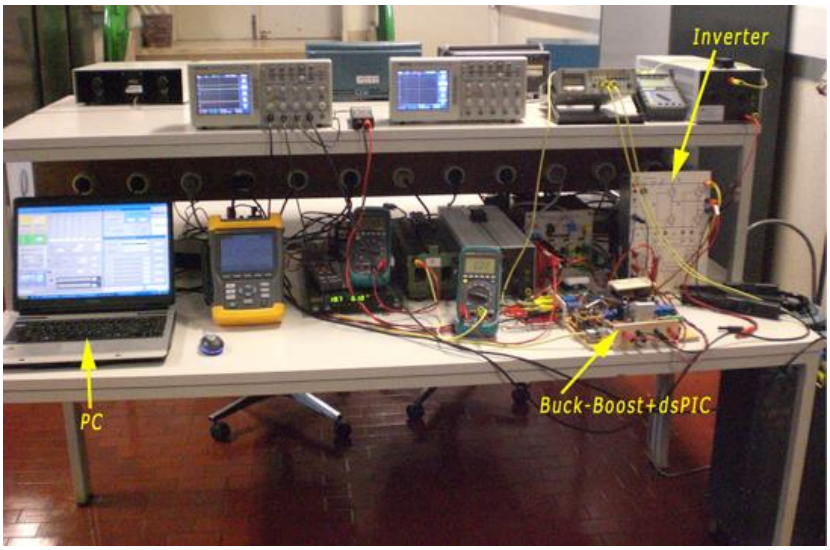

Fig. 62. Grid-connected PV system experimental platform

It is a grid-connected PV system and it consists of a PC to supervise the tests, the PV modules or the PV simulator, the built buck-boost converter with the dsPIC, the DC/AC converter and the load, including measurement devices and an autotransformer to connect the inverter with the grid.

2.6.6 Experimental Platform 3

This platform has been designed to prove the proposed method for PV systems under partial shading conditions. Three PV modules have been connected in series and the P-V curves could present from one maximum to three maximum, depending on the irradiance of each panel. The experimental P-V curves are obtained for different values of irradiance and temperature and they are compared with the simulated model, as Fig. 63 depicts. The obtained values coincide about 99 % in the worst cases.

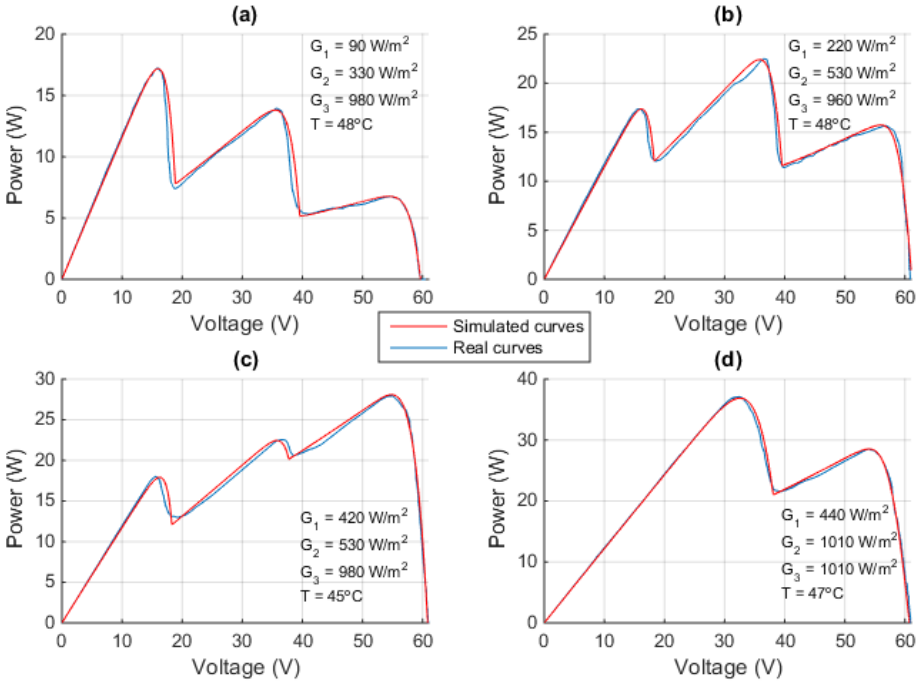

Fig. 63. P-V curves under non-uniform conditions

In the first three cases there are P-V curves with three peaks due to the fact that each solar module has different irradiance from the other panels whereas the last P-V curve shows two maxima because the partial shading is only affecting one PV module. Besides, Fig. X shows three different areas where the peaks are located regardless of the number of peaks. The first area where the maximum is located is about 15 V, then the peak is located approximately in 36 V and finally the maximum can also be located at 56 V. In this case, the experimental platform has been located outdoor to test the proposed method with a webcam, as Fig. 64 depicts.

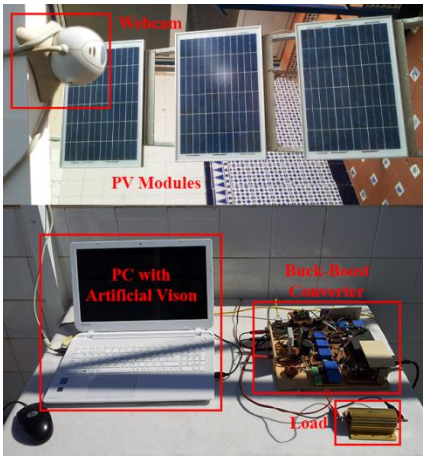

Fig. 64. Experimental platform to validate the artificial vision algorithm

Experimental tests have been carried out so as to validate the proposed AVMPPT algorithm. The experimental results show the achievement of the MPP regardless of the region where the maximum peak is located, the number of peaks, the shape of the shadows and the shaded solar cells area. In this case, the PV modules supplies power to a 150 Ω DC

load through the built buck-boost converter. Then, the backstepping controller is the responsible for the MOSFET switching of the buck-boost converter to regulate the PV modules output voltage. The control loop sampling time is 10 ms and the PWM frequency is 25 kHz. Several partial shading conditions are tested in the experiments to verify that the MPP is achieved under any environmental and partial shading conditions. Table 8 presents the tests shadow intensity and the shadow irradiance.

Table 8. Shadow intensity and shadow irradiance

Interval (s)	**I_SPV_1 (%)**	**I_SPV_2 (%)**	**I_SPV_3 (%)**	**G_SPV_1 (W/m^2)**	**G_SPV_2 (W/m^2)**	**G_SPV_3 (W/m^2)**
[0 - 8)	40	60	0	280	150	1000
[8 - 17)	40	0	0	280	1000	1000
[17 - 28)	40	60	0	280	150	1000
[28 - 40)	40	0	0	280	1000	1000
[40 - 58)	40	60	0	280	150	1000
[58 - 67)	40	0	0	280	1000	1000
[67 - 80]	0	0	0	1000	1000	1000

The first column presents the interval of time and the next three columns shows the shadow intensity. Finally, the last three columns show the shadow irradiance. There is a PV module with a shadow intensity of zero, I_{sPV3}, i. e. that this solar panel is not affected by any shadow, whereas the other two PV modules are partially shaded. The first partially shaded solar panel has a shadow intensity of approximately 40 % from the beginning of the experiment until 67 s when the shadow disappears. The second partially module reaches a shadow intensity of 60 % in an intermittent time. The solar module with $I_{sPV3} = 0$ is related to a shadow irradiance of 1000 W/m^2. Then, the intensity shadow of 40 % corresponds to G_s = 280 W/m^2 and the intensity of 60 % is related to 150 W/m^2. In these partial shading conditions, three different P-V curves are obtained. In next three intervals of time, from 0 s to 8 s, from 17 s to 28 s and from 40 s to 58 s, a three-peak P-V curve is obtained due to the fact that two PV modules are partially shaded and one solar panel is unshaded. In this case, the maximum power point is located at the first zone of the P-V curve, similar to Fig. 63 (a). During the intervals ranged from 8 s to 17s, from 28 s to 40 s and from 58 s to 67 s, there is a two-peak P-V curve because only one PV solar panel is partially shaded and the other two PV modules are unshaded. Now, the MPP is located at the second area of the P-V curve, being the P-V curve similar to Fig. 63 (d). There is a last interval from 67 s to 80 s where the P-V curve only has one peak because the partial shading conditions disappeared and the maximum power point is at the third area of the P-V curve.

Fig. 65 depicts the voltage that provides the maximum power point and the power supplied by the PV system. Fig. 65 (a) presents the theoretical voltage, v_s, that provides the maximum power; the reference voltage achieved by the artificial vision algorithm and it is the voltage that should be tracked, v_{ref}; and the measured PV modules output voltage, v_{PV}. In this case, three different values of voltage are obtained. When the three-peak PV curve

appears, the voltage achieved is 14.3 V. Then, the voltage obtained is 32 V when there are two peaks in the PV curve. Finally, when there is no partial shading, the voltage reached is 49.6 V. These voltages provide the maximum power. It shows how the PV modules output voltage tracks the reference voltage, proving the correct performance of the PV system control.

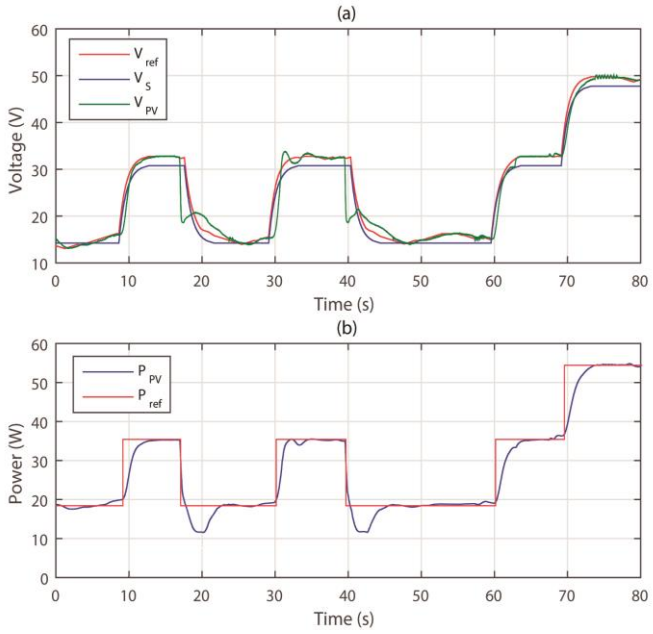

Fig. 65. (a) Shadow voltage, reference voltage and buck-boost converter input voltage. (b) DC/DC converter input power

Fig. 65 (b) presents the power that should be reached for different environmental conditions, P_{ref}, and the power provided by the PV system, P_{PV}. The power extracted from the PV modules reaches the reference power in the three different values obtained, validating the artificial vision algorithm. The maximum power reached is 18.5 W when v_{PV} is 14.3 V and it is related to the three-peak PV curve case. In the case of the two-peak PV curve, the power obtained is 35.6 W when the voltage that supplies the maximum power is 32 V. Finally, when the three PV modules are unshaded and there is only one peak in the PV curve, the maximum power is 54.8 W for a voltage value of 49.6 V. The efficiency of the power tracking is about 99.6 %.

3 Contributions

This Doctoral thesis work is focused on the non-linear backstepping control of a buck-boost power converter and DC/AC power converter to track the maximum power point in PV systems and transfer the power to the electrical network.

First, a backstepping control has been implemented to regulate the PV array output voltage in simulation to achieve the maximum power point. For that, a grid-connected PV system that consists of a PV array, a buck-boost converter, a DC/AC converter and a load has been modeled in Matlab-Simulink. Then, the designed backstepping controller is implemented in the system. The backstepping control is based on Lyapunov functions guaranteeing the locally stability of the system. This control is robust and tests have been carried out to validate its performance.

Once the proposed control is verified in simulation, the method has been proved in an experimental platform. In this case, the experimental platform consists of a commercial PV module, a built buck-boost converter and a DC load to test the backstepping controller in the DC/DC converter. The experiments carried out validate the performance of the proposed control. The voltage that provides the maximum power point is always achieved under changeable environmental conditions, testing the robustness of the control.

Finally, the non-linear backstepping controller is proposed to control the DC/AC power converter in an experimental platform, including the connection to the grid. Thus, backstepping controllers are obtained for distributed hybrid photovoltaic (PV) power supplies of telecommunication equipment. The grid-connected PV system contains the PV array, the built DC-DC buck-boost converters linked to single-phase inverters and telecom equipment as loads. The backstepping approach is robust and able to cope with the grid non-linearity and uncertainties, providing DC input current and voltage controllers for the buck-boost converter to track the PV panel maximum power point, regulating the PV output DC voltage to extract maximum power; unity power factor sinusoidal AC smart-grid inverter currents and constant DC link voltages suited for telecom equipment; and inverter bidirectional power transfer. Experimental results are obtained from a lab set-up controlled by one low-cost dsPIC. Results show the controllers guarantee maximum power transfer to the telecom equipment/AC grid, ensuring steady DC link voltage while absorbing/injecting low harmonic distortion current into the smart-grid.

All these works have been published in different journals between the years 2014/2015. Point 2.2 presents each paper.

Journal paper 1:

Title: Backstepping Controller Design to Track Maximum Power in Photovoltaic Systems.

Authors: A. D. Martin, J. R. Vazquez.

Publication: *Automatika*, vol. 55, no. 1, pp. 22-31, Jan. 2014.

Journal paper 2:

Title: Backstepping Control of a Buck-Boost Converter in an Experimental PV-System

Authors: J. R. Vazquez, A. D. Martin.

Publication: *Journal of Power Electronics*, vol. 15, no. 6, Nov. 2015.

Journal paper 3:

Title: Backstepping control of smart grid-connected distributed photovoltaic power supplies for telecom equipment.

Authors: A. D. Martin, J. M. Cano, J. F. A. Silva, J. R. Vazquez.

Publication: *IEEE Trans. on Energy Conversion*, June 2015, online published:
http://ieeexplore.ieee.org/xpl/articleDetails.jsp?arnumber=7115109&queryText=Aranzazu+D.+Martin&newsearch=true&searchField=Search_All

Los artículos que forman parte de este apartado de la tesis han sido retirados debido a restricciones relativas a los derechos de autor. Dichos artículos han sido sustituidos por la referencia bibliográfica, enlace al texto completo y resumen.

- Delgado Martín, A., Rodríguez Vázquez, J.: "Backstepping Controller Design to Track Maximum Power in Photovoltaic Systems". Automatika. Vol. 55, n. 1, págs. 22-31, (2014). DOI: 10.7305/automatika.2014.01.289

Enlace al texto completo del artículo:
http://dx.doi.org/ 10.7305/automatika.2014.01.289

RESUMEN:
This work presents a new control method to track the maximum power point of a grid-connected photovoltaic (PV) system. A backstepping controller is designed to be applied to a buck-boost DC-DC converter in order to achieve an optimal PV array output voltage. This nonlinear control is based on Lyapunov functions assuring the local stability of the system. Control reference voltages are initially estimated by a regression plane, avoiding local maximum and adjusted with a modified perturb and observe method (P&O). Thus, the maximum power extraction of the generating system is guaranteed. Finally, a DC-AC converter is controlled to supply AC current in the point of common coupling (PCC) of the electrical network. The performance of the developed system has been analyzed by means a simulation platform in Matlab/Simulink helped by SymPowerSystem Blockset. Results testify the validity of the designed control method.

- Rodríguez Vázquez, J., Delgado Martín, A.: "Backstepping Control of a Buck-Boost Converter in an Experimental PV-System". Journal of Power Electronics. Vol. 15, n. 6, págs. 1584-1592 (2015). DOI: 10.6113/JPE.2015.15.6.1584

Enlace al texto completo del artículo:
http://dx.doi.org/10.6113/JPE.2015.15.6.1584

RESUMEN:
This paper presents a nonlinear method to control a DC-DC converter and track the Maximum Power Point (MPP) of a Photovoltaic (PV) system. A backstepping controller is proposed to regulate the voltage at the input of a buck-boost converter by means of Lyapunov functions. To make the control initially faster and avoid local maximum, a regression plane is used to estimate the reference voltages that must be obtained to achieve the MPP and guarantee the maximum power extraction, modifying the conventional Perturb and Observe (P&O) method. An experimental platform has been designed to verify the validity and performance of the proposed control method. In

this platform, a buck-boost converter has been built to extract the maximum power of commercial solar modules under different environmental conditions.

- Delgado Martín, A., Cano, J.M., Silva, J.F.A., Rodríguez Vázquez, J.: "Backstepping control of smart grid-connected distributed photovoltaic power supplies for telecom equipment". IEEE Transactions on Energy Conversion. Vol. 30, n. 4, (2015). DOI: 10.1109/TEC.2015.2431613

Enlace al texto completo del artículo (solo para miembros de la UHU):
http://dx.doi.org/10.1109/TEC.2015.2431613

RESUMEN:
Backstepping controllers are obtained for distributed hybrid photovoltaic (PV) power supplies of telecommunication equipment. Grid-connected PV-based power supply units may contain dc-dc buck-boost converters linked to single-phase inverters. This distributed energy resource operated within the self-consumption concept can aid in the peak-shaving strategy of ac smart grids. New backstepping control laws are obtained for the single-phase inverter and for the buck-boost converter feeding a telecom equipment/battery while sourcing the PV excess power to the smart grid or to grid supply the telecom system. The backstepping approach is robust and able to cope with the grid nonlinearity and uncertainties providing dc input current and voltage controllers for the buck-boost converter to track the PV panel maximum power point, regulating the PV output dc voltage to extract maximum power; unity power factor sinusoidal ac smart grid inverter currents and constant dc-link voltages suited for telecom equipment; and inverter bidirectional power transfer. Experimental results are obtained from a lab setup controlled by one inexpensive dsPIC running the sampling, the backstepping and modulator algorithms. Results show the controllers guarantee maximum power transfer to the telecom equipment/ac grid, ensuring steady dc-link voltage while absorbing/injecting low harmonic distortion current into the smart grid.

4 Additional Research Work

4.1 Additional Papers

A modification of the backstepping control has been also proposed, an adaptive backstepping controller. This non-linear control also tracks the maximum power point regulating the buck-boost converter input voltage regardless of the parameter values of the DC/DC converter.

Apart from the proposed algorithms, other MPPT algorithms have been implemented in order to compare the results of different techniques. A neuro-fuzzy system with fuzzy logic MPPT control is designed and then it is compared with the P&O algorithm, the PI control and the proposed backstepping control.

Finally, the research work about the PV system control under partial shading conditions using artificial vision with backstepping control is sent to a paper, being in revision at this moment.

Additional system performance related with power quality has been proposed. A PV active power line conditioner is designed to transfer the maximum power to the electrical network and to compensate the reactive power and the non-linear loads. Besides, the use of switching output reactances is proposed to improve the compensation of a shunt active power filter. Finally, two power indexes have been tested in a distributed network, the Load Characterization Index (LCI) that identifies linear and non-linear loads in the power systems and the Unbalance Current Ratio (UCR) that assigns the responsibility for system unbalance to load and source sides.

All these works have been published in different journals and international conferences between the years 2013/2015. Next, the reference of each paper is presented.

Paper 1:

Title: Adaptive Backstepping Control of a DC/DC Converter in Photovoltaic Systems.

Authors: A. D. Martin, J. R. Vazquez, R. S. Herrera.

Publication: *IEEE Eurocon*, pp. 949-955, July 2013, presented in International Conference.

Paper 2:

Title: Neuro-Fuzzy Control of a Grid-Connected Photovoltaic System with Power Quality Improvement

Authors: J. R. Vazquez, A. D. Martin, R. S. Herrera.

Publication: *IEEE Eurocon*, pp. 850-856, July 2013, presented in International Conference.

Paper 3:

Title: MPPT Algorithms Comparison in PV Systems. P&O, PI, Neuro-Fuzzy and Backstepping Controls

Authors: A. D. Martin, J. R. Vazquez.

Publication: *IEEE ICIT*, pp. 2841-2847, Mar. 2015, presented in International Conference.

Paper 4:

Title: Unbalance and Harmonic Distortion Assessment in an Experimental Distribution Network

Authors: A. D. Martín, R. S. Herrera, J. R. Vázquez, P. Crolla, G. M. Burt.

Publication: *Electric Power Systems Research*, vol. 127, pp. 271-279, 2015, **published in JCR**.

Paper 5:

Title: Improvement of Shunt Active Power Filter Compensation through Switching Output Reactances

Authors: J. R. Vazquez, A. D. Martin, N. M. Garrido.

Publication: *IEEE ICIT*, pp. 2708-2713, Mar. 2015, presented in International Conference.

Los artículos que forman parte de este apartado de la tesis han sido retirados debido a restricciones relativas a los derechos de autor. Dichos artículos han sido sustituidos por la referencia bibliográfica, enlace al texto completo y resumen.

- Delgado Martín, A., Rodríguez Vázquez, J., Herrera,R.S.: "Adaptive Backstepping Control of a DC/DC Converter in Photovoltaic Systems". IEEE Eurocon, págs. 949-955, (2013). DOI: 10.1109/EUROCON.2013.6625096

Enlace al texto completo del artículo:
http://dx.doi.org/10.1109/EUROCON.2013.6625096

RESUMEN:
This paper presents a new nonlinear control method to regulate the voltage at the output of a DC-DC converter so as to achieve the maximum power point (MPP) of a photovoltaic (PV) system. The proposed adaptive backstepping controller of the system, based on Lyapunov functions to ensure locally stability, is applied to a buck-boost converter. A regression plane is used to initialize reference voltages and to make a modified perturb and observe method (P&O) faster, avoiding local maximum. Therefore, the maximum power extraction of the PV system is guaranteed. This system is grid-connected, thus, a DC-AC converter is connected to the buck-boost converter. The inverter supplies AC current in the point of common coupling (PCC) of the electrical network. The performance of the developed system has been analyzed by means a simulation platform in Matlab/Simulink.

- Rodríguez Vázquez, J., Delgado Martín, A., Herrera, R.S.: "Neuro-Fuzzy Control of a Grid-Connected Photovoltaic System with Power Quality Improvement". IEEE Eurocon, págs. 850-856 (2013). DOI: 10.1109/EUROCON.2013.6625082

Enlace al texto completo del artículo:
http://dx.doi.org/10.1109/EUROCON.2013.6625082

RESUMEN:
This paper presents a Photovoltaic Active Power Line Conditioner, a device designed to extract the maximum power of a photovoltaic (PV) system and to compensate the nonlinear and unbalanced loads of the electrical power systems. The grid-connected PV systems require DC-DC and DC-AC power converters to maximize the generated PV power and to inject an AC current to the network. In this work, a neuro-fuzzy system to achieve the Maximum Power Point (MPP) and a fuzzy logic control loop to ensure the Maximum Power Point Tracking (MPPT) of the PV system connected at DC side are designed. The DC-AC power converter control strategy includes an active compensation of the non-linear and unbalanced loads

connected to the electrical system. The performance of the PV conditioner with the neuro-fuzzy control designed has been analyzed through a simulation platform.

- Delgado Martín, A., Rodríguez Vázquez, J.: "MPPT Algorithms Comparison in PV Systems. P&O, PI, Neuro-Fuzzy and Backstepping Controls". IEEE ICIT, págs. 2841-2847, (2015). DOI: 10.1109/ICIT.2015.7125517

Enlace al texto completo del artículo (solo para miembros de la UHU):
http://dx.doi.org/10.1109/ICIT.2015.7125517

RESUMEN:

This paper presents a comparative analysis of control methods to extract the maximum power and to track the maximum power point (MPP) from photovoltaic (PV) systems under changeable environmental conditions. The PV system consists of a solar module and a DC/DC converter, in this case a buck-boost converter, connected to a load. The maximum power point tracking (MPPT) algorithms compared are the perturb and observe (P&O) method, the PI control, a neuro-fuzzy and fuzzy technique and finally a backstepping control. The parameters considered for the comparison are the efficiency of the MPPT algorithm taking into account the extracted power from the PV system, steady and dynamic response of the system under changeable conditions such as the temperature and the irradiance and the signals ripple. The methods have been compared and the algorithm with the best results has been implemented in an experimental platform.

- Delgado Martín, A., Herrera, R.S., Rodríguez Vázquez, J., Crolla, P., Burt, G.M.: "Unbalance and Harmonic Distortion Assessment in an Experimental Distribution Network". Electric Power Systems Research. Vol. 127, págs. 271-279, (2015). DOI: 10.1016/j.epsr.2015.06.005

Enlace al texto completo del artículo (solo para miembros de la UHU):
http://dx.doi.org/10.1016/j.epsr.2015.06.005

RESUMEN:

The identification of voltage and current harmonic distortion and voltage unbalance sources is one of the main problems in electric distribution systems. In order to overcome it, in this paper the use of two novel indices is proposed. On the one hand, the Load Characterization Index (LCI) is suggested to calculate the harmonic distortion introduced by the load. This index identifies linear and non-linear loads in the power systems. On the other hand, the Unbalance Current Ratio (UCR) is suggested to assign

the responsibility for system unbalance to load and source sides. Both indices can be calculated only from the measurement of the current at the input of the load and the voltage at the Point of Common Connection (PCC). The main objective of this paper is to test the performance of these two indices on an experimental three-phase electrical network. In order to do that, several experimental tests have been considered.

- Rodríguez Vázquez, J., Delgado Martín, A., Garrido, N.M.: "Improvement of Shunt Active Power Filter Compensation through Switching Output Reactances". : IEEE ICIT, págs. 2708-2713, (2015). DOI: 10.1109/ICIT.2015.7125497

Enlace al texto completo del artículo (solo para miembros de la UHU):
http://dx.doi.org/10.1109/ICIT.2015.7125497

RESUMEN:
The increase in non-linear loads in the electrical network deteriorates the voltage waveform quality. One of the most used methods to correct the quality lack is to use shunt, series or mixed topologies of active power filters. Mixed filters can compensate loads that generate voltage harmonics and current harmonics, but the economic investment is high. Commercial shunt filters are more widespread due to their design, modularity and cost; although their non-linear load tracking capability is limited. The aim of this work is to improve the shunt active filter reference tracking, designing a variable reactance at the filter output. The validity of the proposed design is analyzed through a Matlab-Simulink platform.

5 Conclusions and Future Work

5.1 Results and Conclusions

The main objective of this thesis is to design a non-linear backstepping controller to regulate the buck-boost converter input voltage to track the maximum power point in PV systems. Besides, another backstepping control is proposed to control the energy transfer from the PV system to the electrical network through a DC/AC converter. Thus, the main conclusions drawn from this Doctoral Thesis work can be summarized as:

1. A novel backstepping controller is designed and implemented to track the MPP in PV systems. For that, a grid-connected PV system is simulated in Matlab-Simulink to validate the performance of the system using the control proposed. In this work, the backstepping control has been applied to a buck-boost converter. This control has been proved to guarantee global asymptotic stability by means of Lyapunov functions. Besides, the robustness of the control has been also verified under perturbations, i. e. rapid changes in environmental conditions, obtaining a transient response of 0.04s. This control does not present an oscillatory behavior unlike the P&O algorithm. The performance of the system is 98.5% in the worst cases. Thus, the effectiveness of the backstepping method to control a buck-boost converter to extract the maximum power of a PV system has been validated.
2. Once the proposed control method is verified in simulation, an experimental platform is built to validate the backstepping control. In this case, PV commercial modules have been used connected to a built buck-boost converter. Then, the PV array supplies power to a DC load. The on-line supervised backstepping control has been implemented in a low-cost microcontroller, a dsPIC30F3013. The results confirm that the control works correctly because the reference voltage is always achieved for any environmental conditions. Thus, the tracking efficiency obtained for this non-linear control is higher than 99%. In stationary state, the control does not present an oscillatory behavior whereas the transient response is faster than the P&O algorithm because the power is stabilized after 3.3 s under a change in the irradiance and the P&O requires 8.4 s to stabilize the power under the same irradiance change. Finally, the efficiency of the built power converter block is about 90% in the worst cases, obtaining an efficiency of 99% in the best cases.
3. Besides, another non-linear backstepping controller is proposed to control the DC/AC converter to transfer power to the electrical network in an experimental grid-connected PV system. In this case, a PV array is feeding a buck-boost converter, and DC linked to a telecom load and a single-phase AC-DC converter connected to a smart-grid, configuring a sub-set of a distributed hybrid photovoltaic power supply for telecom equipment within the self-consumption concept. The backstepping control laws guarantee the MPP achievement, obtaining MPPT efficiency between 98.2% and 99.9%. The backstepping control

laws for the inverter regulate the DC telecom load voltage and control the AC grid current, absorbing/injecting nearly sinusoidal (THD = 1.6%, lower than the 3% required by the standards) grid currents at near unity power factor and the self-consumption can contribute to the smart-grid peak power shaving strategy. All the control laws (backstepping control laws for the buck-boost converter and for the DC/AC converter), fixed frequency converter modulators, voltage and current sampling and grid synchronization have been implemented in the low-cost microcontroller dsPIC30F4011. Besides, the experimental results show the performance of the PV self-consumption system using the backstepping control and the system dynamic behavior when the DC/AC converter changes operation from inverter to rectifier to adapt itself to the telecom load requirements. The robustness of the control laws allow the capacitance of real capacitors can vary almost 10 times around the rated value, while inductances can vary from 30% to nearly 300% of the rated value.

Additional research work is developed.

1. A backstepping control is also used in a PV system under partial shading conditions. For that, a novel artificial vision with the backstepping control is proposed to detect the shadows and track the maximum power point even when there is more than one peak in the P – V curves. This algorithm can avoid local maxima and it can lead the voltage directly to the area where the global maximum is located. The artificial vision algorithm provides the shadow irradiance of each solar panel, the area affected by the partial shading and the voltage that supplies the maximum power. Then, the backstepping controller tracks this reference voltage. An experimental platform using the built buck-boost converter is used to validate the performance of the proposed control. The results verify the detection of the shadows and the calculation of the shadow irradiance as well as the achievement of the maximum power point under different environmental conditions under partial shading conditions. The global maximum is always reached regardless of where it is located and the number of peaks of the P-V curve. The tracking efficiency is between 98.7% and 99.6%.
2. A modification of this control is proposed as well, the adaptive backstepping control. The adaptive backstepping controller also tracks the MPP of a PV system controlling the buck-boost converter input voltage and it is able to make the system adapt itself when there is uncertainty in the values of the inductor and the capacitor of the buck-boost converter. The control has a learning capacity to solve model uncertainty by means of an-online estimation of the unknown or changeable parameters. Thus, the adaptive backstepping controller can be used regardless of the buck-boost converter parameter values. This control has been validated in simulation. The simulation results show that the efficiency of the PV system is between 98% and 99.8% and the transient response is about 0.01 s under sudden changes in the environmental conditions.
3. Apart from the backstepping controls, a neuro-fuzzy system and a fuzzy logic controller are designed to track the maximum power point in PV systems. In this

case, the neuro-fuzzy system calculates the PV array output reference voltage that provides the MPP and a fuzzy logic control loop to achieve the reference voltage given by the neuro-fuzzy system. This method has been tested in simulation, achieving better results than the methods based on P&O and without oscillations.

4. Finishing the MPPT algorithms, a comparison between four different methods have been made. In this case, the techniques compared are the conventional P&O algorithm, a PI control, the neuro-fuzzy and fuzzy logic controller and the proposed backstepping control. One of the main conclusions obtained by the comparison is that the signals ripple of the P&O algorithm involves an oscillatory behavior about the MPP voltage even in stationary state, leading to power losses. The other three methods do not present oscillation and they have smooth transient response. Taking into consideration the MPPT efficiency, the backstepping control achieves better results, obtaining a performance between 98.2% and 99.9%.
5. Regarding power quality, a PV active power line conditioner system has been proposed. Thus, the global control strategy supplies the maximum power to the electrical network through a DC/AC converter and compensates the non-linear and unbalanced loads connected to the electrical system. In this work, sine compensation is designed to obtain balanced, sine and direct sequence network current. This control is effective, simple and easy to implement with a reduced computation time, achieving a transient response lower than half a period. The results obtained in simulation show that the source current THD (Total Harmonic Distortion) can be reduced from 48% to 1.26% when the PV active power line conditioner is connected.
6. Besides, continuing with power quality, two quality indices have been tested to assess the harmonic distortion and the unbalance introduced by different loads connected to the same point of common coupling in an experimental distribution network. The first index is the UCR that assigns responsibility for system unbalance to load and source sides and the LCI that calculates the harmonic introduced by the load. These indices have been compared with other common indices. Results show both indices work properly even with unbalanced and distorted voltages. Moreover, LCI identifies the capacitors as linear loads according to the Standard proposition when other methods fail to identify them as linear loads.
7. Finally, a shunt active power line conditioner with a power stage including a switching output reactance has been designed to improve the conditioner tracking when it works with variable non-linear loads. The simulation results show the effectiveness of the proposed design. The obtained voltage THD is low and similar to the conventional active power conditioner whereas the current THD is reduced about 50% with respect to the former conditioner. Thus, the conditioner tracking capability has been improved significantly.

5.2 Future Work

Proposed future work can be divided in the following topics:

1. Validation of the artificial vision algorithm proposed method in a grid-connected PV system under partial shading conditions. In this work, the backstepping control designed for the DC/AC converter will be added to the backstepping control for the buck-boost converter and the artificial vision to track the MPP under non-uniform irradiance and transfer the power to the electrical network. All the controls will be implemented in the same low-cost microcontroller.
2. Besides, the PV active power line conditioner will be tested in an experimental platform including non-linear loads to validate the global control strategy that supplies the maximum power to the grid and compensates the non-linear and unbalanced loads.
3. The improved shunt active power line conditioner with the switching output reactance will be also verified in an experimental platform to validate the simulation results.
4. Finally, a PV active power line conditioner with the switching output reactance and the backstepping control to track the MPP can be connected in a distributed generation network to help shave midday peaks of grid power consumption.

6 Resumen en Español.

6.1 Introducción

La demanda de energía y el número de sistemas de generación distribuida está creciendo por todo el mundo durante los últimos años. Por esa razón, es esencial el uso de energías renovables además de las convencionales, [1]-[3]. Hoy en día el uso de las energías renovables está muy extendido y particularmente los sistemas de energía fotovoltaica. La energía fotovoltaica suministra electricidad a casas aisladas y a dispositivos autónomos e inyecta energía eléctrica en las redes de potencia. Estos sistemas producen electricidad a grande escala también a través de las redes de distribución.

Los sistemas fotovoltaicos están basados en la generación de energía por medio de células fotovoltaicas (FV). Las células solares convierten la energía solar en energía eléctrica para ser transferida a los sistemas eléctricos, [4]. El modelo la célula FV está formado por un fuente de corriente, un diodo en antiparalelo, una resistencia en paralelo y otra en serie, [4]. El modelo puede ser simulado en Matlab-Simulink, [5]. Una única célula FV genera poca energía y es necesaria la asociación de células para obtener la tensión y la intensidad requerida. Por lo tanto, las células se conectan en serie y en paralelo para conseguir un módulo FV o un array fotovoltaico. La potencia generada por los módulos FV depende de las condiciones ambientales, tales como la temperatura y la irradiancia. Las curvas características I – V y P – V se obtienen de los módulos FV para determinar donde se encuentra el máximo de la curva, [6]-[7]. El máximo pico de la curva P – V es el punto de máxima potencia (MPP) que puede ser generado por el módulo FV. Por lo tanto, el sistema debería trabajar en ese punto para obtener mayor eficiencia. Así, hay un solo punto de trabajo para unas condiciones determinadas de cada módulo, siendo la potencia máxima únicamente para una determinada tensión de salida, [8]. El MPP cambia cuando varía la temperatura y la irradiancia.

El sistema FV conectado a red está formado por módulos FV, un convertidor DC/DC, un convertidor DC/AC y un sistema de control, [9]. Los módulos FV y el convertidor DC/DC se pueden conectar a una carga o puede ser conectado a la red eléctrica usando un inversor para inyectar corriente sinusoidal en fase con la tensión de la red.

El objetivo del convertidor DC/DC es regular la tensión de salida del módulo FV para mantenerla en el MPP, [10]. Para ello, la variación del nivel de tensión se consigue con el uso y control de los dispositivos de conmutación. Los convertidores DC/DC son circuitos electrónicos que controlan la carga y descarga de sus elementos pasivos modificando su ciclo de trabajo, [11]. Hay diferentes topologías de convertidores, [12]. En este trabajo, se usa un convertidor buck-boost, cuya tensión de salida puede ser mayor o menor que la tensión de entrada. Se trabajará en modo de conducción continua, donde la intensidad fluye continuamente por el inductor sin llegar a ser cero, [11].

Posteriormente, una estrategia de control se diseña para obtener la máxima transferencia de bajo cualquier condición ambiental para que el array PV trabaje en el MPP. Hay diferentes algoritmos para el seguimiento del punto de máxima potencia (MPPT), [13].

Los algoritmos calculan el MPP en cada instante de tiempo para cualquier irradiancia y temperatura, ya que el MPP cambia debido a que las condiciones ambientales están continuamente variando. El algoritmo más usado es el Perturb and Observe (P&O), [10], [14]-[15]. Otro control usado frecuentemente es el control proporcional e integral (PI), [16], aunque existen bastantes métodos, como el de conductancia incremental, [17]-[19], el de Fractional Open Circuit Voltage, [20]-[21], Fractional Short Circuit Current, [22]-[23] y Ripple Correlation Control, [24]-[25]. Existen otros algoritmos basados en redes neuronales artificiales, [26]-[27], y lógica difusa, [28]-[29]. Otra técnica es el Sliding Mode control, [10], [32]-[33].

Los algoritmos MPPT convencionales son capaces de alcanzar el MPP bajo condiciones estándar. Sin embargo, pueden aparecer problemas en los sistemas FV tales como pérdidas cuando las células FV no son idénticas o cuando aparece sombreado parcial, [34]-[36], conduciendo este fenómeno a la obtención de curvas P – V con múltiples máximos y haciendo que los antiguos algoritmos no alcanzan el máximo global. Bajo condiciones de sombreado parcial, un módulo PV es expuesto a diferentes valores de irradiancia y las células sombreadas absorben la energía suministrada por las no sombreadas que están expuestas a una irradiancia mayor llevando a una alta disipación de potencia localizada y convirtiendo esta potencia en calor. Esto puede ser perjudicial para los módulos FV y la eficiencia del sistema FV se ve seriamente deteriorada, [37]-[40]. Para resolver este problema se usan diodos bypass conectados en los módulos FV, [41]-[42], para impedir que los módulos sombreados consuman la potencia generada por los módulos no sombreados. Por lo tanto, las curvas P – V presentan múltiples máximos bajo condiciones no uniformes de irradiancia, complicando el seguimiento del MPP, [43]-[45]. Diferentes métodos MPPT han sido modificados para realizar el seguimiento, [46], como el P&O, [47]-[48], conductancia incremental, [49], redes neuronales, [50]-[52], lógica difusa, [53]-[54], o DEPSO, [55]-[56]. Otros métodos se centran en la medida de la tensión de circuito abierto y corriente de cortocircuito o de la irradiancia, [57]-[59], entre otros, [60]-[61].

Los sistemas FV conectados a red necesitan un convertidor DC/AC para conectar el Sistema a la red, [62]-[64]. Los inversores pueden ser monofásicos o trifásicos. Su objetivo es transferir la máxima potencia active a la red en los sistemas FV. Los inversores están controlados para inyectar corrientes sinusoidales en fase con la red eléctrica, [65]-[66]. Están formados por un circuito de control que calcula la intensidad de referencia y un circuito de potencia que sigue la referencia e inyecta la corriente final a la red. El circuito de potencia incluye transistores para obtener la salida AC deseada con una conmutación de los transistores específica. La tensión de salida se suministra a la carga o a la red eléctrica. Para poder inyectar potencia a la red, el inversor debe ser controlado, [67]. El control más usado es el PI, [68]. El objetivo del control del inversor es inyectar intensidad co-lineal con la tensión en el punto de conexión común y mantener constante la tensión de entrada del inversor. Por lo tanto, un control de corriente por histéresis puede ser usado para inyectar toda la potencia del array FV a la red, [69]-[70].

Cuando el número de paneles FV es elevado, el sombreado en algunos paneles reduce fuertemente la potencia de salida. Dado que paneles individuales sólo generan unos pocos cientos de vatios, es deseable usar una arquitectura distribuida FV en la que cada

panel tiene su propio convertidor DC/DC para optimizar localmente el MPP incluso considerando el sombreado parcial o diferentes condiciones de operación, [10], [71]. Así, las salidas de los convertidores distribuidos son conectadas en paralelo para alimentar una carga o a la red con uno o varios inversores distribuidos. Por lo tanto, la combinación de módulos FV en serie y paralelo crea arrays FV capaces de suministrar potencia durante las horas pico de consumo del día, usando los sistemas FV conectados a redes inteligentes. Los sistemas de energía distribuida operan dentro del concepto de autoconsumo de potencia eléctrica, [72]-[73], donde cada cliente de electricidad tiene la oportunidad de conectar un sistema FV capaz de producir energía, según las leyes de cada país. Los sistemas FV son beneficiosos para el concepto de redes inteligentes porque pueden suministrar o almacenar la potencia extra mientras que el consumidor puede confiar en el almacenamiento o en la red eléctrica durante las horas sin sol. Además, este concepto viene bien para aplicaciones con equipos de telecomunicaciones, ya que su consumo es aproximadamente constante, [76].

6.2 Objetivos

En este trabajo, un Sistema FV que contiene módulos FV, un convertidor DC/DC, un convertidor DC/AC, una carga y un sistema de control es modelado en Matlab-Simulink. Una vez que la simulación es validada, entonces se construye una plataforma experimental para verificar los métodos de control propuestos.

Primero, se obtienen las curvas I – V y P – V de los módulos FV para conocer el punto óptimo de trabajo y saber dónde debería trabajar el sistema. Las curvas características se obtienen en primer lugar en simulación y se comparan después con las logradas por módulos FV reales, probando así la validez del modelo.

Posteriormente, se requiere un convertidor DC/DC para controlar la salida de tensión del array FV. Se ha elegido un convertidor buck-boost, [11], conectado a la salida de los módulos, porque convierte la tensión DC de un nivel a otro mayor o menor a la tensión de entrada según las necesidades. Un adecuado control del convertidor a través de su ciclo de trabajo permite obtener el valor necesario de tensión a su entrada para poder alcanzar el MPP. Para llevar a cabo los experimentos, se ha desarrollado una plataforma experimental que incluye la construcción del convertidor buck-boost, usando microcontroladores de bajo coste mientras que otros trabajos usan tarjetas comerciales de control y adquisición de datos, [77]-[79].

El convertidor buck-boost debe ser controlado para lograr el MPP. Dos algoritmos básicos se han desarrollado, el P&O y el control PI, para alcanzar el máximo y comparar estas técnicas con el método de control propuesto. El algoritmo convencional conlleva un comportamiento oscilatorio, por lo que en este trabajo se propone conseguir el punto de máximo trabajo usando un control no lineal, el control backstepping, [80]-[81]. Este control garantiza un estado estacionario sin oscilaciones y un modo de operación robusto y estable asintóticamente usando funciones de Lyapunov. Se ha elegido un control no lineal debido a la estructura variable, naturaleza variante del tiempo y las no linealidades del convertidor buck-boost. Un control lineal implicaría un modelo de linealización que es simple pero que no puede controlar al convertidor en un amplio rango. En este caso, el controlador

backstepping regula la tensión de salida del array FV a través del ciclo de trabajo del convertidor buck-boost para alcanzar el MPP bajo cualquier condición ambiental. Un plano de regresión calculado off-line se usa para obtener las tensiones de salida del array FV de referencia que suministra los MPPs para diferentes valores de temperatura e irradiancia para conseguir un control inicialmente más rápido. Además, también se ha propuesto un controlador backstepping adaptativo, [82]. En este caso, el control está basado en el hecho de que los elementos del buck-boost, bobina y condensador, son desconocidos o pueden sufrir variaciones. La ventaja de este método es que el control puede ser usado en el buck-boost sin importar los valores de los parámetros porque tiene una capacidad de aprendizaje para resolver las incertidumbres del modelo usando una estimación on-line de los parámetros desconocidos o que cambian.

En condiciones de sombreado parcial, se ha propuesto un nuevo método usando visión artificial para el seguimiento del MPP en tiempo real y para la detección del número de células FV afectadas por sombra parcial así como la intensidad de las sombras. Las webcams son usadas de manera habitual en las plantas FV como sistemas de vigilancia y este control puede usar esas mismas cámaras para la detección de sombras. La cámara debería estar dirigida hacia los módulos FV (en este caso conectados en serie). La visión artificial es comúnmente usada en muchas aplicaciones en tiempo real como los sistemas de seguimiento para detectar vehículos o incluso personas, para vigilancia, misiones militares, comunicación por vídeo o videojuegos, [83]-[85]. Esta técnica se usa para identificar el sombreado parcial de las células de una forma rápida y robusta, detectando los cambios de formas e intensidad de las sombras en tiempo real.

Con respecto a los convertidores DC/AC, en vez de usar compensadores lineales PI para regular la tensión a la entrada del inversor e inyectar intensidades sinusoidales a la red, [86]-[87], se propone usar el control backstepping para originar nuevos controladores para el inversor considerando la dinámica lenta y rápida del inversor monofásico, [88]-[90]. La separación de las dinámicas es necesaria ya que la potencia de la red inyectada/recuperada del inversor no es constante a los largo de un período. El controlador backstepping asegura una operación robusta y estable trabajando como inversor (sistema de fase mínima) o rectificador (sistema de fase no mínima), siendo capaz de enfrentarse a las variaciones de tensión AC de la red y los modos de operación de las microredes, [91]. Por lo tanto, las ventajas del control backstepping están relacionadas con el uso de las dinámicas directas del modelo de los convertidores. Este control garantiza la estabilidad y robustez del sistema mediante el uso de funciones de Lyapunov mejorando el rendimiento del sistema, [92]. Así, el convertidor DC/AC puede trabajar como inversor o como rectificador, dependiendo de la necesidad de la carga. Otra aplicación del sistema es cuando existe un exceso de energía FV durante las horas pico de sol. Esta energía puede ser usada para rebajar el pico de consumo de redes inteligentes durante la tarde si se añaden baterías. Adicionalmente, si hay una falta en la red que conduzca a una sag, el array FV y la batería de este sistema de potencia híbrido continuará suministrando energía a la carga sin verse afectada por el sag.

Como prestaciones adicionales, el control del inversor del sistema FV también puede ser usado para compensar armónicos, potencia reactiva y cargas desequilibradas del sistema eléctrico, [93]-[94], usando una estrategia de control basada en una modificación de la teoría

vectorial, [95]. Así, el control global hace posible la extracción de la máxima potencia del sistema FV, compensa las cargas desequilibradas y no lineales del sistema eléctrico y regula la tensión de entrada del inversor. De esta forma, la calidad de la potencia de la red eléctrica se mejora, [96]-[97]. Entonces, este sistema global es denominado acondicionador activo de potencia FV. Además, se propone una mejora en el filtro activo paralelo que consiste en usar una reactancia de salida conmutable para mejorar el seguimiento del acondicionador cuando trabaja con cargas no lineales. Finalmente, se han probado experimentalmente dos índices de calidad, el Load Characterization Index (LCI) que identifica las cargas lineales y no lineales en sistemas de potencia y el Unbalance Current Ratio (UCR) que asigna la responsabilidad del desequilibrio del sistema a la carga o a la fuente, [98]-[99].

Por lo tanto, los objetivos resumidos son:

- Modelar un Sistema PV conectado a red en Matlab-Simulink.
- Obtención de las curvas características I – V y P – V.
- Desarrollo de una plataforma experimental para validar el funcionamiento de los métodos de control propuestos. En este caso, el convertidor buck-boost ha sido construido.
- Diseñar un control no lineal para el convertidor buck-boost. En este caso, se han propuesto dos controladores, un control backstepping y un controlador backstepping adaptativo.
- Diseñar un control no lineal para el inversor, un control backstepping.
- Controlar la operación del convertidor DC/AC funcionamiento como inversor o como rectificador cuando trabaja conectado a una red inteligente.
- Comparar diferentes algoritmos MPPT con el control backstepping propuesto.
- Diseñar un algoritmo MPPT para condiciones de sombreado parcial, proponiendo un seguimiento del punto de máxima potencia mediante visión artificial.
- Obtener prestaciones adicionales del sistema FV en relación con la calidad de potencia: proponer un acondicionador activo de potencia FV para transferir la máxima energía y compensar las cargas desequilibradas y no lineales, probar dos índices de calidad y diseñar una reactancia variable para mejorar el seguimiento de los filtros activos.

6.3 Contribuciones

Esta tesis doctoral está centrada en el diseño de un control no lineal backstepping para controlar un convertidor buck-boost y un inversor para realizar el seguimiento del punto de máxima potencia en sistemas FV y transferir la potencia a la red eléctrica.

Primero, se ha implementado un controlador backstepping para regular la tensión de salida de un array FV en simulación para conseguir el punto de máxima potencia. Para ello, un sistema FV conectado a red que está formado por un array FV, un convertidor buck-boost, un inversor y una carga ha sido modelado en Matlab-Simulink. Después, el controlador diseñado ha sido implementado en el sistema. Este control está basado en el uso de funciones de Lyapunov para garantizar la estabilidad local del sistema. Además, el

control backstepping es robusto y los experimentos llevados a cabo validan su funcionamiento.

Journal paper 1:

Title: Backstepping Controller Design to Track Maximum Power in Photovoltaic Systems.

Authors: A. D. Martin, J. R. Vazquez.

Publication: *Automatika*, vol. 55, no. 1, pp. 22-31, Jan. 2014.

Una vez que el control propuesto se ha verificado en simulación, el método ha sido validado en una plataforma experimental. En este caso, la plataforma experimental desarrollada está compuesta por un módulo FV comercial, un convertidor buck-boost construido y una carga para comprobar el funcionamiento del backstepping en el convertidor DC/DC. Los experimentos llevados a cabo validan la eficiencia del control propuesto. La tensión que suministra el punto de máxima potencia se alcanza siempre incluso con condiciones ambientales cambiantes, comprobando así la robustez del control.

Conference paper 2:

Title: Adaptive Backstepping Control of a DC/DC Converter in Photovoltaic Systems.

Authors: A. D. Martin, J. R. Vazquez, R. S. Herrera.

Publication: *IEEE Eurocon*, pp. 949-955, July 2013.

Finalmente, se ha propuesto el diseño de un controlador backstepping para el control del convertidor DC/AC en una plataforma experimental, incluyendo la conexión a red. Así, los controladores backstepping se obtienen para suministros de potencia FV en distribuciones híbridas para equipos de telecomunicación. El sistema FV conectado a red en este caso contiene un array FV, el convertidor buck-boost construido unido con inversores monofásicos y con equipos de telecomunicaciones como cargas. El método backstepping es robusto y capaz de enfrentarse a las no linealidades e incertidumbres de la red eléctrica, suministrando los controladores la tensión e intensidad DC requerida para que el convertidor buck-boost siga el punto de máxima potencia del array FV, regulando la tensión de salida de los módulos FV para extraer la máxima potencia. Además, los controladores consiguen que las intensidades AC del inversor sean sinusoidales con factor de potencia unitario y una tensión de entrada al inversor constante apropiada para el suministro de equipos de telecomunicaciones. Por último, este control logra que la transferencia de potencia por el convertidor DC/AC sea bidireccional, ya que éste puede trabajar como inversor o como rectificador. Los resultados experimentales obtenidos en el laboratorio se han conseguido implementando los controladores en un microcontrolador de bajo coste, un dsPIC. Los resultados muestran que el control garantiza la máxima transferencia de potencia al equipo de telecomunicación o a la red eléctrica, asegurando una tensión constante a la entrada del

inversor mientras que absorbe o inyecta una intensidad con baja distorsión armónica a la red inteligente.

Journal paper 3:

Title: Backstepping Control of a Buck-Boost Converter in an Experimental PV-System

Authors: J. R. Vazquez, A. D. Martin.

Publication: *Journal of Power Electronics*, vol. 15, no. 6, Nov. 2015.

6.4 Trabajo Adicional

Se ha propuesto una modificación del control backstepping, un control backstepping adaptativo. Este control también sigue el MPP regulando la tensión de entrada del convertidor buck-boost sin importar los valores de los parámetros del convertidor.

Aparte de los algoritmos propuestos, otros algoritmos MPPT han sido implementados para compararlos. Un sistema neuro-fuzzy con un control MPPT lógico difuso se ha diseñado para compararlo con el algoritmo P&O, con el control PI y con el control propuesto backstepping.

Finalmente, se ha propuesto un control basado en visión artificial con backstepping para la detección de sombras para los sistemas FV con sombreado parcial. Este trabajo está actualmente enviado a una revista bajo revisión.

Se han propuesto prestaciones adicionales del sistema relacionadas con la calidad de potencia. Se ha diseñado un acondicionador activo de potencia FV para transferir la máxima potencia a la red y compensar la potencia reactiva y las cargas no lineales. Además, se propone usar una reactancia conmutable para mejorar el seguimiento de los filtros activos. Por último, se han probado dos índices de calidad.

Todos estos trabajos han sido publicados en diferentes revistas y congresos internacionales entre los años 2013/2015:

Paper 1:

Title: Adaptive Backstepping Control of a DC/DC Converter in Photovoltaic Systems.

Authors: A. D. Martin, J. R. Vazquez, R. S. Herrera.

Publication: *IEEE Eurocon*, pp. 949-955, July 2013, presented in International Conference.

Paper 2:

Title: Neuro-Fuzzy Control of a Grid-Connected Photovoltaic System with Power Quality Improvement

Authors: J. R. Vazquez, A. D. Martin, R. S. Herrera.

Publication: *IEEE Eurocon*, pp. 850-856, July 2013, presented in International Conference.
Paper 3:

Title: MPPT Algorithms Comparison in PV Systems. P&O, PI, Neuro-Fuzzy and Backstepping Controls

Authors: A. D. Martin, J. R. Vazquez.

Publication: *IEEE ICIT*, pp. 2841-2847, Mar. 2015, presented in International Conference.

Paper 4:

Title: Unbalance and Harmonic Distortion Assessment in an Experimental Distribution Network

Authors: A. D. Martín, R. S. Herrera, J. R. Vázquez, P. Crolla, G. M. Burt.

Publication: *Electric Power Systems Research*, vol. 127, pp. 271-279, 2015, **published in JCR**.

Paper 5:

Title: Improvement of Shunt Active Power Filter Compensation through Switching Output Reactances

Authors: J. R. Vazquez, A. D. Martin, N. M. Garrido.

Publication: *IEEE ICIT*, pp. 2708-2713, Mar. 2015, presented in International Conference.

Paper 6 in revision:

Title: MPPT in PV Systems under Partial Shading Conditions using Artificial Vision

Authors: A. D. Martin, J. R. Vazquez, J. M. Cano.

6.5 Resultados y Conclusiones

El objetivo principal de esta tesis es el diseño de controladores backstepping para el convertidor buck-boost y para el inversor. Estos controladores no lineales regulan la tensión de entrada del convertidor buck-boost para seguir el MPP en sistemas FV. Además, el controlador backstepping propuesto para el inversor controla la transferencia de energía del sistema FV a la red eléctrica. Así, los principales resultados y conclusiones de la tesis son:

- El diseño e implementación de un controlador backstepping para seguir el MPP en sistemas FV. Para ello, un sistema FV conectado a red es simulado en Matlab-Simulink para validar el funcionamiento del sistema usando el control propuesto. En este trabajo, el controlador ha sido aplicado a un convertidor buck-boost. Se ha probado para garantizar la estabilidad asintótica global usando funciones de

Lyapunov. Además, la robustez del control ha sido verificada bajo perturbaciones, como por ejemplo cambios rápidos en las condiciones ambientales, obteniendo una respuesta transitoria de 0.04s. Este control no presenta un comportamiento oscilatorio a diferencia del algoritmo P&O. El rendimiento del sistema es del 98.5 % en el peor de los casos. Así, la efectividad del uso del controlador backstepping es validada para la extracción de la máxima potencia de un sistema FV.

- Una vez que el método propuesto ha sido verificado en simulación, se ha desarrollado una plataforma experimental para validar el control backstepping. En este caso, se ha usado un módulo FV comercial conectado al convertidor buck-boost construido. Entonces, el array FV suministra potencia a una carga. El control backstepping supervisado on-line ha sido implementado en un microcontrolador de bajo coste, un dsPIC30F3013. Los resultados confirman que el control trabaja de forma correcta porque la referencia de tensión siempre se alcanza para cualquier condición ambiental. Así, se tiene una eficiencia en el seguimiento mayor al 99%. En estado estacionario el control no presenta comportamiento oscilatorio mientras que la respuesta transitoria es más rápida que usando el algoritmo P&O, ya que la potencia se estabiliza después de 3.3s bajo un cambio de irradiancia y con el P&O se requiere 8.4s para estabilizar la potencia ante el mismo cambio de irradiancia. Finalmente, la eficiencia del convertidor buck-boost construido está del 90% en los peores casos, obteniendo una rendimiento del 99% en los mejores.
- Además, se ha propuesto un controlador backstepping para el controlar del inversor para transferir la máxima potencia a la red eléctrica en un sistema FV conectado a red experimental. En este caso, el array FV suministra la energía al convertidor buck-boost construido, unido a un equipo de telecomunicaciones y a un inversor monofásico conectado a una red inteligente, configurando un sistema híbrido distribuido FV. Las leyes de control del backstepping del convertidor DC/DC garantizan alcanzar el MPP, obteniendo una eficiencia del seguimiento entre el 98.2% y el 99.9%. Las leyes de control del backstepping para el convertidor DC/AC regulan la tensión de la carga de telecomunicaciones y controla la intensidad que se absorbe o se inyecta a la red, que es casi sinusoidal (THD = 1.6%, menor que el 3% requerido por los estándares) y cercana al factor de potencia unitario. Todas las leyes de control (del convertidor buck-boost y del inversor), los moduladores de convertidores de frecuencia fija, el muestreo de tensión e intensidad así como la sincronización con la red están implementadas en el microcontrolador de bajo coste. Además, los resultados experimentales muestran el funcionamiento del sistema FV de autoconsumo usando el control backstepping y el comportamiento dinámico del sistema cuando cambia el modo de operación de inversor a rectificador para adaptarse a los requerimientos de las cargas de telecomunicaciones. La robustez del control permite que la capacidad de los condensadores reales puedan variar casi 10 veces sobre el valor calculado mientras que las inductancias pueden variar entre el 30% y el 300% su valor.

Las conclusiones del trabajo adicional son resumidas:

- Se ha propuesto una modificación del control backstepping, un control backstepping adaptativo. Este control también sigue el MPP controlando la tensión de entrada del convertidor buck-boost y además puede adaptarse cuando hay incertidumbre en los valores de la bobina y del condensador del convertidor debido a su capacidad de aprendizaje por medio de una estimación on-line de los parámetros. Este control ha sido validado en simulación y los resultados muestran que la eficiencia del seguimiento está entre 98% y 99% y la respuesta transitoria es aproximadamente 0.01s ante cambios bruscos de las condiciones ambientales.
- Aparte de los controles backstepping, un sistema neuro-fuzzy con lógica difusa se ha diseñado para el seguimiento del MPP. En este caso el sistema neuro-fuzzy calcula la tensión de referencia de salida del array PV y el controlador fuzzy sigue la tensión de referencia. Este método ha sido probado en simulación, consiguiendo mejores resultados que con el algoritmo P&O, no obteniendo oscilaciones.
- Para terminar con los algoritmos MPPT, se ha realizado una comparativa entre el algoritmo P&O, el control PI, el sistema neuro-fuzzy con controlador fuzzy y el método propuesto de backstepping. Una de las principales conclusiones de la comparativa está en las señales de rizado del P&O que implican un comportamiento oscilatorio sobre el MPP incluso en estado estacionario, conduciendo esto a pérdidas de potencia. Los otros métodos no presentan oscilaciones y tiene una respuesta transitoria suave. Teniendo en cuenta la eficiencia de los métodos, el que mejor resultados obtiene es el backstepping, logrando una eficiencia del seguimiento entre 98.2% y 99.9%.
- Para sistemas FV con condiciones de sombra se propone un control backstepping con visión artificial para detectar las sombras y realizar el seguimiento, incluso cuando las curvas P – V presentan múltiples picos. Este algoritmo puede evitar los máximos locales y puede conducir a la tensión directamente a la zona donde está situado el máximo global. El algoritmo de visión artificial suministra la irradiancia de la sombra de cada panel, el área afectada por las sombras y la tensión de referencia que da el MPP. Después, el controlador backstepping sigue esa tensión de referencia. Se ha diseñado una plataforma experimental usando el convertidor buck-boost construido para validar el funcionamiento de este método. Los resultados verifican la detección de sombras y el cálculo de la irradiancia de sombra así como el seguimiento de MPP. El máximo global se alcanza siempre sin importar donde está localizado ni el número de máximos de la curva P – V. La eficiencia del seguimiento está entre 98.7% y 99.6%.
- Con respecto a la calidad de potencia, un acondicionador activo FV ha sido propuesto. Así, la estrategia de control global suministra potencia a la red a través de un inversor y compensa las cargas desequilibradas y no lineales del sistema eléctrico. En este trabajo, se ha diseñado una compensación sinusoidal para obtener corriente de red de secuencia directa, sinusoidal y equilibrada. Este control es efectivo, simple y fácil de implementar con un tiempo reducido de

computación, consiguiendo una respuesta transitoria menor a medio periodo. Los resultados obtenidos en simulación muestran que el THD de la intensidad de fuente puede ser reducido del 48% al 1.26% cuando se conecta el acondicionador FV.

- Continuando con calidad de la potencia, dos índices han sido probados para evaluar la distorsión armónica y el desequilibrio introducido por diferentes cargas conectadas en el punto de conexión común en una red de distribución experimental. El primer índice, el UCR asigna responsabilidad del desequilibrio del sistema a la carga o a la red y el LCI calcula la distorsión introducida por la carga. Estos índices han sido comparados con otros índices comunes. Los resultados muestran que ambos índices trabajan adecuadamente incluso con tensiones distorsionadas y desequilibradas. Además, el LCI identifica los condensadores como cargas lineales según los estándares cuando otros métodos fallan en identificarlos como cargas lineales.
- Finalmente, se propone mejorar los acondicionadores activos incluyendo una reactancia conmutable para mejorar el seguimiento del acondicionador cuando trabaja con cargas no lineales. Los resultados de simulación muestran la efectividad del diseño propuesto. Se obtiene un THD en la tensión bajo y similar a los filtros activos convencionales mientras que el THD de la intensidad se reduce un 50% con respecto a los anteriores acondicionadores.

6.6 Trabajo Futuros

El trabajo futuro propuesto se resume a continuación:

- Validación experimental del controlador backstepping adaptativo en el convertidor DC/DC y en el inversor.
- Validación de otros algoritmos MPPT en la plataforma experimental desarrollada.
- Validación del algoritmo de visión artificial propuesto en un sistema FV conectado a red bajo condiciones de sombreado parcial.
- Validación del acondicionador FV en una plataforma experimental incluyendo cargar no lineales para verificar la estrategia de control global para que suministre la máxima potencia a la red y compense cargas no lineales y desequilibradas en redes de generación distribuidas.